Supplementary Information

Structure-Property Relationships to Direct the Dynamic Properties of Acylsemicarbazide-Based Materials

Stefan J.D. Maessen,[a] Siebe Lekanne Deprez,[b] Pascal Vermeeren,[b] Bart W.L. van den Bersselaar,[a] Martin Lutz,[c] Johan P.A Heuts,[a] Célia Fonseca Guerra[b] and Anja R.A. Palmans*[a]

a. Department of Chemical Engineering & Chemistry and Institute for Complex Molecular Systems, Eindhoven University of Technology, P.O. Box 513, 5600 MB Eindhoven, The Netherlands.

b. Department of Chemistry and Pharmaceutical Sciences, Amsterdam Institute of Molecular and Life Sciences (AIMMS), Vrije Universiteit Amsterdam, De Boelelaan 1108, 1081 HZ Amsterdam, The Netherlands.

c. Structural Biochemistry, Bijvoet Centre for Biomolecular Research, Faculty of Science, Utrecht University, Universiteitsweg 99, 3584 CG Utrecht, The Netherlands.

*corresponding author:

a.palmans@tue.nl

Contents

1. Experimental section

1.1 Materials and Methods

Materials

Unless stated otherwise, all reagents and chemicals were obtained from commercial sources at the highest purity available and used without further purification. Polydimethylsiloxane, hydride terminated, viscosity 7-10 cSt and polydimethylsiloxane, monohydride terminated, viscosity 5-9 cSt were obtained from ABCR. All solvents were obtained from Biosolve except for acetonitrile which was obtained from Actu-All Chemicals. Dry solvents were obtained from an MBraun solvent purification system (MB SPS-800). Dry unstabilized THF from the solvent purification system was stored under argon and further dried with activated 4 Å molecular sieves, and filtered through a Whatman 2 µm PTFE syringe filter before use. Deuterated chloroform ($CDCl_3$) was purchased from Cambridge Isotope Laboratories and kept dry with 4 Å molecular sieves. Deuterated DMSO (DMSO-d_6) and deuterated THF (THF-d_8) were purchased from Deutero GmbH and used as received.

General Methods

Reactions were followed by thin-layer chromatography (TLC) 60-F254 silica gel plates from Merck and visualized by 254 nm UV light or by staining with a ceric ammonium molybdate solution. Automated column chromatography was performed on a Grace Reveleris X2 automated column machine with Reveleris Silica Flash Cartridges and on a Biotage Isolera 1 with Biotage SNAP KP-SIL columns.

NMR spectroscopy

^{1}H, ^{13}C NMR spectra were recorded on a 400 MHz Bruker Avance III Spectrometer (^{1}H using 400 MHz, ^{13}C using 100 MHz). Peak multiplicities are abbreviated as s: singlet, d: doublet, t: triplet, q: quartet, p: pentet, m: multiplet, dd: doublet of doublets, td: triplet of doublets, tt: triplet of triplets. Proton and carbon chemical shifts are reported in parts per million (ppm) downfield

from tetramethylsilane (TMS) using the deuterated solvent resonance frequency as internal standard (7.26 ppm for $CDCl_3$ and 2.50 ppm for DMSO-d_6).

Matrix-assisted laser desorption/ionization time-of-flight

Matrix-assisted laser desorption/ionization time-of-flight followed by mass spectrometry (MALDI-ToF-MS) mass analysis measurements were performed on a Bruker Autoflex Speed using α-cyano-4-hydroxycinnamic acid (CHCA) and *trans*-2-[3-(4-tert-butylphenyl)-2-methyl-2-propenylidene]malononitrile (DCTB) as matrices. Samples for MALDI-ToF-MS were dissolved with a concentration of 1 mg mL^{-1} in either chloroform, DCM or THF.

Fourier transform infrared spectroscopy

Fourier transform infrared spectroscopy (FTIR) spectra were recorded on a Shimadzu IRTracer-100 spectrometer using the MIRacle 10 single reflection ATR accessory.

Growth of single crystals

Crystals suitable for single-crystal X-ray diffraction were prepared via a vapor diffusion method. Saturated solutions of PhASCPh and PhASCBz in methanol were prepared and diluted two-fold. An open GCMS vial was charged with 0.2 mL of this half-saturated solution, which was then placed in a large closed vial containing 2 mL of countersolvent (diethyl ether for PhASCPh, methyl *tert*-butyl ether for PhASCBz). After several days, the formation of crystals was observed.

X-Ray crystal structure determination of PhASCPh

$C_{14}H_{13}N_3O_2$, Fw = 255.27, colorless needle, 0.33 × 0.15 × 0.05 mm^3, orthorhombic, Pbca (no. 61), a = 9.9581(3), b = 9.1704(3), c = 27.6575(7) Å, V = 2525.70(12) $Å^3$, Z = 8, D_x = 1.343 g/cm^3, μ = 0.09 mm^{-1}. The diffraction experiment was performed on a Bruker Kappa ApexII diffractometer with sealed tube and Triumph monochromator (λ = 0.71073 Å) at a temperature of 150(2) K up to a resolution of $(\sin\theta/\lambda)_{max}$ = 0.65 $Å^{-1}$. The intensities were integrated with the Eval15 software[1]. A multi-scan absorption correction and scaling was performed with SADABS[2] (correction range 0.65-0.75). A total of 41429 reflections was measured, 2887 reflections were unique (R_{int} = 0.062), 2119 reflections were observed [$I>2\sigma(I)$]. The structure was solved with Patterson superposition methods using SHELXT.[3] Structure refinement was performed with SHELXL-2018[4] on F^2 of all reflections. Non-hydrogen atoms were refined freely with anisotropic displacement parameters. All hydrogen atoms were located in difference Fourier maps. N-H hydrogen atoms were refined freely with isotropic displacement parameters, C-H hydrogen atoms were refined with a riding model. 184 Parameters were refined with no restraints. R1/wR2 [$I > 2\sigma(I)$]: 0.0453 / 0.1023. R1/wR2 [all refl.]: 0.0683 / 0.1130. S = 1.062. Residual electron density between -0.19 and 0.23 e/$Å^3$. Geometry calculations and checking for higher symmetry was performed with the PLATON program.[5]

X-Ray crystal structure determination of PhASCBz

$C_{15}H_{13}N_3O_3$, Fw = 283.28, colorless plate, 0.37 × 0.35 × 0.08 mm^3, monoclinic, $P2_1/c$ (no. 14), a = 9.7633(3), b = 27.5437(7), c = 10.4855(3) Å, β = 98.644(2) °, V = 2787.70(13) $Å^3$, Z = 8, D_x = 1.350 g/cm^3, μ = 0.10 mm^{-1}. The diffraction experiment was performed on a Bruker Kappa ApexII diffractometer with sealed tube and Triumph monochromator (λ = 0.71073 Å) at a temperature of 150(2) K up to a resolution of $(\sin\theta/\lambda)_{max}$ = 0.65 $Å^{-1}$. The intensities were integrated with the Eval15 software[1]. A multi-scan absorption correction and scaling was performed with SADABS[2] (correction range 0.68-0.75). A total of 53558 reflections was

measured, 6410 reflections were unique (R_{int} = 0.034), 5233 reflections were observed [I>2σ(I)]. The structure was solved with Patterson superposition methods using SHELXT.[3] Structure refinement was performed with SHELXL-2018[4] on F^2 of all reflections. Non-hydrogen atoms were refined freely with anisotropic displacement parameters. All hydrogen atoms were located in difference Fourier maps. N-H hydrogen atoms were refined freely with isotropic displacement parameters, C-H hydrogen atoms were refined with a riding model. 403 Parameters were refined with no restraints. R1/wR2 [I > 2σ(I)]: 0.0402 / 0.1033. R1/wR2 [all refl.]: 0.0503 / 0.1084. S = 1.060. Residual electron density between -0.33 and 0.43 e/Å^3. Geometry calculations and checking for higher symmetry was performed with the PLATON program.[5]

Compression molding

Compression molding was performed in a Fontijne LabEcon 300 hot press. The pDMS-ASC were placed in a mold and sandwiched between 0.05 mm thick Teflon sheets and 4 mm thick stainless steel sheets, which was placed under 100 kN of force at 140 °C for 60 minutes. The samples were cooled rapidly and inspected. In all cases, more polymer was added and the samples were molded again under 100 kN of force at 140 °C for 30 minutes. The pDMS-ASC polymers were pressed into 0.7-1 mm thick films, from which rectangles were cut for DMTA experiments and 8 mm disks were punched for creep experiments.

Size Exclusion Chromatography (SEC)

SEC was performed on Varian/Polymer Laboratories PL-SEC 50 equipment equipped with refractive index (RI) and UV (254 nm) detectors. The system was equipped with a combination of Agilent PLgel 5-μm mixed-C column and Agilent PLgel 5-μm mixed-D column. The mobile phase was THF with BHT stabilizer and run at a flow rate of 1 mL min^{-1} at 40 °C. Polystyrene was used as calibration standard.

Thermogravimetric analysis (TGA)

The thermal stabilities of the pDMS-ASC materials were determined using a TGA 550 (TA instruments) under N_2 flow. Temperature ramps were performed by ramping from 20 °C to 40 °C at 20 °C min^{-1}, keeping the sample isothermal at 40 °C for 5 minutes, followed by a ramp to 800 °C at 10 °C min^{-1}. Temperature calibration was performed using the Curie points of high purity ferromagnetic standards.

Differential scanning calorimetry (DSC)

DSC was performed in a Q2000 DSC (TA instruments) calibrated with an indium standard. Measurements were performed using standard aluminum pans between -40 °C and 160 °C. Heating and cooling runs were performed at 10 °C min^{-1}. The first cooling and second heating runs were reported for all materials.

Variable temperature infrared spectroscopy (VTIR)

VTIR spectra were obtained at the Bruker Tensor 27. A sample was heated to 160 or 200 °C and cooled back to 25 °C, both with a heating rate of 3 °C min^{-1}. At 200 °C, the sample was first equilibrated for 5 min before cooling. IR spectra were collected every 5 °C.

Dynamic mechanical thermal analysis (DMTA)

DMTA was performed on rectangular shaped compression molded samples using the film tension setup in a Discovery DMA 850 (TA instruments). Samples were cooled to -150 °C and left to equilibrate for 2 hours. Then, a temperature ramp was performed at 3 °C min^{-1} from -

150 °C to 200 °C. A preload force of 1.0 N and a force track of 125% was used. The storage and loss modulus were recorded as a function of temperature.

Medium- and wide-angle x-ray scattering (MAXS and WAXS)

Bulk small-angle X-ray scattering (SAXS) was performed on a Ganesha instrument from SAXSLab. The flight tube and sample holder are all under vacuum in a single housing, with a GeniX-Cu ultra-low divergence X-ray generator. The source produces X-rays with a wavelength (λ) of 0.154 nm and flux of 1 × 108 ph s^{-1}. Scattered X-rays were captured on a 2-dimensional Pilatus 300K detector with 487 × 619 pixel resolution. The sample-to-detector distance was 0.084 m (WAXS mode) or 0.48 m (MAXS mode). The instrument was calibrated with diffraction patterns from silver behenate.

Probing dynamics in bulk experiments

Around 50 mg of the pDMS-ASC polymers were dissolved in 20 mL of THF (using a heat gun for ASC-HDI and ASC-PDI, at room temperature for ASC-BDI). Around 50 mg of the corresponding monoASCs (H-monoASC for ASC-HDI, P-monoASC for ASC-PDI and B-monoASC for ASC-BDI) were added to the polymer and dissolved. The mixtures were divided equally over 10 vials (2 mL per vial) and the solvent was allowed to evaporate over the course of 24 hours, after which the mixtures were dried in a vacuum oven at 50 °C overnight. For the measurements, an oven was preheated at 120 °C and 7 vials were put in. The vials were taken out at time intervals of 1, 2, 4, 8, 16, 24 and 48 hours. The mixtures were then dissolved in 4 mL of THF (using a heat gun for ASC-HDI and ASC-PDI, at room temperature for ASC-BDI) and SEC measurements were performed (~2 mg mL^{-1} in THF). For ASC-PDI, the samples were additionally diluted two-fold due to aggregation during the SEC measurements (~1 mg mL^{-1} in THF). The SEC chromatograms were baseline corrected at a retention time of 12 minutes, and normalized on the highest intensity polymer peak above 2000 Da.

Creep-recovery measurements

Creep recovery measurements were performed using a Discovery HR 20 (TA instruments) with environmental temperature control (ETC) setup and 8 mm parallel-plate geometry. All experiments were performed with an axial force range of 3 ± 0.1 N. Samples were equilibrated at the measurement temperature for 3 minutes, after which they were subjected to an oscillatory time sweep for 2 minutes under 1.0% oscillatory strain and at an angular frequency of 1 Hz. Creep measurements were performed between 100 and 140 °C. 20 kPa of shear stress was applied to the sample for 1800 seconds, with a recovery period of 5400 seconds. The slope of the creep compliance was determined between 1400 and 1800 s.

Tensile tests

Tensile tests were performed on rectangular shaped samples using the film tension setup in a Discovery DMA 850 (TA instruments). Samples were compression molded to a thickness between 0.3 and 0.4 mm for these measurements. A sample with an initial length of 5.0 mm ± 0.2 mm and a width of 5.3 mm was clamped in the setup. A rate of 0.1 mm/min (~2%/min) was used to put the sample in tension. The stress-strain curves were obtained at room temperature.

Frequency sweep experiments

Frequency sweep experiments from 10^{2} rad/s to 10^{-3} rad/s were performed using a Discovery HR 20 (TA instruments) with environmental temperature control (ETC) setup and 8 mm parallel-plate geometry. The oscillation amplitude was set to 1% strain.

1.2 Synthetic procedures

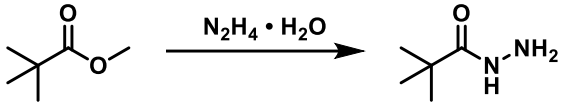

Synthesis of *tert*-butyl hydrazide: Methyl pivalate (5 mL, 38 mmol, 1 eq) was added to a 25 mL round-bottom flask equipped with an oil bath and reflux cooler. Hydrazine monohydrate (10 mL, 206 mmol, 5.5 eq) was to the flask and the mixture was stirred at 80 °C overnight. The liquid was dried in under high vacuum for 6 hours, after which a white crystalline powder was obtained which was used without further purification (3.5 g, 80%). ^{1}H NMR (400 MHz, DMSO-d_6) δ = 8.78 (s, 1H), 3.99 (s, 2H), 1.08 (s, 9H). ^{13}C NMR (100 MHz, DMSO-d_6) δ = 177.31, 37.59, 27.79.

Synthesis of ASC model compounds: *General procedure:* The hydrazide (1 eq) was dissolved in acetonitrile (dried on 3 Å molecular sieves) in a dried 50 mL round-bottom flask under argon atmosphere. The isocyanate (1 eq) was added to the suspension directly and the mixture was left to stir overnight. The next day, the suspension was filtered using filter paper in a funnel and washed with 2x 10 mL of acetonitrile and with 2x 10 mL of diethyl ether. The solid was collected in a vial and dried in a vacuum oven at 50 °C overnight, yielding the pure product.

MeASCPh: 300 mg (4.05 mmol) of acethydrazide in 10 mL of acetonitrile, 0.440 mL (4.05 mmol) of phenyl isocyanate, 10 mL of acetonitrile. Product obtained as a white solid (573 mg, 73%). ^{1}H NMR (400 MHz, DMSO-d_6) δ = 9.63 (d, J = 2.1 Hz, 1H), 8.70 (s, 1H), 7.96 (d, J = 2.1 Hz, 1H), 7.44 (d, J = 7.3 Hz, 2H), 7.25 (t, J = 7.2 Hz, 2H), 6.95 (tt, J = 7.0 Hz, 1.2 Hz, 1H), 1.87 (s, 3H). ^{13}C NMR (100 MHz, DMSO-d_6) δ = 169.29, 155.43, 139.66, 128.65, 121.89, 118.50, 20.64. MALDI-ToF-MS: m/z calc. for $C_9H_{11}N_3O_2$: 193.09 Da; found 194.12 Da $[M+H]^+$, 216.09 Da $[M+Na]^+$.

BuASCPh: 300 mg (2.94 mmol) of butyric acid hydrazide in 10 mL of acetonitrile, 0.321 mL (2.94 mmol) of phenyl isocyanate. Product obtained as a white solid (427 mg, 66%). ^{1}H NMR (400 MHz, DMSO-d_6) δ = 9.59 (s, 1H), 8.68 (s, 1H), 7.96 (s, 1H), 7.44 (d, J = 7.4 Hz, 2H), 7.24 (t, J = 7.6, 2H), 6.94 (tt, J = 7.4, 1.2 Hz, 1H), 2.12 (t, J = 7.3 Hz, 2H), 1.55 (h, J = 7.4 Hz, 2H), 0.89 (t, J = 7.4 Hz, 3H). ^{13}C NMR (100 MHz, DMSO-d_6) δ = 172.10, 155.41, 139.68, 128.65, 121.82, 118.36, 35.11, 18.38, 13.58. MALDI-ToF-MS: m/z calc. for $C_{11}H_{15}N_3O_2$: 221.12 Da; found 222.15 Da $[M+H]^+$, 244.12 Da $[M+Na]^+$.

BnASCPh: 500 mg (3.33 mmol) of phenylacetic hydrazide in 10 mL of acetonitrile, 0.362 mL (3.3 mmol) of phenyl isocyanate. Product obtained as a white solid (820 mg, 91%). ^{1}H NMR (400 MHz, DMSO-d_6) δ = 9.95 (s, 1H), 8.72 (s, 1H), 8.08 (s, 1H), 7.44 (d, J = 7.3 Hz, 2H), 7.35 – 7.20 (m, 7H), 6.95 (t, J = 7.4 Hz, 1H), 3.50 (s, 2H). ^{13}C NMR (100 MHz, DMSO-d_6) δ = 170.07, 155.31, 139.61, 135.73, 129.12, 128.67, 128.23, 126.48, 121.89, 118.42, 40.14. MALDI-ToF-MS: m/z calc. for $C_{15}H_{15}N_3O_2$: 269.12 Da; found 270.14 Da $[M+H]^+$, 292.11 Da $[M+Na]^+$, 308.08 Da $[M+K]^+$.

PhASCPh: 500 mg (3.67 mmol) of benzhydrazide in 10 mL of acetonitrile, 0.400 mL (3.67 mmol) of phenyl isocyanate. Product obtained as a white solid (832 mg, 89%). ^{1}H NMR (400 MHz, DMSO-d_6) δ = 10.30 (s, 1H), 8.86 (s, 1H), 8.18 (s, 1H), 7.93 (d, J = 6.9 Hz, 2H), 7.58 (tt, J = 7.6 Hz, 1.2 Hz, 1H), 7.54 – 7.43 (m, 4H), 7.26 (t, J = 7.3 Hz, 2H), 6.96 (tt, J = 7.3, 1.2 Hz, 1H). ^{13}C NMR (100 MHz, DMSO-d_6) δ = 166.42, 155.65, 139.69, 132.58, 131.78, 128.65,

128.39, 127.56, 121.90, 118.53. MALDI-ToF-MS: m/z calc. for $C_{14}H_{14}N_3O_2$: 255.10 Da; found 256.10 Da $[M+H]^+$, 278.08 Da $[M+Na]^+$, 294.06 Da $[M+K]^+$.

***t*-BuASCPh:** 500 mg (3.67 mmol) of *tert*-butyl hydrazide in 15 mL of acetonitrile, 0.470 mL (3.67 mmol) of phenyl isocyanate. Product was hot-filtrated with acetonitrile and the filtrate was recrystallized from acetonitrile due to some diphenyl urea impurities. Obtained as a colorless crystals (280 mg, 28%). ^{1}H NMR (400 MHz, DMSO-d_6) δ = 9.36 (d, J = 2.1 Hz, 1H), 8.67 (s, 1H), 7.82 (s, 1H), 7.43 (d, J = 7.4 Hz, 2H), 7.26 (t, J = 7.3 Hz, 2H), 6.95 (t, J = 7.4 Hz, 1H), 1.16 (s, 9H). ^{13}C NMR (100 MHz, DMSO-d_6) δ = 177.97, 155.98, 140.18, 129.16, 122.21, 118.61, 37.86, 27.63. MALDI-ToF-MS: m/z calc. for $C_{12}H_{17}N_3O_2$: 235.13 Da; found 236.17 Da $[M+H]^+$, 258.14 Da $[M+Na]^+$, 274.11 Da $[M+K]^+$.

PhASCBu: 300 mg (2.20 mmol) of benzhydrazide in 20 mL of acetonitrile, 0.245 mL (2.20 mmol) of butyl isocyanate. Product obtained as a white solid (78 mg, 15%). Low yield obtained due to gelation of the reaction mixture leading to loss of stirring during the reaction. ^{1}H NMR (400 MHz, DMSO-d_6) δ = 10.10 (s, 1H), 7.89 (d, J = 7.2 Hz, 2H), 7.78 (s, 1H), 7.56 (t, J = 7.3 Hz, 1H), 7.48 (t, J = 7.5 Hz, 2H), 6.45 (t, J = 5.7 Hz, 1H), 3.02 (q, J = 6.6 Hz, 2H), 1.38 (p, J = 7.0 Hz, 2H), 1.27 (h, J = 7.2 Hz, 2H), 0.87 (t, J = 7.2 Hz, 3H). ^{13}C NMR (100 MHz, DMSO-d_6) δ = 166.28, 158.33, 132.76, 131.58, 128.26, 127.53, 38.86, 31.99, 19.42, 13.72. MALDI-ToF-MS: m/z calc. for $C_{12}H_{17}N_3O_2$: 235.13 Da; found 236.18 Da $[M+H]^+$, 258.14 Da $[M+Na]^+$, 274.29 Da $[M+K]^+$.

PhASCBn: 500 mg (3.67 mmol) of benzhydrazide in 10 mL of acetonitrile, 0.454 mL (3.67 mmol) of benzyl isocyanate. Product obtained as a white solid (678 mg, 69%). ^{1}H NMR (400 MHz, DMSO-d_6) δ = 10.18 (s, 1H), 7.98 (s, 1H), 7.91 (d, J = 7.0 Hz, 2H), 7.56 (tt, J = 7.6 Hz, 1.2 Hz, 1H), 7.48 (t, J = 7.4 Hz, 2H), 7.35 – 7.16 (m, 5H), 7.08 (s, 1H), 4.25 (d, J = 6.1 Hz, 2H). ^{13}C NMR (100 MHz, DMSO-d_6) δ = 166.41, 158.50, 140.65, 132.74, 131.64, 128.27, 128.10, 127.61, 126.94, 126.49, 42.63. MALDI-ToF-MS: m/z calc. for $C_{15}H_{15}N_3O_2$: 269.12 Da; found 270.14 Da $[M+H]^+$, 292.11 Da $[M+Na]^+$, 308.08 Da $[M+K]^+$.

PhASCBz: 369 mg (2.79 mmol) of benzhydrazide in 10 mL of acetonitrile, 369 mg (2.71 mmol) of benzoyl isocyanate. Product obtained as a white solid (680 mg, 89%). ^{1}H NMR (400 MHz, DMSO-d_6) δ = 11.11 (s, 1H), 10.67 (s, 1H), 10.20 (s, 1H), 8.03 (d, J = 7.2 Hz, 2H), 7.93 (d, J = 7.0 Hz, 2H), 7.69 – 7.49 (m, 6H). ^{13}C NMR (100 MHz, DMSO-d_6) δ = 168.07, 165.55, 153.77, 133.05, 132.23, 132.19, 131.98, 128.61, 128.51, 128.34, 127.56. MALDI-ToF-MS: m/z calc. for $C_{15}H_{13}N_3O_3$: 283.10 Da; found 284.11 Da $[M+H]^+$, 306.09 Da $[M+Na]^+$, 322.06 Da $[M+K]^+$.

Synthesis of methyl ester-terminated pDMS: Polydimethylsiloxane, hydride terminated, viscosity 7-10 cSt (40.0 g, 1 eq) was mixed with methyl undec-10-enoate (14.0 g, 70.6 mmol, ~2.4 eq) in bulk in a dried 100 mL round-bottom flask under argon atmosphere. The mixture was cooled with a room-temperature water bath, and Karstedt's catalyst (2 wt% in xylene) was added (5-6 drops), after which the mixture was stirred for 24 hours. The mixture was transferred to a separatory funnel and extracted with 3x 50 mL of acetonitrile to remove excess methyl undec-10-enoate. After this, the polymer oil was dissolved in 100 mL of DCM and filtered over a plug of activated charcoal in a glass filter to remove the platinum catalyst. The charcoal plug was washed with 3x 50 mL of DCM. The solvent was removed in *vacuo* after which the product was obtained as a colorless oil (50.0 g, 99%). ^{1}H NMR (400 MHz, $CDCl_3$) δ = 3.65 (s, 6H), 2.29 (t, J = 7.5 Hz, 4H), 1.62 (p, J = 7.3 Hz, 4H), 1.39 – 1.17 (m, 28H), 0.57 – 0.47 (m, 4H), 0.06 (m, 96H). ^{13}C NMR (100 MHz, $CDCl_3$) δ = 174.43, 51.52, 34.26, 33.60, 29.69, 29.65, 29.52, 29.42, 29.32, 25.12, 23.38, 18.42, 1.31, 1.20, 1.18. SEC (RI detector): M_n: 1.7 kg mol^{-1}, M_w: 1.9 kg mol^{-1}, PDI: 1.1.

Synthesis of acyl hydrazide terminated pDMS: Methyl ester-terminated pDMS (45.0 g) was dissolved in 150 mL of isopropanol in a 250 mL round-bottom flask equipped with an oil bath and reflux cooler. Hydrazine monohydrate (22.0 g, 0.44 mol) was added to the solution, after which the mixture was left to stir at 50 °C for 72 hours. The isopropanol was removed in *vacuo*, and the mixture was dissolved in 150 mL of DCM. The mixture was transferred to a separatory funnel and extracted with 3x 200 mL of demineralized water to remove excess hydrazine. After this, the DCM layer was dried over Na_2SO_4, filtered using gravity and the filter washed with 50 mL of DCM. The solvent was removed in *vacuo* after which the product was obtained as a colorless viscous oil (43.0 g, 96%). ^{1}H NMR (400 MHz, $CDCl_3$) δ = 6.77 (s, 2H), 3.90 (s, 4H), 2.14 (t, J = 7.6 Hz, 4H), 1.62 (p, J = 7.2 Hz, 4H), 1.37 – 1.17 (m, 28H), 0.52 (t, J = 7.5 Hz, 4H), 0.24 – -0.17 (m, 96H). ^{13}C NMR (100 MHz, $CDCl_3$) δ = 174.24, 34.70, 33.57, 29.68, 29.64, 29.50, 29.45, 29.43, 25.66, 23.34, 18.38, 1.29, 1.17, 1.15. SEC (UV detector): M_n: 2.0 kg mol^{-1}, M_w: 2.8 kg mol^{-1}, PDI: 1.4. SEC (RI detector): M_n: 1.4 kg mol^{-1}, M_w: 1.9 kg mol^{-1}, PDI: 1.3.

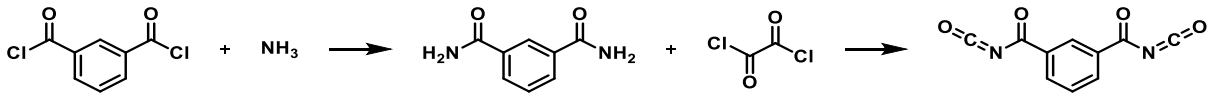

Synthesis of isophthalamide: Ammonium hydroxide (50 mL, 25% in water) was added to a dried 100 mL round-bottom flask that was cooled with an ice bath and equipped with a dropping funnel under argon. Isophthaloyl chloride (5.0 g, 24.6 mmol) was dissolved in 20 mL of dry THF and transferred to the dropping funnel. The THF solution was added dropwise to the flask over 5 minutes, after which the mixture was stirred for an additional 15 minutes. The mixture was allowed to warm to room temperature after which the precipitate was filtered using a Büchner filter and washed with 3x 100 mL of demineralized water. over a plug of activated charcoal in a glass filter to remove the platinum catalyst. The charcoal plug was washed with 3x 50 mL of DCM. The solid dried in a vacuum oven at 60 °C overnight after which the product was obtained as a white powder (3.8 g, 95%). ^{1}H NMR (400 MHz, DMSO-d_6) δ = 8.39 (t, J = 1.8 Hz, 1H), 8.07 (s, 2H), 8.01 (dd, J = 7.7, 1.8 Hz, 2H), 7.53 (t, J = 7.7 Hz, 1H), 7.49 (s, 2H). ^{13}C NMR (100 MHz, DMSO-d_6) δ = 167.41, 134.23, 129.88, 128.06, 126.59.

Synthesis of isophthaloyl diisocyanate (BDI): Isophthalamide (2.0 g, 12.2 mmol, 1 eq) was added to a dried 500 mL flat-bottom flask equipped with an oil bath. The flask was purged several times by alternating high vacuum and argon. 1,2-Dichloroethane (90 mL, dried on 4 Å molecular sieves and filtered through a Whatman 2 µm PTFE syringe filter) was added to the flask. Oxalyl chloride (3.6 mL, 42.0 mmol, 3.4 eq) was added to the mixture, after which the mixture was left to stir at 80 °C for 24 hours. Then, a clear solution was obtained. The temperature was reduced to 60 °C and the solvent was removed in *vacuo* via the Schlenk line with a cold trap in between. The flask was refilled with argon, and the stopper was exchanged for a sublimation cooler. The product was purified via sublimation for between 80-100 °C at high vacuum for 4 hours, forming colorless crystal needles on the sublimation cooler. The flask was evacuated and transferred to a glove-box, in which the flask was opened and the pure product was obtained as colorless crystals (1.6 g, 61%). The product was stored in the glovebox due its extreme water sensitivity. ^{1}H NMR (400 MHz, $CDCl_3$) δ = 8.73 (td, J = 1.7, 0.6 Hz, 1H), 8.34 (dd, J = 7.8, 1.8 Hz, 2H), 7.64 (td, J = 7.8, 0.6 Hz, 2H). ^{13}C NMR (100 MHz, $CDCl_3$) δ = 164.40, 136.21, 132.67, 132.43, 132.09, 129.76.

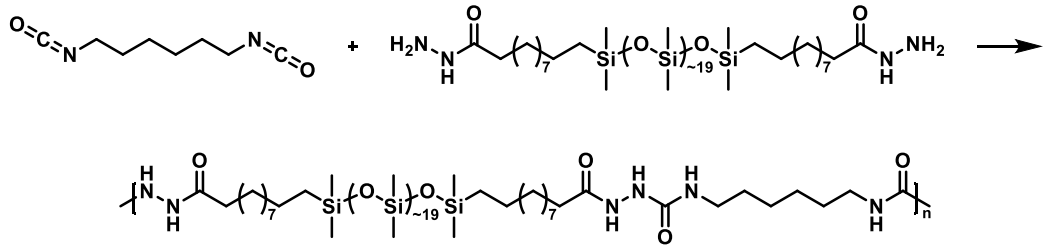

Synthesis of ASC-HDI: Hydrazide terminated pDMS (2.026 g) was dissolved in 15 mL of dry THF in a 100 mL round-bottom flask equipped with an oil bath under argon. The mixture was heated to 50 °C while stirring vigorously. Hexamethylene diisocyanate (HDI, 179 mg, 1.06 mmol) was dissolved in a vial in 5 mL of dry THF and added to the solution. Within 30 minutes, a gel was formed. Part of the solvent was removed in vacuo and the gel was further dried in a vacuum oven at 60 °C overnight after which the product was obtained as a translucent, opaque plastic (2.2 g, quantitative yield). ^{1}H NMR (400 MHz, THF-d_8) δ = 9.54 (m, 1H), 7.75 (m, 1H), 6.36 (m, 1H), 3.18 (m, 4H), 2.17 (m, 4H), 1.60 (m, 4H), 1.32 (m, 36H), 0.70 – 0.45 (m, 4H), 0.33 – -0.16 (m, 108H). Solubility too poor for ^{13}C NMR. SEC (UV detector): M_n: 13.9 kg mol^{-1}, M_w: 24.2 kg mol^{-1}, PDI: 1.7. SEC (RI detector): M_n: 20.9 kg mol^{-1}, M_w: 28.7 kg mol^{-1}, PDI: 1.4.

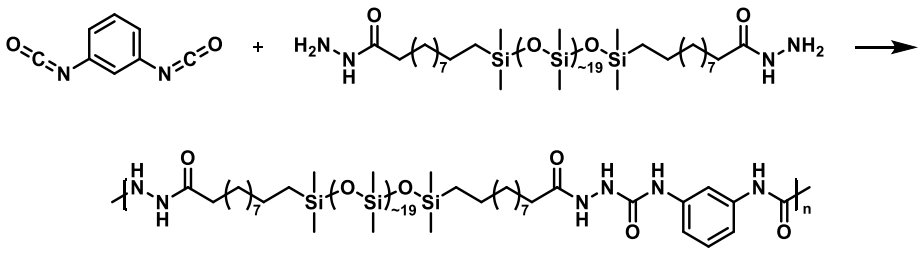

Synthesis of ASC-PDI: Hydrazide terminated pDMS (2.0 g) was dissolved in 20 mL of dry THF in a 100 mL round-bottom flask equipped with an oil bath under argon. The mixture was heated to 50 °C while stirring vigorously. 1,3-Phenylene diisocyanate (PDI, 191 mg, 1.19 mmol) was dissolved in 4 mL of dry THF after which it was added to the solution. Within 60 minutes, a gel was formed. Part of the solvent was removed in vacuo and the gel was further dried in a vacuum oven at 50 °C overnight after which the product was obtained as a slightly yellow, translucent, opaque plastic (2.2 g, quantitative yield). ^{1}H NMR (400 MHz, THF-d_8) δ = 9.48 (s, 1H), 8.46 (s, 1H), 7.86 (s, 1H), 7.00 (m, 3H), 2.17 (m, 4H), 1.59 (m, 4H), 1.49 – 1.10 (m, 29H), 0.58 (t, J = 7.7 Hz, 4H), 0.33 – -0.17 (m, 92H). Solubility too poor for ^{13}C NMR. SEC (UV detector): M_n: 7.7 kg mol^{-1}, M_w: 16.5 kg mol^{-1}, PDI: 2.1. SEC (RI detector): M_n: 7.8 kg mol^{-1}, M_w: 16.5 kg mol^{-1}, PDI: 2.1.

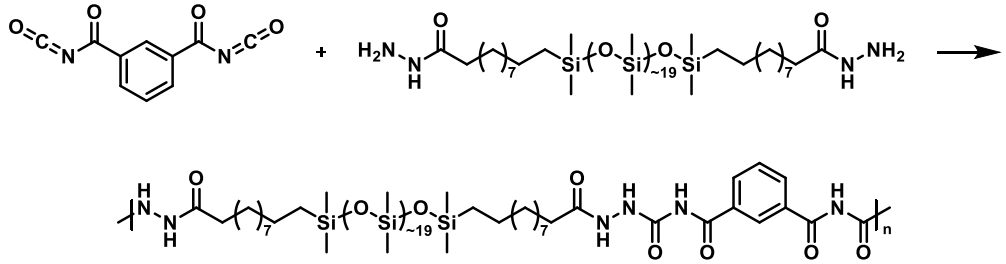

Synthesis of ASC-BDI: Hydrazide terminated pDMS (2.0 g) was dissolved in 10 mL of dry THF in a 50 mL round-bottom flask in a glovebox. The mixture was stirred vigorously. Isophthaloyl diisocyanate (BDI, 272 mg, 1.26 mmol) was dissolved in 5 mL of dry THF after which it was added to the solution. The mixture was left to stir for 1 hour, after which it was precipitated in 150 mL of cold methanol to remove cyclic oligomers. The precipitate was centrifuged, and the isolated solid was dried in a vacuum oven at 50 °C for 4 hours. The

polymer was redissolved in 10 mL of THF and the precipitation procedure was repeated once more. The polymer was dried in a vacuum oven at 50 °C overnight after which the product was obtained as a translucent, opaque plastic (1.6 g, 70%). ^{1}H NMR (400 MHz, THF-d_8) δ = 10.15 (s, 3H), 9.23 (s, 2H), 8.58 (s, 1H), 8.19 (d, J = 7.8 Hz, 2H), 7.65 (t, J = 7.8 Hz, 1H), 2.31 – 2.06 (m, 4H), 1.63 (m, 4H), 1.33 (m, 28H), 0.68 – 0.46 (m, 4H), 0.30 – -0.13 (m, 97H). Solubility too poor for ^{13}C NMR. SEC (UV detector): M_n: 13.5 kg mol^{-1}, M_w: 31.3 kg mol^{-1}, PDI: 2.3. SEC (RI detector): M_n: 15.9 kg mol^{-1}, M_w: 31.7 kg mol^{-1}, PDI: 2.0.

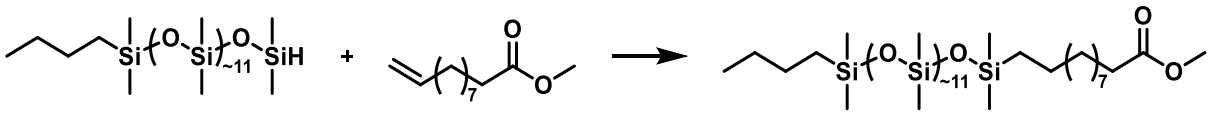

Synthesis of monofunctional methyl ester-terminated pDMS: Polydimethylsiloxane, monohydride terminated, viscosity 5-9 cSt (10.0 g, 1 eq) was combined with methyl undec-10-enoate (2.35 g, 11.9 mmol, ~1.4 eq) in bulk in a dried 50 mL round-bottom flask under argon atmosphere. The mixture was cooled with a room-temperature water bath, and Karstedt's catalyst (2 wt% in xylene) was added (3-4 drops), after which the mixture was left to stir for 24 hours. The bulk mixture was transferred to a separatory funnel and extracted with 3x 25 mL of acetonitrile to remove excess methyl undec-10-enoate. After this, the polymer oil was dissolved in 30 mL of DCM and filtered over a plug of activated charcoal in a glass filter to remove the platinum catalyst. The charcoal plug was washed with 3x 15 mL of DCM. The solvent was removed in *vacuo* after which the product was obtained as a colorless oil (10.4 g, 89%). ^{1}H NMR (400 MHz, $CDCl_3$) δ = 3.66 (s, 3H), 2.30 (t, J = 7.5 Hz, 2H), 1.61 (p, J = 7.2 Hz, 2H), 1.29 (m, 19H), 0.93 – 0.84 (t, 3H), 0.60 – 0.46 (m, 4H), 0.25 – -0.16 (m, 78H). ^{13}C NMR (100 MHz, $CDCl_3$) δ = 174.45, 51.54, 34.27, 33.62, 29.71, 29.66, 29.54, 29.44, 29.34, 26.53, 25.62, 25.14, 23.39, 18.43, 18.12, 13.96, 1.32, 1.20, 0.34, 0.32. SEC (RI detector): M_n: 1.3 kg mol^{-1}, M_w: 1.5 kg mol^{-1}, PDI: 1.1.

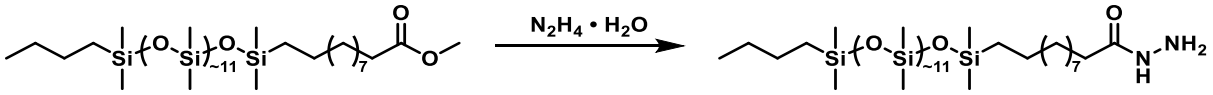

Synthesis of monofunctional acyl hydrazide terminated pDMS: Monofunctional methyl ester-terminated pDMS (10.0 g) was dissolved in 10 mL of isopropanol in a 50 mL round-bottom flask equipped with an oil bath and reflux cooler. Hydrazine monohydrate (4.0 g, 79.9 mmol) was added to the solution, after which the mixture was left to stir at 50 °C for 24 hours. The isopropanol was removed in *vacuo*, and the mixture was dissolved in 100 mL of DCM. The mixture was transferred to a separatory funnel and extracted with 3x 100 mL of demineralized water to remove excess hydrazine. After this, the DCM layer was dried over Na_2SO_4, filtered using gravity and the filter washed with 50 mL of DCM. The solvent was removed in *vacuo* after which the product was obtained as a colorless viscous oil (9.0 g, 90%). ^{1}H NMR (400 MHz, $CDCl_3$) δ = 6.64 (s, 1H), 3.88 (s, 2H), 2.20 – 2.08 (m, 2H), 1.63 (p, J = 7.3 Hz, 2H), 1.29 (m, 18H), 0.93 – 0.83 (m, 3H), 0.59 – 0.45 (m, 4H), 0.25 – -0.16 (m, 81H). ^{13}C NMR (100 MHz, $CDCl_3$) δ = 174.21, 34.73, 33.63, 33.60, 29.70, 29.67, 29.52, 29.47, 29.45, 26.50, 25.66, 25.59, 23.37, 18.41, 18.09, 13.94. SEC (UV detector): M_n: 1.7 kg mol^{-1}, M_w: 2.2 kg mol^{-1}, PDI: 1.3. SEC (RI detector): M_n: 1.3 kg mol^{-1}, M_w: 1.6 kg mol^{-1}, PDI: 1.3.

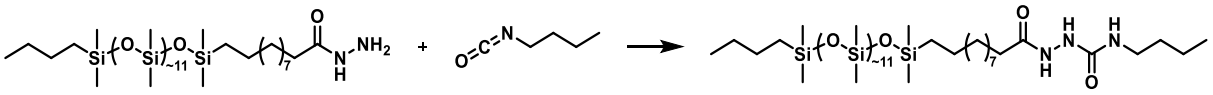

Synthesis of MonoASC with butyl isocyanate (H-monoASC): Monofunctional hydrazide-terminated pDMS (1.0 g, 1 eq) was dissolved in 10 mL of dry THF in a 50 mL round-bottom flask equipped with an oil bath and reflux cooler. Phenyl isocyanate (0.164 mL, 1.48 mmol, 2

eq) was added to the solution, after which the mixture was left to stir for 24 hours. Ammonium hydroxide (1 mL, 25% in water) was added to the mixture to quench excess isocyanate. Then, 50 mL of chloroform and 50 mL of demineralized water were added to the mixture, which was transferred to a separatory funnel and extracted with 3x 50 mL of demineralized water. After this, the organic layer was dried over Na_2SO_4, filtered using gravity and the solvent was removed in *vacuo*. The product was further purified using flash column chromatography (liquid injection from DCM), with an eluent system of 10 column volumes of 100% DCM, followed by 20% acetone in DCM. The product fractions were combined and the solvent was removed in *vacuo* after which the product was obtained as colorless waxy solid (603 mg, 56%). ^{1}H NMR (400 MHz, $CDCl_3$) δ = 8.28 (s, 1H), 7.65 (s, 1H), 5.63 (s, 1H), 3.18 (q, J = 6.6 Hz, 2H), 2.23 (t, J = 7.7 Hz, 2H), 1.64 (m, 2H), 1.54 – 1.41 (m, 2H), 1.41 – 1.17 (m, 20H), 1.02 – 0.78 (m, 6H), 0.61 – 0.42 (m, 4H), 0.26 – -0.18 (m, 73H). ^{13}C NMR (100 MHz, $CDCl_3$) δ = 172.99, 158.21, 40.05, 34.29, 33.65, 32.23, 29.78, 29.72, 29.58, 29.54, 29.47, 26.51, 25.59, 25.57, 23.40, 20.11, 18.43, 18.10, 13.95, 13.89, 1.31, 1.20, 0.32. SEC (UV detector): M_n: 1.4 kg mol^{-1}, M_w: 1.5 kg mol^{-1}, PDI: 1.1. SEC (RI detector): M_n: 1.2 kg mol^{-1}, M_w: 1.4 kg mol^{-1}, PDI: 1.1.

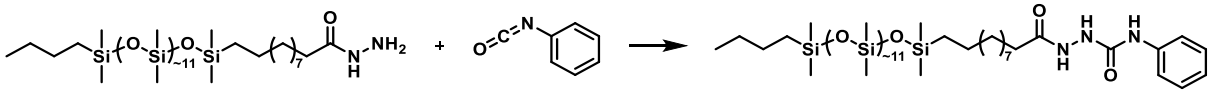

Synthesis of MonoASC with phenyl isocyanate (P-monoASC): Monofunctional hydrazide-terminated pDMS (1.0 g, 1 eq) was dissolved in 10 mL of dry THF in a 50 mL round-bottom flask equipped with an oil bath and reflux cooler. Phenyl isocyanate (0.161 mL, 1.48 mmol, 2 eq) was added to the solution, after which the mixture was left to stir for 24 hours. Ammonium hydroxide (1 mL, 25% in water) was added to the mixture to quench excess isocyanate. 50 mL of chloroform and 50 mL of demineralized water were added to the mixture. Then, the mixture was transferred to a separatory funnel and extracted with 3x 50 mL of demineralized water. After this, the organic layer was dried over Na_2SO_4, filtered using gravity and the solvent was removed in *vacuo*. The product was further purified using flash column chromatography (liquid injection from DCM), with an eluent system of 10 column volumes of 100% DCM, followed by 5% acetone in DCM. The product fractions were combined and the solvent was removed in *vacuo* after which the product was obtained as colorless waxy solid (631 mg, 58%). ^{1}H NMR (400 MHz, $CDCl_3$) δ = 8.78 (s, 1H), 8.24 (s, 1H), 8.17 (s, 1H), 7.28 (d, J = 7.6 Hz, 3H), 7.19 (t, J = 7.7 Hz, 2H), 6.98 (t, J = 7.4 Hz, 1H), 2.26 (t, J = 7.7 Hz, 2H), 1.69 – 1.52 (m, 2H), 1.43 – 1.12 (m, 18H), 0.97 – 0.81 (m, 3H), 0.53 (m, 4H), 0.26 – -0.17 (m, 81H). ^{13}C NMR (100 MHz, $CDCl_3$) δ = 173.98, 155.67, 138.26, 129.03, 123.43, 119.52, 34.23, 33.67, 29.79, 29.70, 29.58, 29.50, 29.45, 26.51, 25.59, 25.49, 23.41, 18.44, 18.10, 13.95, 1.32, 1.20, 0.33. SEC (UV detector): M_n: 1.4 kg mol^{-1}, M_w: 1.6 kg mol^{-1}, PDI: 1.1. SEC (RI detector): M_n: 1.4 kg mol^{-1}, M_w: 1.5 kg mol^{-1}, PDI: 1.1.

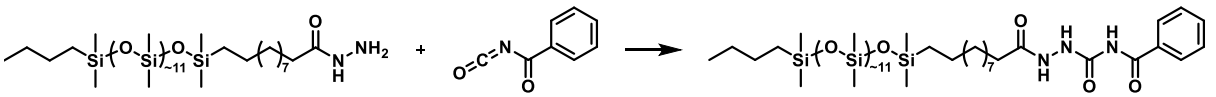

Synthesis of MonoASC with benzoyl isocyanate (B-monoASC): Monofunctional hydrazide-terminated pDMS (0.5 g, 1 eq) was dissolved in 10 mL of dry THF in a 50 mL round-bottom flask equipped with an oil bath and reflux cooler. Benzoyl isocyanate (65 mg, 0.44 mmol, 1.2 eq) was added to the solution, after which the mixture was left to stir for 24 hours. Then, 50 mL of chloroform and 50 mL of demineralized water were added to the mixture, which was transferred to a separatory funnel and extracted with 3x 50 mL of demineralized water. After this, the organic layer was dried over Na_2SO_4, filtered using gravity and the solvent was removed in *vacuo*. The product was further purified using flash column chromatography (liquid injection from DCM), with an eluent system of 15 column volumes of 100% DCM, followed by

5% acetone in DCM. The product fractions were combined and the solvent was removed in *vacuo* after which the product was obtained as colorless waxy solid (366 mg, 66%). ^{1}H NMR (400 MHz, $CDCl_3$) δ = 10.33 (d, J = 3.1 Hz, 1H), 8.85 (s, 1H), 7.87 (d, J = 7.1 Hz, 2H), 7.61 (t, J = 7.4 Hz, 1H), 7.56 (s, 1H), 7.49 (t, J = 7.7 Hz, 2H), 2.28 (t, J = 7.6 Hz, 2H), 1.69 (p, J = 7.6 Hz, 2H), 1.43 – 1.15 (m, 18H), 0.95 – 0.82 (m, 3H), 0.61 – 0.44 (m, 4H), 0.25 – -0.17 (m, 77H). ^{13}C NMR (100 MHz, $CDCl_3$) δ = 171.71, 167.52, 153.62, 133.61, 129.14, 127.88, 34.38, 33.63, 29.75, 29.68, 29.55, 29.50, 29.42, 26.50, 25.59, 25.47, 23.39, 18.42, 18.09, 13.95, 1.32, 1.20, 0.33. SEC (UV detector): M_n: 1.5 kg mol^{-1}, M_w: 1.6 kg mol^{-1}, PDI: 1.1. SEC (RI detector): M_n: 1.4 kg mol^{-1}, M_w: 1.6 kg mol^{-1}, PDI: 1.1.

2. Crystal structures of ASC model compounds

2.1 PhASCPh

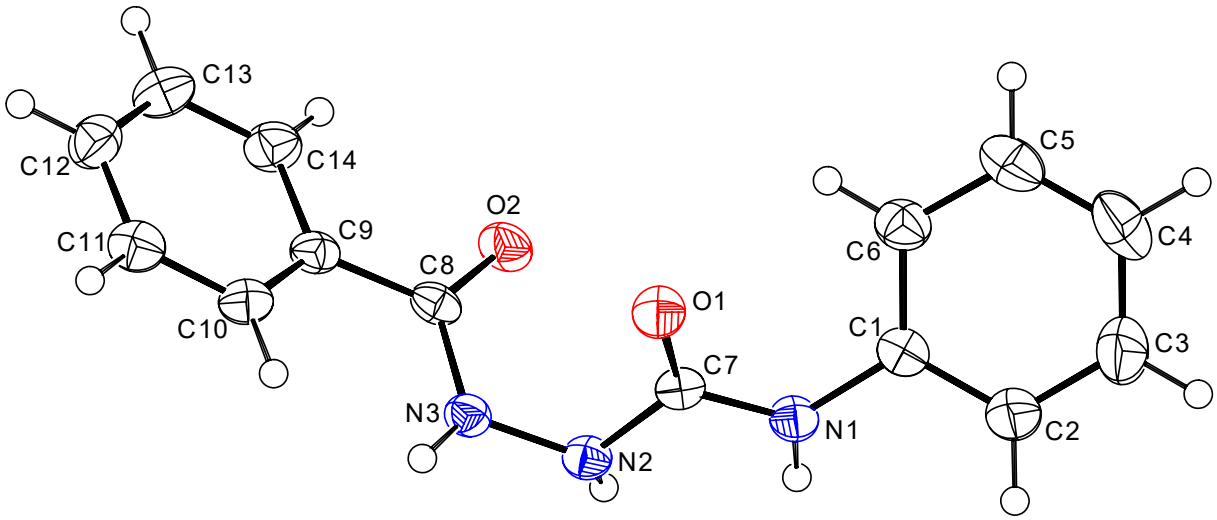

Figure S1: Molecular structure of PhASCPh in the crystal. Displacement ellipsoids are drawn at the 50% probability level, hydrogen atoms with arbitrary radii.

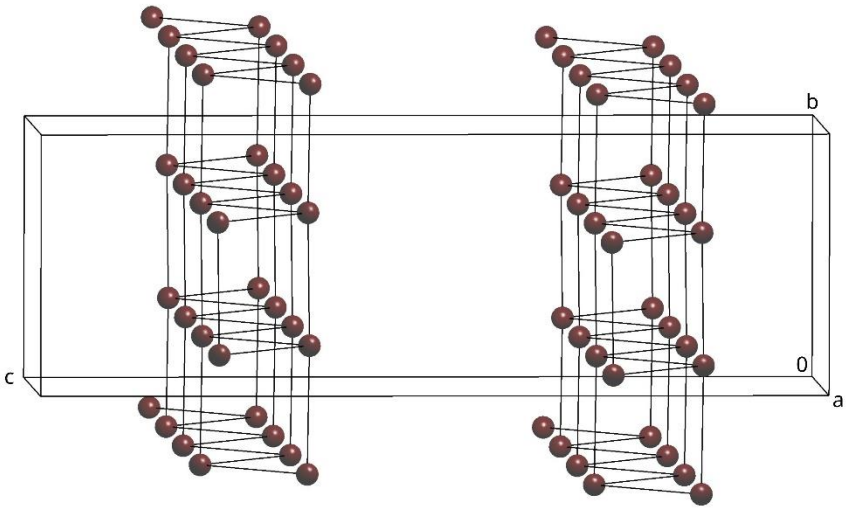

Figure S2: Topology of the hydrogen bonding network in the crystal structure of PhASCPh. Molecules are simplified to spheres (nodes). The connecting lines represent N-H…O hydrogen bonds. The hydrogen bonded two-dimensional sheets are oriented parallel to the

crystallographic a,b-plane. The simplification and the drawing were created with the ToposPro software[6].

Table S1: Selected torsion angles [°] in the crystal structure of PhASCPh.

C2-C1-N1-C7	151.63(16)	C7-N2-N3-C8	61.83(18)
C1-N1-C7-N2	171.06(13)	N2-N3-C8-C9	-169.31(13)
N1-C7-N2-N3	-167.70(13)	N3-C8-C9-C10	11.9(2)

Table S2: Hydrogen bonding geometries in the crystal structure of PhASCPh.

	D-H [Å]	H...A [Å]	D....A [Å]	D-H...A [°]
N1-H1N...O1^{i}	0.87(2)	1.97(2)	2.7919(17)	158.1(16)
N2-H2N...O1^{i}	0.878(19)	2.190(18)	2.9480(18)	144.4(14)
N3-H3N...O2^{ii}	0.886(18)	1.965(19)	2.8361(17)	167.5(16)

Symmetry codes *i*: ½-x, y+½, z; *ii*: x-½, y, ½-z.

2.2 PhASCBz

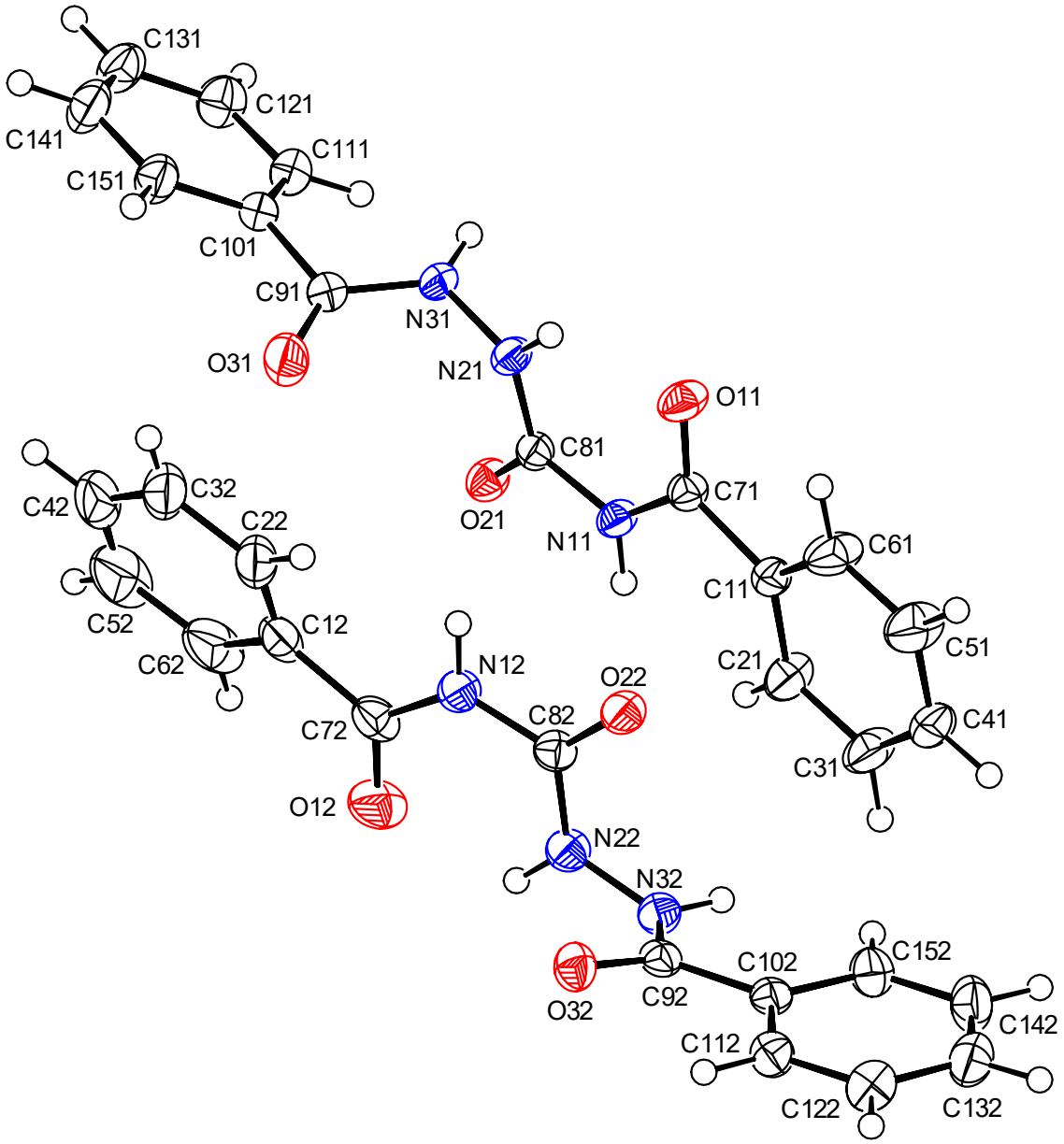

Figure S3: Two independent molecules of PhASCBz in the asymmetric unit of the crystal structure. Projection along the crystallographic c-axis. Displacement ellipsoids are drawn at the 50% probability level, hydrogen atoms with arbitrary radii.

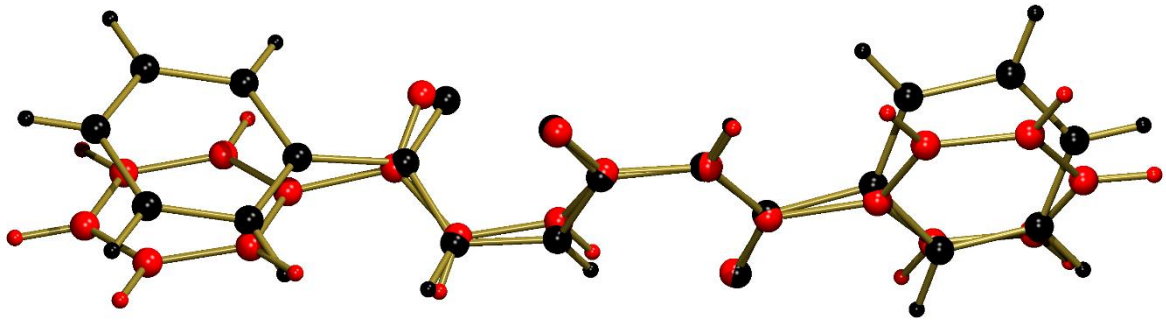

Figure S4: Overlay of the two independent molecules in the crystal structure of PhASCBz.

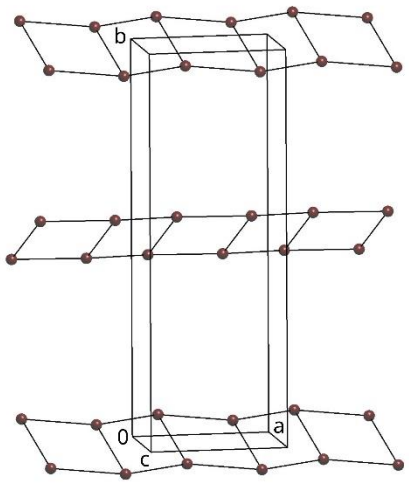

Figure S5: Topology of the hydrogen bonding network in the crystal structure of PhASCBz. Molecules are simplified to spheres (nodes). The connecting lines represent N-H…O hydrogen bonds. The hydrogen bonded one-dimensional chains are running along the crystallographic a-axis. The two independent molecules take part in the same chain. The simplification and the drawing were created with the ToposPro software[6].

Table S3: Selected torsion angles [°] in the two independent molecules in the crystal structure of PhASCBz.

	x = 1	x = 2
C2x-C1x-C7x-N1x	5.65(19)	-20.1(2)
C1x-C7x-N1x-C8x	-178.61(11)	178.17(12)
C7x-N1x-C8x-N2x	-9.51(18)	-1.9(2)
N1x-C8x-N2x-N3x	173.53(10)	-175.06(11)
C8x-N2x-N3x-C9x	85.95(15)	68.96(15)
N2x-N3x-C9x-C10x	-175.04(11)	-162.43(10)
N3x-C9x-C10x-C11x	32.08(18)	-172.40(11)

Table S4: Hydrogen bonding geometries in the crystal structure of PhASCBz.

	D-H [Å]	H...A [Å]	D....A [Å]	D-H...A [°]
N11-H11N...O22	0.902(17)	2.008(17)	2.9010(14)	170.6(14)
N21-H21N...O11	0.858(18)	1.973(17)	2.6174(14)	131.1(15)
N31-H31N...O32^{i}	0.881(17)	1.985(17)	2.8373(15)	162.3(15)
N12-H12N...O21	0.908(18)	1.937(18)	2.8325(14)	168.6(15)
N22-H22N...O12	0.903(18)	2.023(17)	2.6570(15)	126.1(14)
N32-H32N...O21^{ii}	0.901(18)	2.044(18)	2.8922(15)	156.3(15)

Symmetry codes *i*: x+1, y, z, z; *ii*: 1-x, 1-y, -z.

CCDC 2377270 and 2377271 contain the supplementary crystallographic data for this paper. These data can be obtained free of charge from The Cambridge Crystallographic Data Centre via www.ccdc.cam.ac.uk/data_request/cif.

3. NMR kinetics experiments

Dissociation kinetics of ASC model compounds were measured by first making a 50 mM stock solution of benzylamine in DMSO-d_6 with added dimethyl sulfone ($DMSO_2$) as internal standard. This stock solution was added to the model compounds to a concentration of 50 mM, making a 1:1 ratio of model compound to benzylamine. Subsequently, 0.6 mL of the mixture was transferred to an NMR tube and submerged in an oil bath at the desired temperature. At certain time intervals, an NMR tube was quenched in ice water. Then, a ^{1}H NMR spectrum was recorded and the same sample was used for the next time interval. Dissociation rates were determined by setting the integral of $DMSO_2$ to 100, and following the decrease in intensity of an ASC model compound peak over time. The peaks used for integration is mentioned below the respective model compound in Table S5. As the system follows pseudo first-order kinetics, k_d was determined from the slope of $\ln\left(\frac{c}{c_0}\right)$ as a function of time (eqn(S1)). The activation energy, E_{act}, was determined from the slope of k_d as a function of inverse temperature (eqn(S2)).

$$\ln\left(\frac{c}{c_0}\right) = -k_d t \tag{S1}$$

$$k_d = Ae^{-\frac{E_{act}}{RT}} \tag{S2}$$

Table S5: Model compound kinetics data. Chemical shift δ of the peak tracked to follow conversion is indicated below the corresponding ASC model compound (in ppm).

Model compound	Temperature (°C)	Time (min)	Peak signal ($DMSO_2$ = 100)	ln(c/c$_0$) (-)	k_d (min^{-1})	E_{act} (kJ mol^{-1})
MeASCPh	130	0	46.01	0	0.0179	112 ± 7
δ = 1.87		10	38.41	0.181		
		20	32.04	0.362		
		30	26.9	0.537		
		40	22.59	0.711		
	120	0	53.68	0	0.00962	
		15	46.34	0.147		
		30	39.92	0.296		
		45	34.76	0.435		
		60	30.32	0.571		
	110	0	46.61	0	0.00364	
		15	44.15	0.0542		
		30	41.86	0.107		
		45	39.49	0.166		
		60	37.48	0.218		
	100	0	46.4	0	0.00127	
		30	44.47	0.0425		
		60	43.24	0.0705		
		90	41.29	0.117		
		120	39.83	0.153		
BuASCPh	130	0	28.35	0	0.0223	112 ± 6
δ = 2.12		10	22.64	0.225		
		20	17.91	0.459		
		30	14.45	0.674		
		40	11.74	0.882		

	120	0	33.18	0	0.0117	
		15	27.71	0.180		
		30	23.09	0.363		
		45	19.53	0.530		
		60	16.54	0.696		
	110	0	28.18	0	0.00451	
		15	26.48	0.0622		
		30	24.76	0.129		
		45	22.95	0.205		
		60	21.45	0.272		
	100	0	28.49	0	0.00164	
		30	27.14	0.0485		
		60	25.87	0.0965		
		90	24.54	0.149		
		120	23.39	0.197		
BnASCPh	130	0	31.88	0	0.0274	108 ± 6
δ = 3.49		10	24.23	0.274		
		20	18.26	0.557		
		30	13.97	0.825		
		40	10.76	1.086		
	120	0	36.48	0	0.0148	
		15	29.17	0.224		
		30	23.13	0.456		
		45	18.75	0.666		
		60	15.13	0.880		
	110	0	31.93	0	0.00579	
		15	29.39	0.0829		
		30	27.12	0.163		
		45	24.71	0.256		
		60	22.35	0.357		
	100	0	36.49	0	0.00211	
		30	34.41	0.0587		
		60	31.89	0.135		
		90	30.3	0.186		
		120	28.35	0.252		
PhASCPh	130	0	31.22	0	0.0305	113 ± 8
δ = 7.93		10	22.43	0.331		
		20	16.42	0.643		
		30	12.32	0.930		
		40	9.55	1.185		
	120	0	36.5	0	0.0167	
		15	28.04	0.264		
		30	21.45	0.532		
		45	17.05	0.761		
		60	13.76	0.976		
	110	0	31.52	0	0.00634	
		15	28.24	0.110		
		30	25.93	0.195		
		45	23.71	0.285		
		60	21.67	0.375		
	100	0	30.99	0	0.00208	
		30	29.1	0.0629		
		60	27.55	0.118		

		90	25.69	0.188		
		120	24.07	0.253		
t-BuASCPh	130	0	58.69	0	0.0628	120 ± 7
δ = 1.16		5	40.93	0.360406		
		10	29.11	0.701188		
		15	22.28	0.96858		
		20	17.87	1.189146		
	120	0	58.86	0	0.023	
		15	40.79	0.366725		
		30	29.01	0.707521		
		45	20.28	1.065527		
		60	15.44	1.3382		
	110	0	57.64	0	0.011	
		15	48.63	0.169976		
		30	41.14	0.337236		
		45	34.94	0.500584		
		60	29.91	0.656024		
	100	0	57.74	0	0.0033	
		30	52.77	0.090007		
		60	47.35	0.198383		
		90	42.84	0.298478		
		120	39.16	0.388294		
PhASCBu	140	0	29.97	0	0.00707	139 ± 9
δ = 7.89		10	27.93	0.0705		
		20	25.74	0.152		
		30	24.26	0.211		
		40	22.69	0.278		
	130	0	34	0	0.00270	
		15	32.79	0.0362		
		30	31.26	0.0840		
		45	30.11	0.122		
		60	28.94	0.161		
	120	0	32.7	0	0.00114	
		60	30.12	0.0822		
		120	28.31	0.144		
		180	26.54	0.209		
		240	25.12	0.264		
	110	0	35.36	0	0.000279	
		60	34.72	0.0183		
		120	34.21	0.0331		
		180	33.51	0.0537		
		240	33.17	0.0639		
PhASCBn	140	0	32.14	0	0.00700	139 ± 2
δ = 7.91		10	29.9	0.0722		
		20	27.78	0.146		
		30	26.06	0.210		
		40	24.37	0.277		
	130	0	37.11	0	0.00250	
		15	35.65	0.0401		
		30	34.31	0.0785		
		45	33.17	0.112		

		60	32	0.148		
	120	0	31.91	0	0.000847	
		30	31.07	0.0267		
		60	30.25	0.0534		
		90	29.54	0.0772		
		120	28.89	0.0994		
	110	0	37	0	0.000299	
		60	36.34	0.0180		
		120	35.67	0.0366		
		180	35.04	0.0544		
		240	34.46	0.0711		
PhASCBz	100	0	33.47	0	0.0200	127 ± 1
δ = 7.92		10	27.52	0.196		
		20	22.59	0.393		
		30	18.54	0.591		
		40	14.83	0.814		
	90	0	32.3	0	0.00676	
		15	29.11	0.104		
		30	25.97	0.218		
		45	23.82	0.305		
		60	21.72	0.397		
	80	0	33.65	0	0.00207	
		15	32.5	0.0348		
		30	31.56	0.0641		
		45	30.61	0.0947		
		60	29.83	0.120		
	70	0	32.18	0	0.000566	
		30	31.77	0.0128		
		60	31.16	0.0322		
		90	30.55	0.0520		
		120	30.03	0.0691		

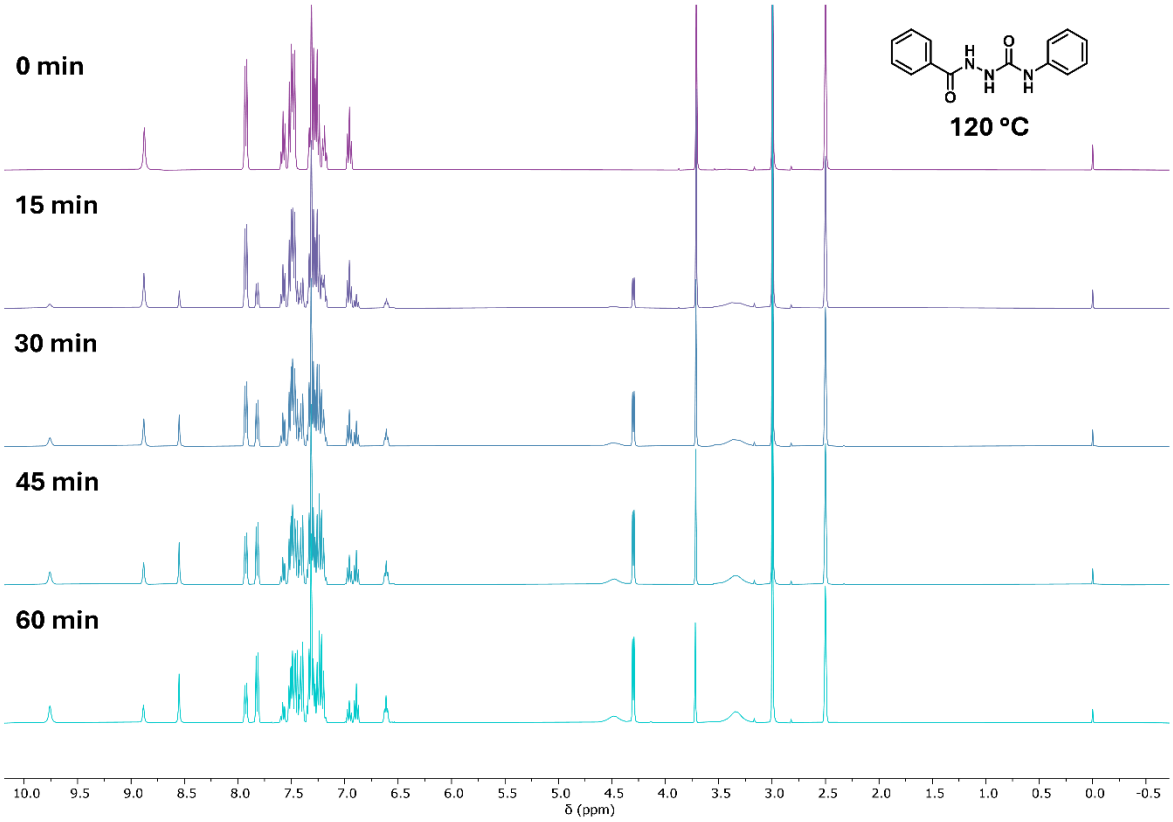

Figure S6: Example ^{1}H NMR spectra in DMSO-d_6 of PhASCPh during kinetic experiment at 120 °C.

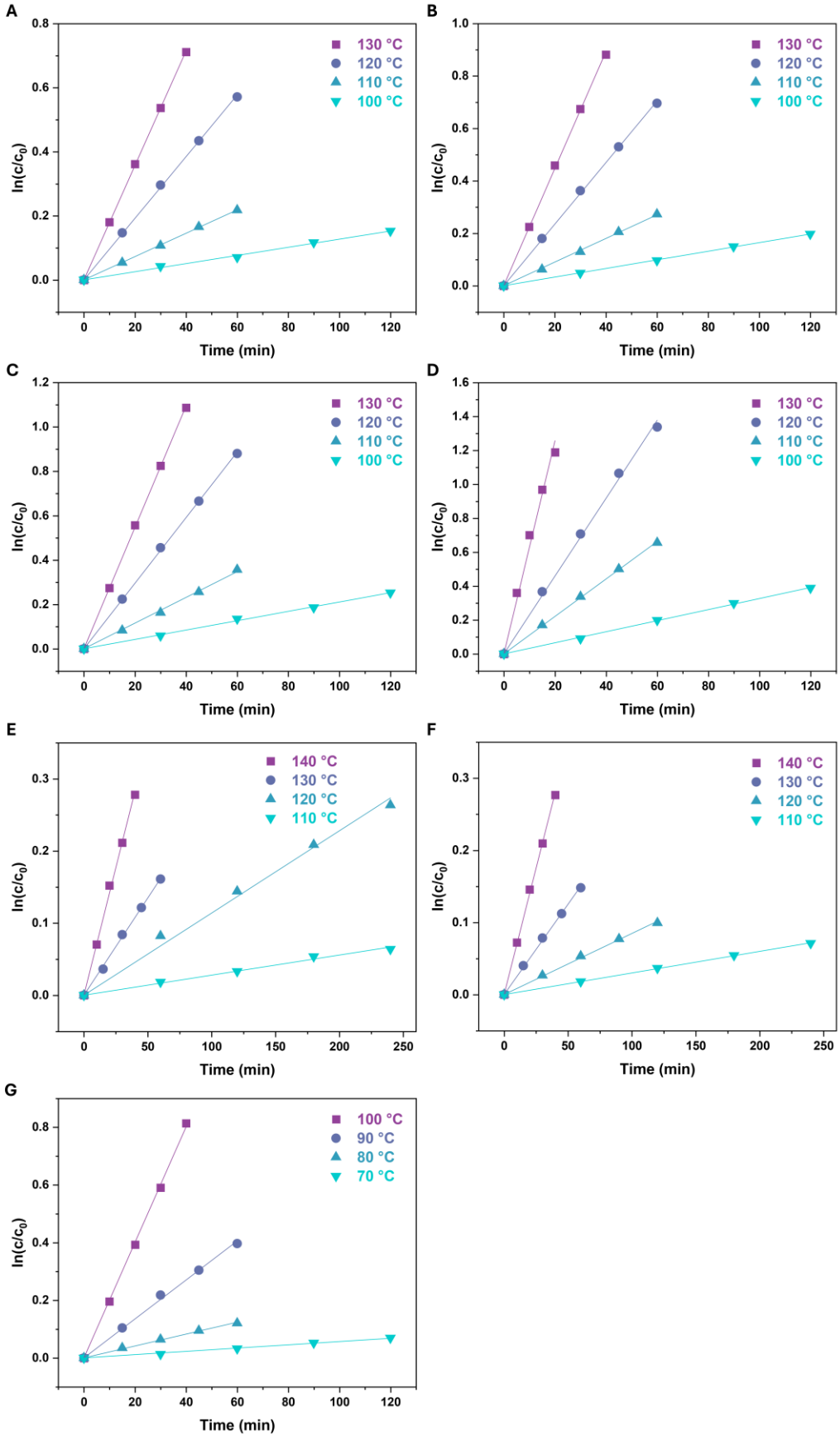

Figure S7: Kinetic measurements of model ASC at various temperatures. A) MeASCPh, B) BuASCPh, C) BnASCPh, D) *t*-BuASCPh, E) PhASCBu, F) PhASCBn and G) PhASCBz. The lines represent linear fits through the origin of the corresponding data points.

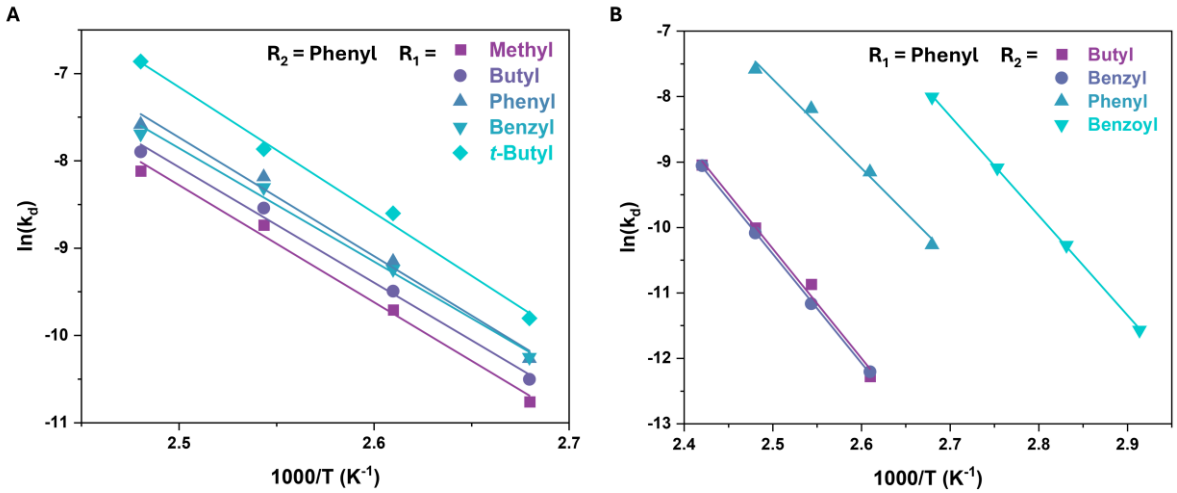

Figure S8: Arrhenius plots of ASCs with various hydrazide (A) and isocyanate (B) substituents. The lines represent linear fits of the corresponding data points.

4. Supporting figures

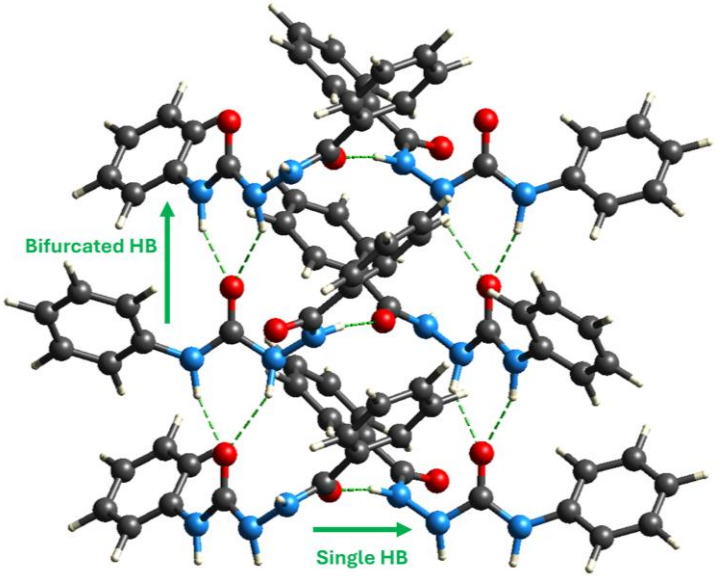

Figure S9: Crystal structure of PhASCPh. Hydrogen bonds visualized in green using the CrystalExplorer[7] software.

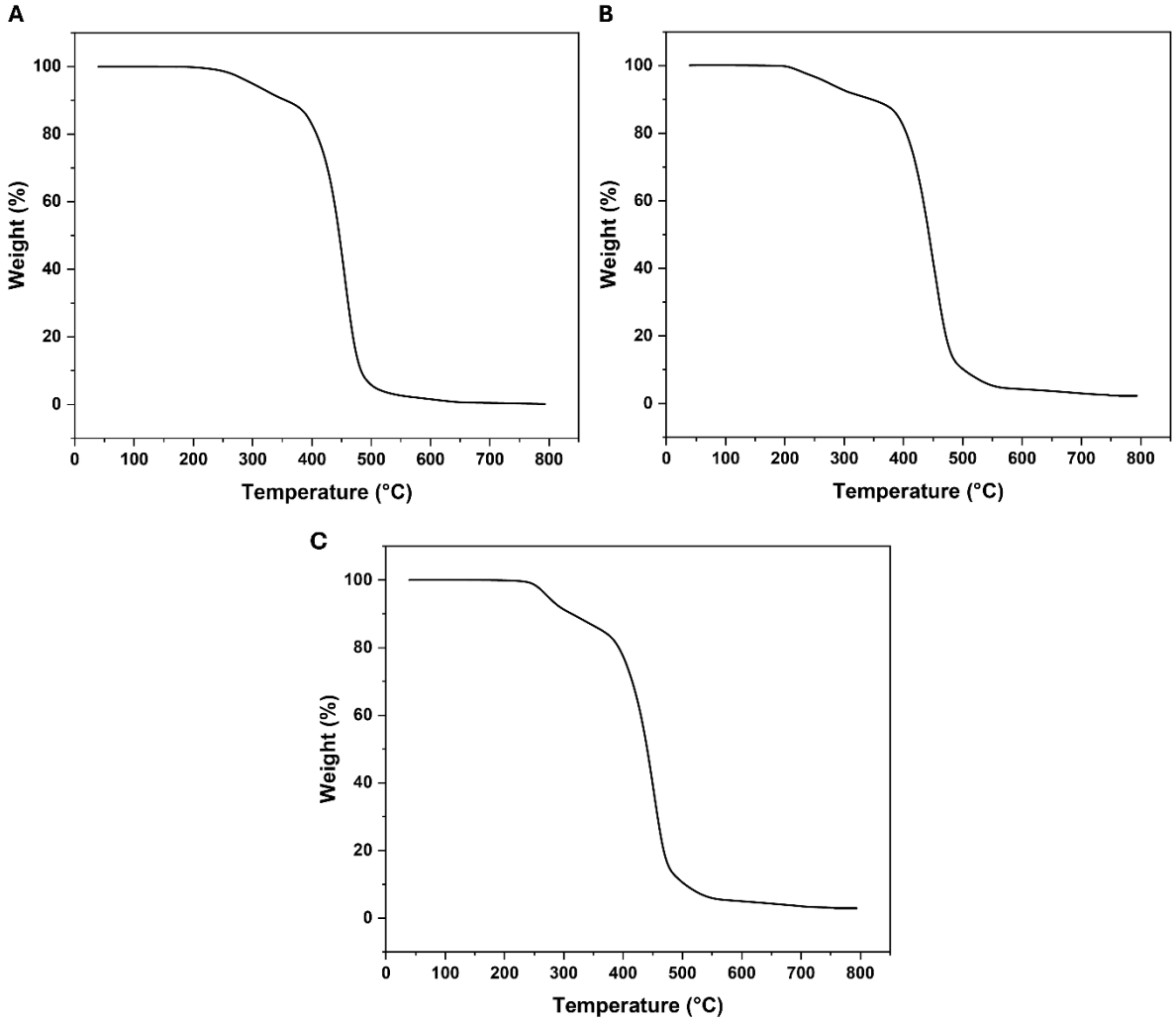

Figure S10: TGA curves of ASC-HDI (A), ASC-PDI (B) and ASC-BDI (C). Heating rate is 10 °C min^{-1}.

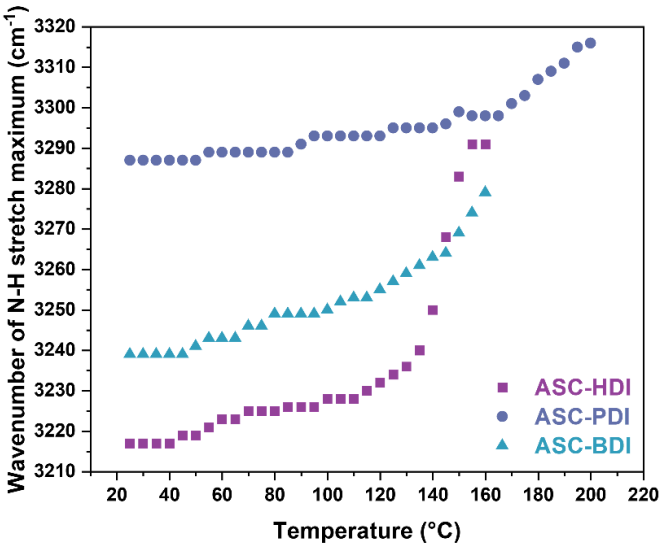

Figure S11: Wavenumbers of N-H stretch maximum of pDMS-ASC materials as a function of temperature.

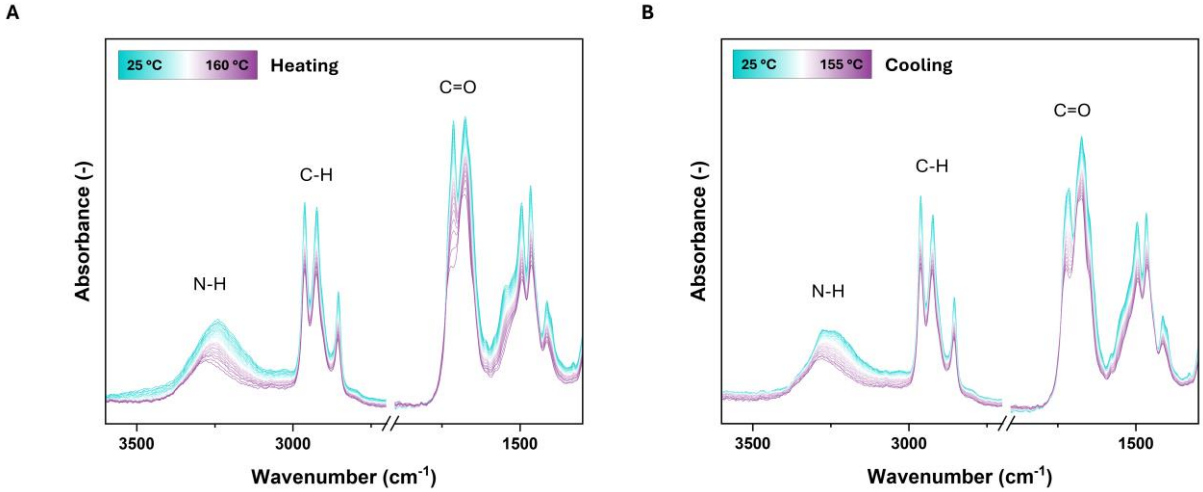

Figure S12: Variable temperature infrared spectroscopy spectrum of ASC-BDI during first heating (A) and first cooling (B) with intervals of 5 °C.

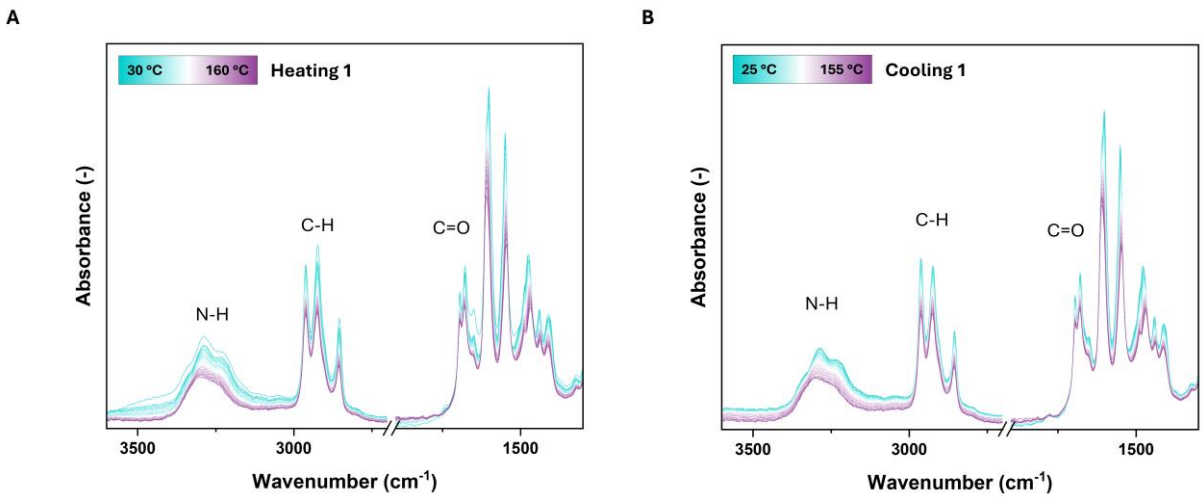

Figure S13: Variable temperature infrared spectroscopy spectrum of ASC-PDI up to 160 °C during first heating (A) and first cooling (B) with intervals of 5 °C.

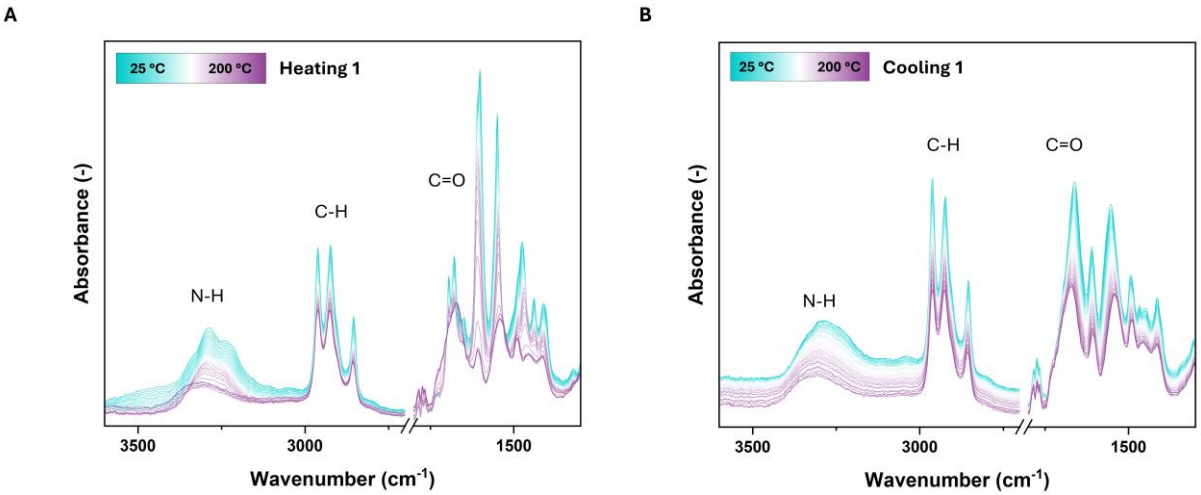

Figure S14: Variable temperature infrared spectroscopy spectrum of ASC-PDI up to 200 °C during first heating (A) and first cooling (B) with intervals of 5 °C.

Detailed analysis of VTIR of ASC-HDI

Before heating, ASC-HDI shows two well-defined N-H stretch peaks at 3217 and 3344 cm^{-1}, C=O stretches at 1656 and 1588 cm^{-1}, and an N-H bending peak at 1549 cm^{-1} (Figure S14). Upon heating, the N-H stretches broaden and eventually fuse into one feature. The carbonyl peaks shift to higher wavenumbers at elevated temperatures and the relative intensities of the peaks change drastically. Upon cooling, all shifted peaks return to their values before heating, but there are significant differences in intensity remaining. The intensity differences before and after heating suggest that kinetic trapping of the material takes place during compression molding. The unchanged peak positions, however, suggest that the trapped state is very similar to the thermodynamically stable state. To check whether the morphology was stable after heating once, a second VTIR heating run was performed (Figure S14C and D). This run showed similar behavior to the first run, with now only minor intensity differences before and after heating.

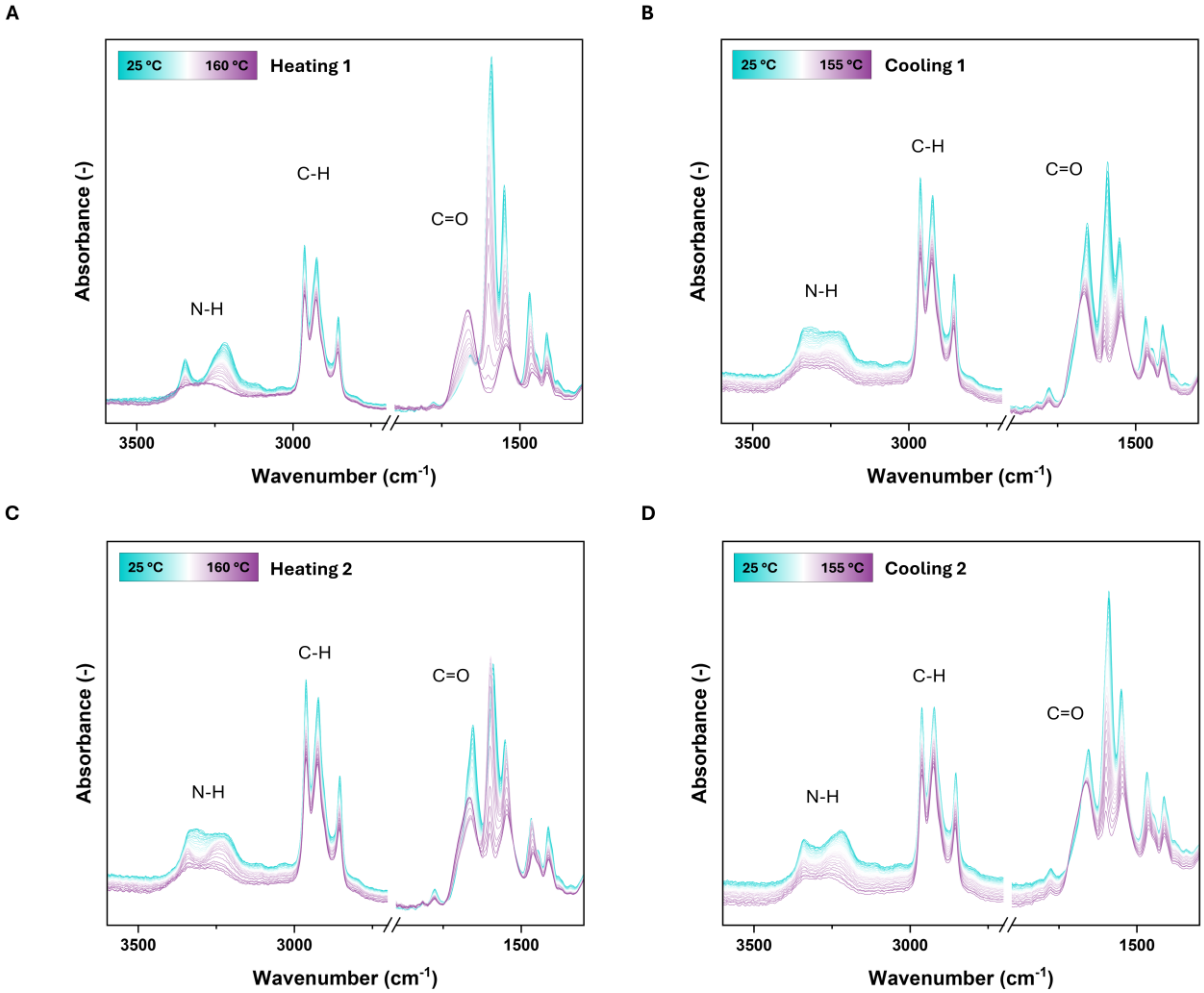

Figure S15: Variable temperature infrared spectroscopy spectrum of ASC-HDI during first heating (A), first cooling (B), second heating (C) and second cooling (D) with intervals of 5 °C.

To test the stability of the hydrogen bonding patterns of the pDMS-ASC materials, isothermal IR spectra were taken at 140 °C (Figure S15). Here, for ASC-HDI there is some gradual change in the N-H and C=O stretch regions over a duration of 4 hours, indicating some change in hydrogen-bonding patterns. The other pDMS-ASC materials showed little to no change in hydrogen-bonding patterns during this time period.

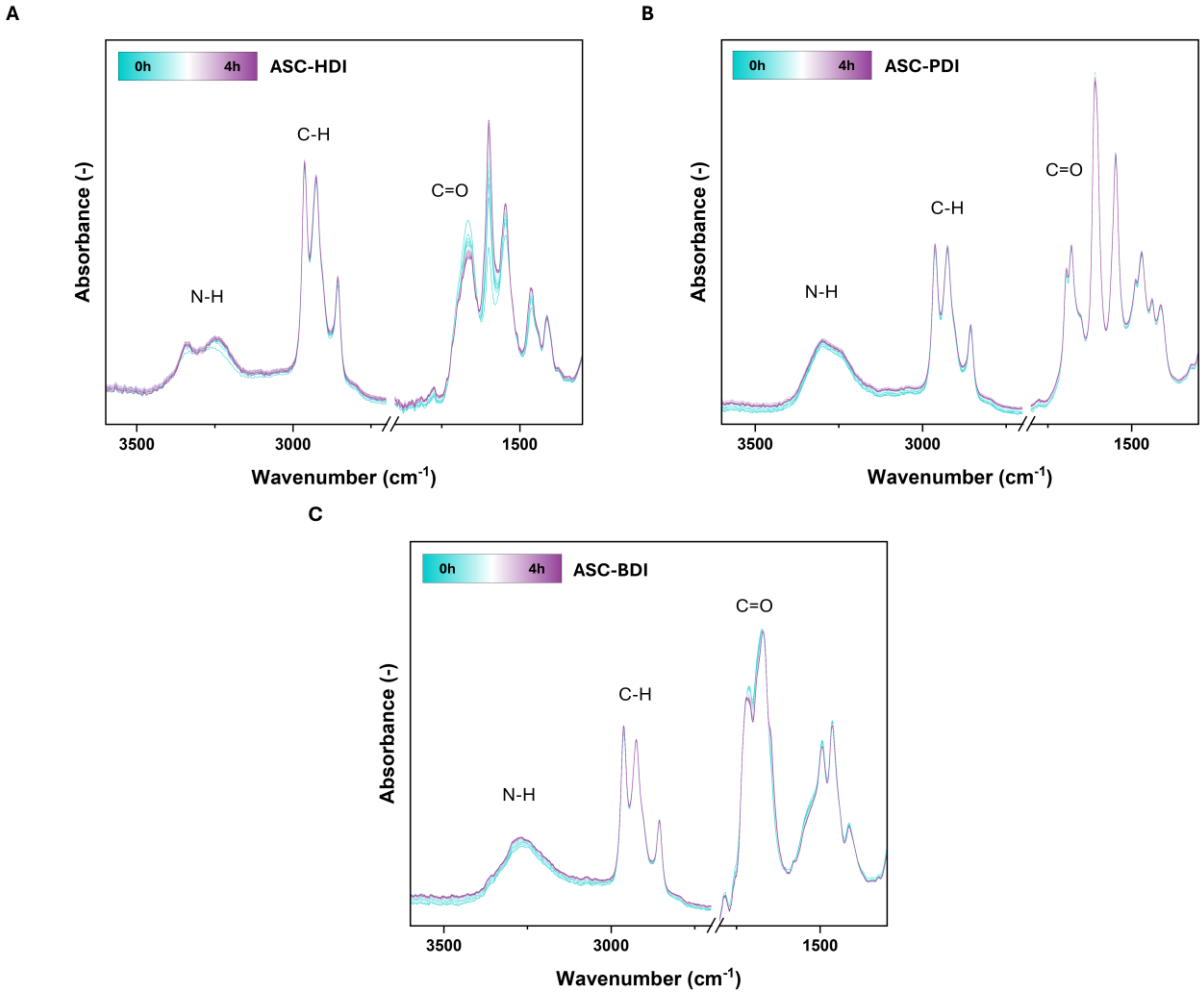

Figure S16: Isothermal IR spectra of ASC-HDI (A), ASC-PDI (B) and ASC-BDI (C) at 140 °C for 4 hours with intervals of 10 minutes.

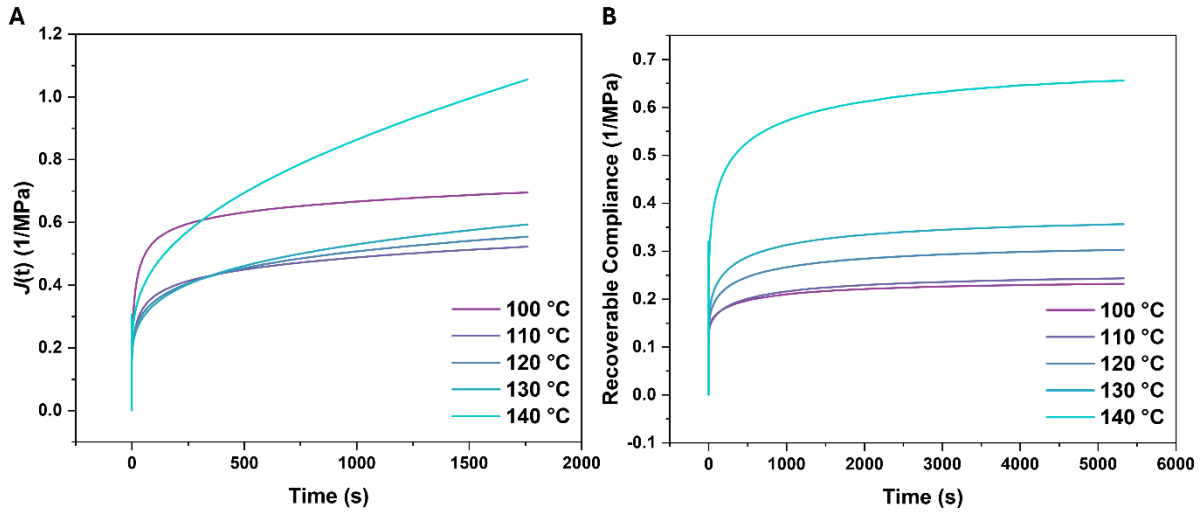

Figure S17: A) Creep compliance of ASC-HDI at various temperatures. B) Recoverable compliance of ASC-HDI at various temperatures. Stress is 20 kPa.

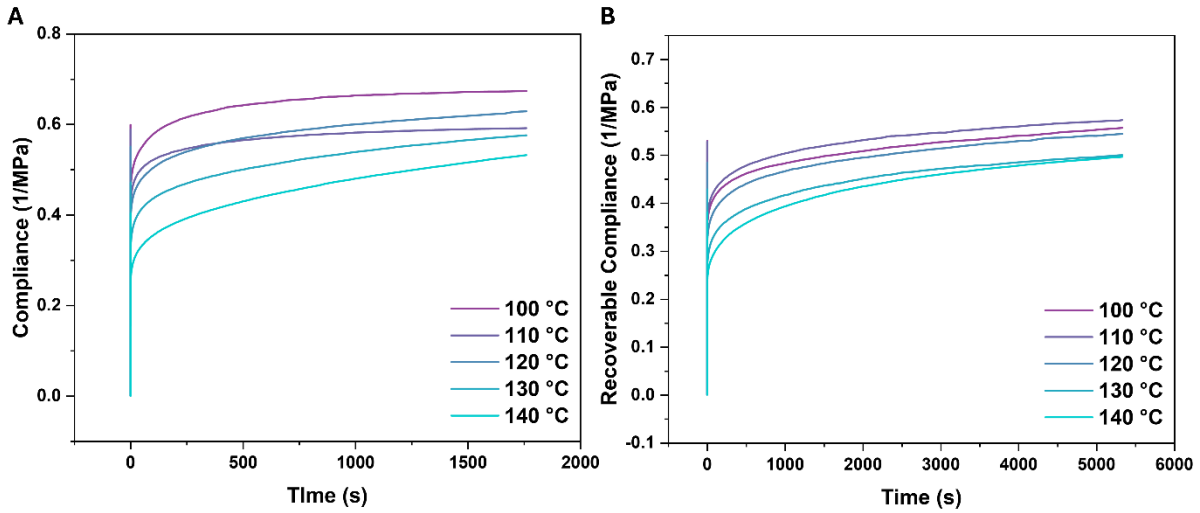

Figure S18: A) Creep compliance of ASC-PDI at various temperatures. B) Recoverable compliance of ASC-PDI at various temperatures. Stress is 40 kPa.

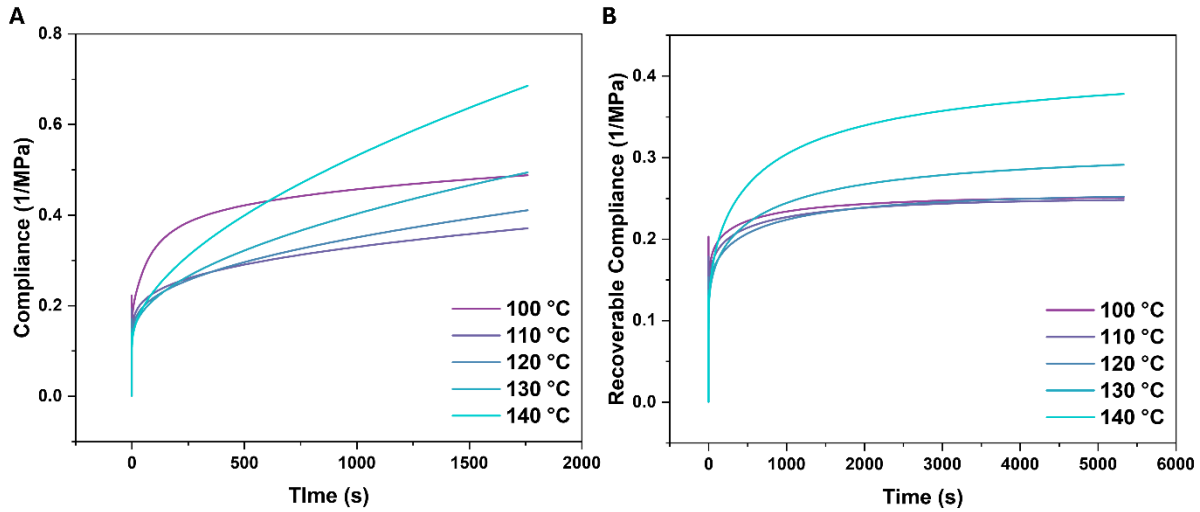

Figure S19: A) Creep compliance of ASC-BDI at various temperatures. B) Recoverable compliance of ASC-BDI at various temperatures. Stress is 20 kPa.

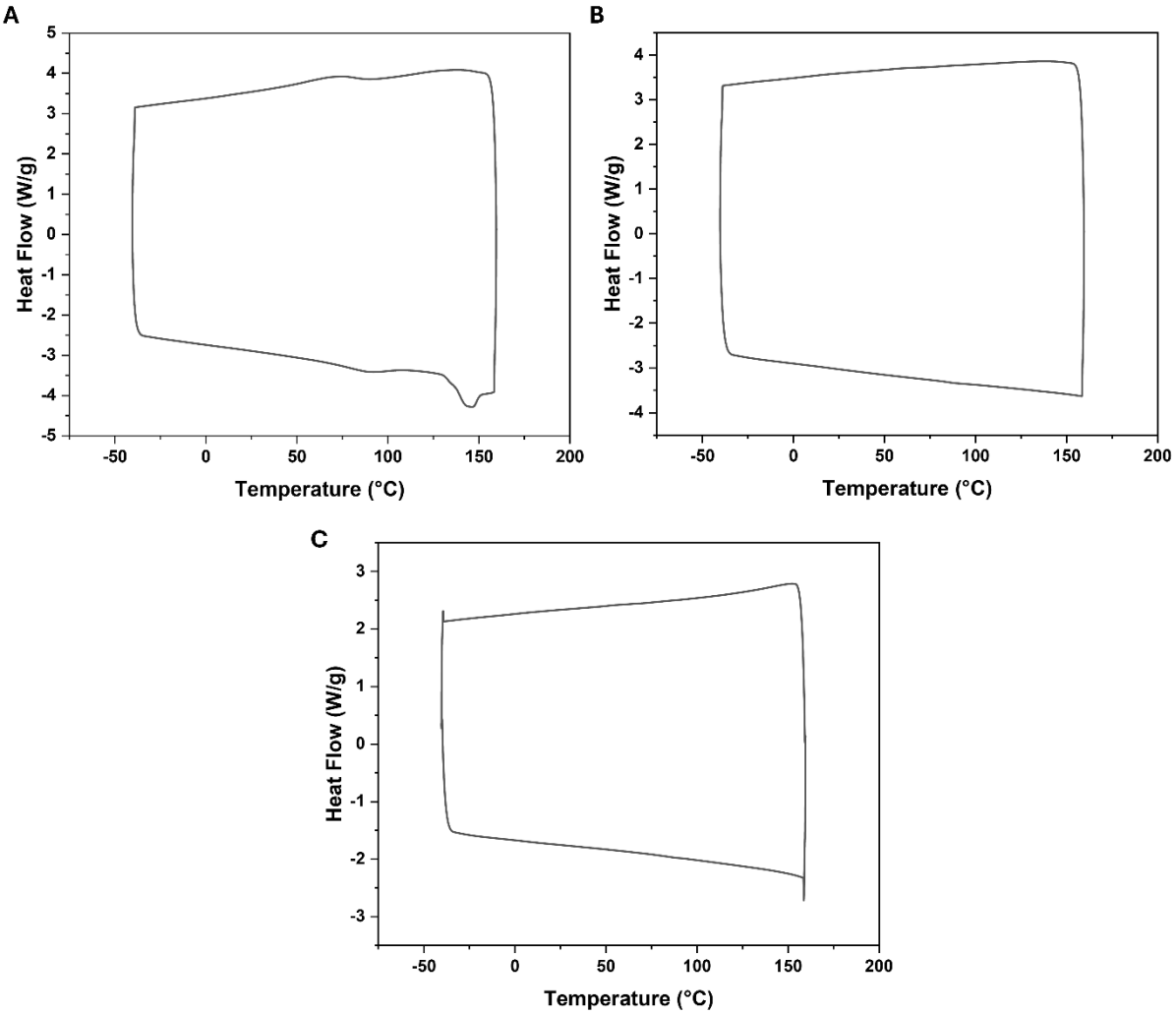

Figure S20: DSC thermograms of the first cooling and second heating of ASC-HDI (A), ASC-PDI (B) and ASC-BDI (C). Heating rate and cooling rates are 10 °C min^{-1}. Exo up.

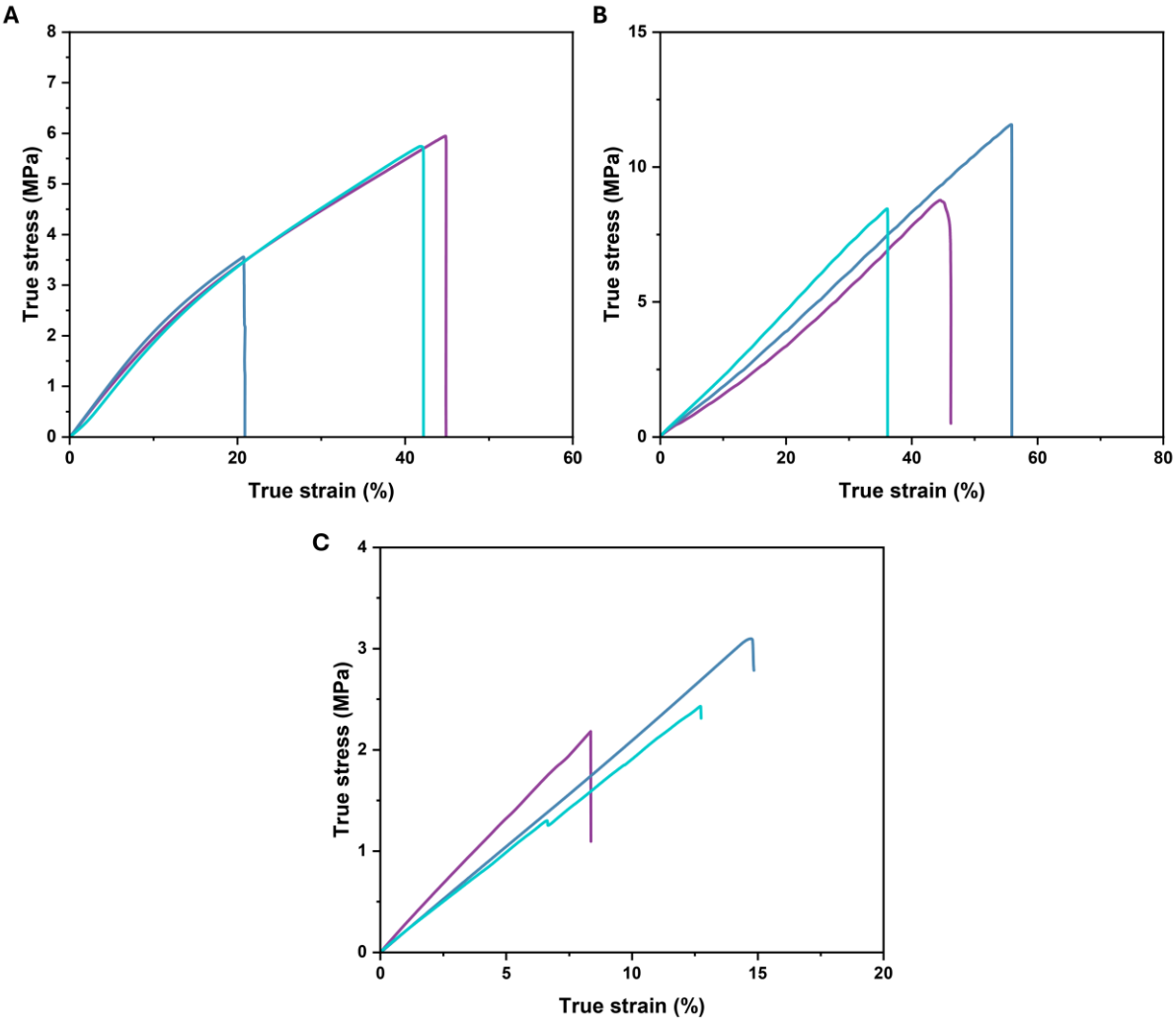

Figure S21: Stress-strain curves of ASC-HDI (A), ASC-PDI (B) and ASC-BDI (C) in triplicate.

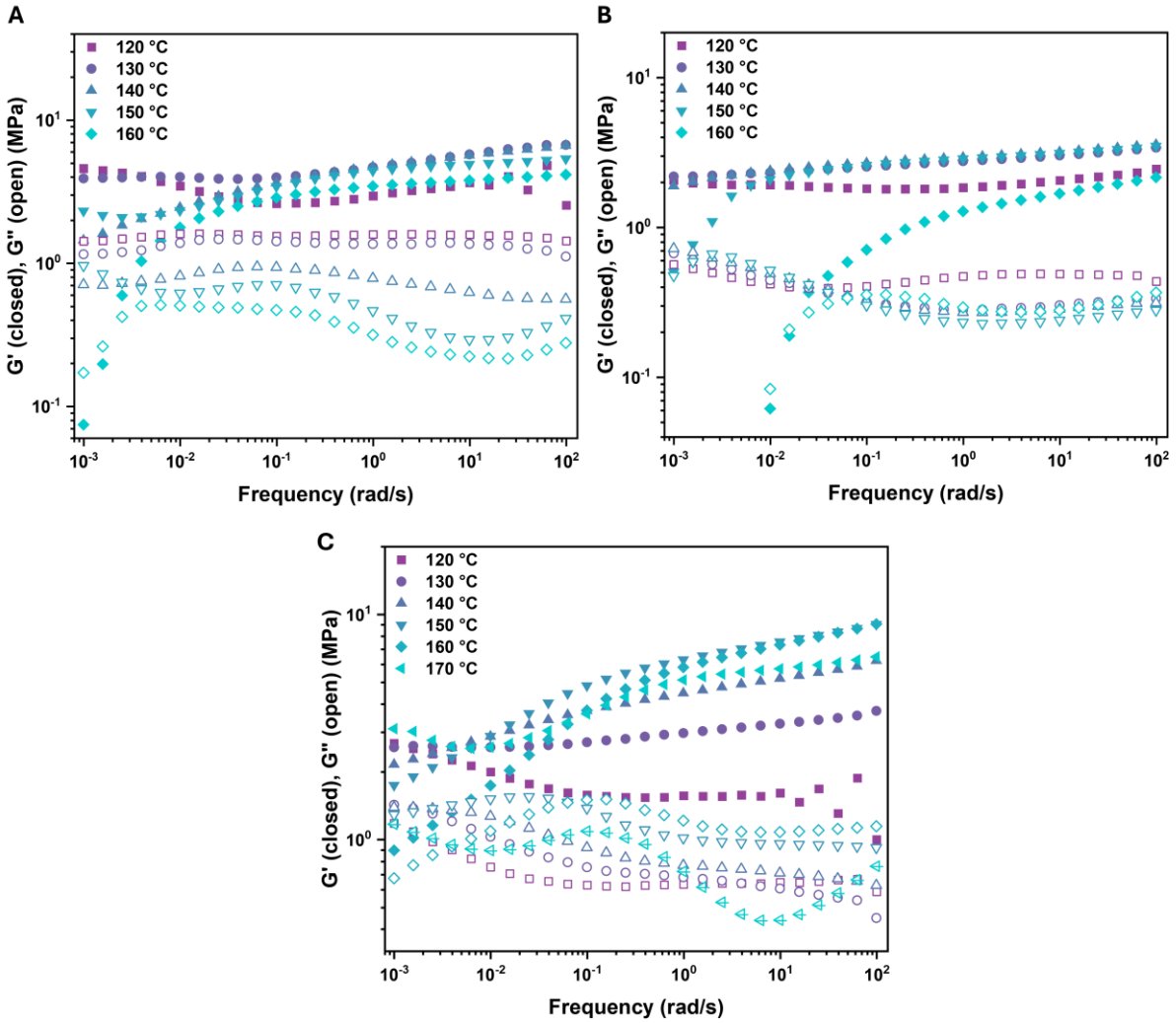

Figure S22: Frequency sweep data at different temperatures under 1% strain of ASC-HDI (A), ASC-PDI (B) and ASC-BDI (C).

5. Detailed DFT analysis of model compound crystal structures

This section contains analyses of hydrogen bonding motives present in crystal structures obtained for PhASCPh and PhASCBz (see Scheme S1).

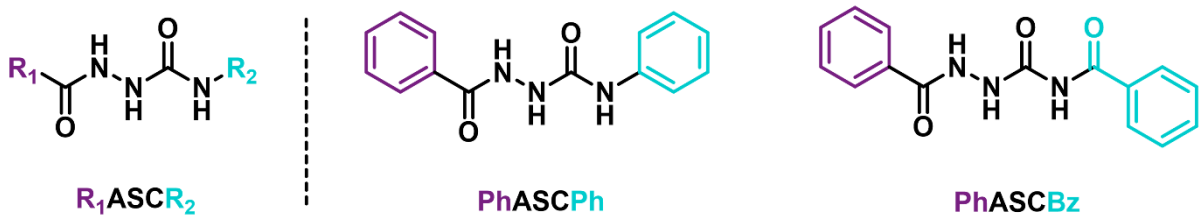

Scheme S1: Structures of ASC motives considered in this study.

First, the PhASCPh motif is studied through comparing the experimentally determined crystal structure with the computationally optimized crystal structure (section 5.1). Hydrogen-bond patterns are examined, and the effect of hydrogen bonds on both experimental and theoretical IR spectra is established. Similar analyses for PhASCBz crystals are discussed in section 5.2.

5.1 PhASCPh

Crystal structure

Experimentally determined crystal structures for PhASCPh (R_1, R_2 = Phenyl; CIF ID: l1330a) were taken as a starting point for periodic DFT calculations at a ZORA-BLYP-D3(BJ)/TZP level of theory (see Computational Details). The structures are reported in Figure S23 and several points can be observed.

First, the computational and experimental structures show a high degree of similarity, particularly in their structural patterns (Figure S23). Bond angles and lengths are identical with a margin of 3 degrees and 0.02 Å, respectively. The most notable differences occur in C–H and N–H bond lengths, which are elongated by a maximum of 0.15 Å in the theoretical structure. However, as will be discussed in later sections, these variations only affect the magnitude of interaction strengths while the trends remain consistent. Consequently, the computationally determined crystal structure is considered valid and hence used for further, detailed analyses. Data derived from the experimental structure are always highlighted in grey.

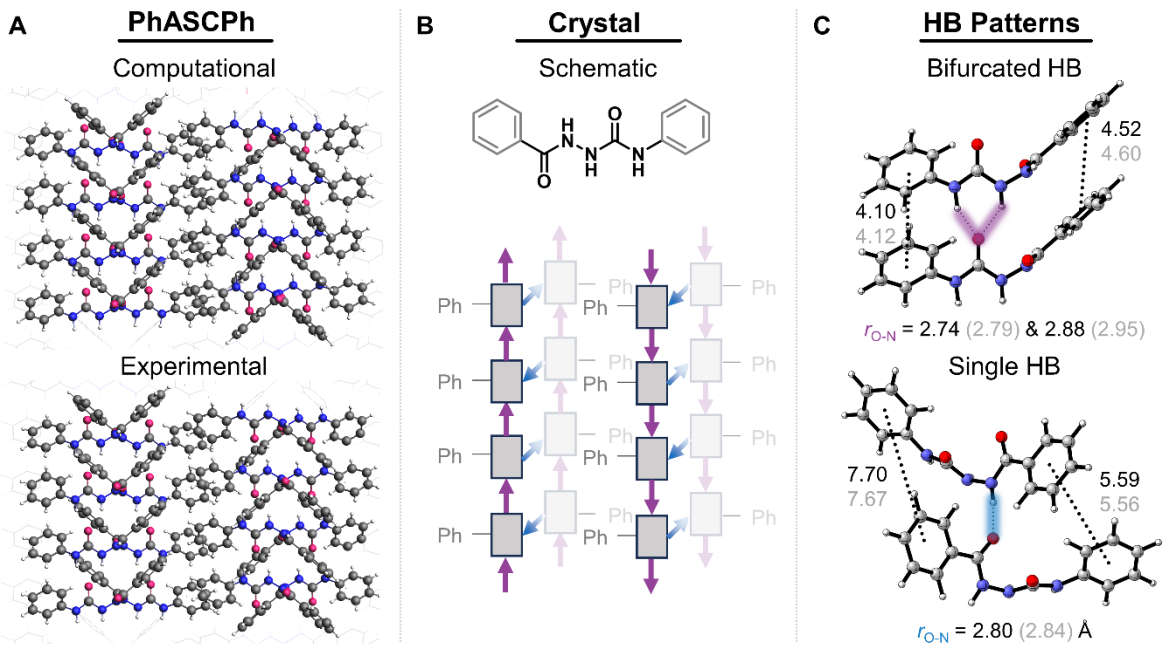

Figure S23: Experimental and optimized crystal structure of PhASCPh (A) including a schematic representation (B) and structural HB patterns, being "bifurcated HB" and "single HB" (C). Values in parenthesis depict experimental bond lengths in Å. Computed at a ZORA-BLYP-D3(BJ)/TZP level of theory.

Second, the crystal structure exhibits multiple hydrogen bond (HB) patterns that form chains in different directions. The schematic representation (Figure S23B and C) illustrates these patterns, being the "bifurcated HB" and "single HB" patterns. Bifurcated HBs occur between urea scaffolds (part of the ASC motif, shown in purple) with hydrogen bond lengths ($r_{O\text{-}N}$) of 2.74 and 2.88 Å. Single HBs (shown in blue) form between the remaining atoms of the ASC motif with a length of 2.80 Å. These hydrogen-bonding patterns create chains of bifurcated HBs in one direction, which are connected perpendicularly by single HBs. Both the single HBs, *i.e.*, in and out of the screen, and the bifurcated HB chains, *i.e.*, up and down, alternate directions (Figure S23).

Interaction decomposition

Both hydrogen-bond patterns are analyzed further to determine their strength and compared to other intermolecular interactions present, such as the interaction between the phenyl substituents. To accomplish this, the interacting PhASCPh dimer is fragmented and bonds between R_1/R_2 and ASC motifs are replaced by hydrogen atoms[8]: r (**H–**C_{ph}) = 1.083 Å, r (**H–**C=O) = 1.08 Å), and r (**H–**NH) = 1.01 Å (see Scheme S2). The fragmentation defines two fragments, A and B, with various ASC and substituents combinations, allowing us to isolate the hydrogen bond interaction (ASC_A-ASC_B) from interactions between substituents.

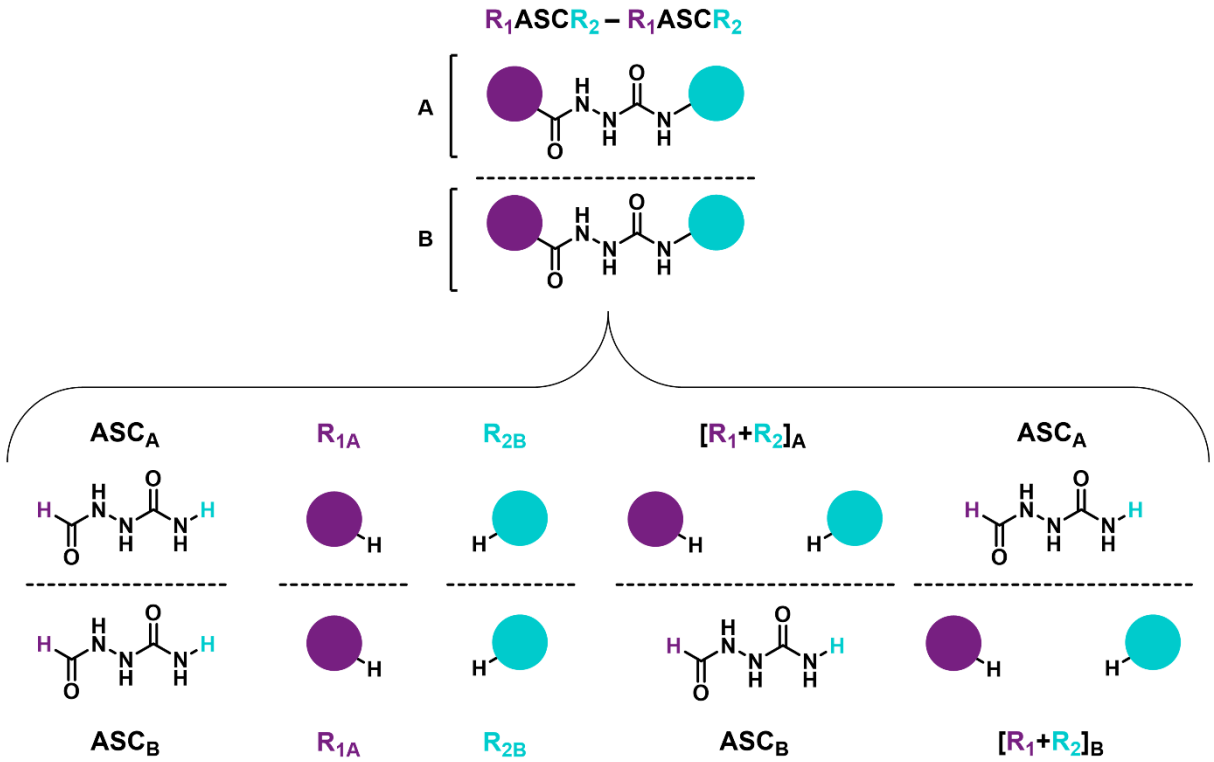

Scheme S2: Fragmentation scheme for studying the interaction between two R_1ASCR_2 monomers forming a hydrogen-bonded dimer.

The decomposition results are shown in Table S6. The interaction energy (ΔE_{int}) summed over all fragmentations closely approximates the interaction energy of the complete dimer, with a maximum difference of 1.6 kcal mol^{-1}, validating the employed fragmentation scheme. The decomposition reveals that the hydrogen bond component is the most important interaction for both the bifurcated and single HB dimer, accounting for half of the total interaction energy in both HB patterns. The energy decomposition analysis (EDA, see Theoretical Methods) shows strong electrostatic interactions (ΔV_{elstat}) between the negatively charged HB acceptor ($C{=}O^{\delta-}$) and positively charged HB donor ($N{-}H^{\delta+}$), alongside significant donor-acceptor interactions (ΔE_{oi}), where the lone pair on the C=O donates electrons to the σ* orbital of the H–N.[9,10] The other half of the interaction in the PhASCPh dimer stems from contributions of phenyl–phenyl (π–π stacking) and mixed ASC–phenyl interactions, each contributing a small amount to the overall interaction.

Table S6: Gas–phase decomposition of the interaction energy ΔE_{int}[a] (in kcal mol^{-1}) of PhASCPh dimers decomposed into components defined in Scheme S2.

System	Structure	ΔE_{int}	ΔV_{elstat}	ΔE_{Pauli}	ΔE_{oi}	ΔE_{disp}
Bifurcated Hydrogen Bond						
$[PhASCPh]_A$ – $[PhASCPh]_B$	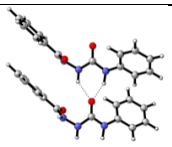	–20.2 –20.3	–24.3 –17.1	36.0 20.8	–13.6 –7.3	–18.3 –16.7
ASC_A – ASC_B		–10.1 –10.4	–19.9 –13.1	25.1 11.9	–10.9 –5.1	–4.5 –4.0
Ph_A – Ph_B		–2.5 –2.7	–2.0 –1.5	5.3 4.1	–0.8 –0.7	–5.0 –4.6
Ph_A – Ph_B	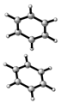	–2.1 –2.2	–1.0 –0.7	2.1 1.5	–0.7 –0.5	–2.6 –2.5
$[Ph+Ph]_A$ – ASC_B	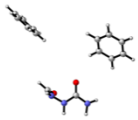	–1.6 –1.5	–0.7 –0.6	0.8 0.7	–0.5 –0.4	–1.2 –1.1
ASC_A – $[Ph+Ph]_B$	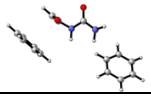	–5.5 –5.7	–3.7 –2.9	8.0 5.5	–2.1 –1.6	–7.6 –6.8
Sum[b]		–21.8 –22.5	–27.2 –18.9	41.3 23.7	–14.9 –8.3	–20.9 –19.0
Single Hydrogen Bond						
$[PhASCPh]_A$ – $[PhASCPh]_B$	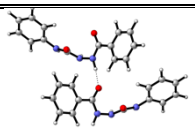	–15.3 –14.3	–18.4 –12.3	24.6 12.8	–11.2 –5.5	–10.3 –9.3
ASC_A – ASC_B	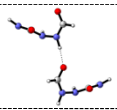	–7.2 –6.3	–11.8 –8.2	13.6 7.1	–7.0 –3.3	–2.0 –1.9
Ph_A – Ph_B	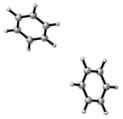	–1.6 –1.8	–1.0 –0.5	3.1 1.7	–0.8 –0.5	–2.9 –2.5
Ph_A – Ph_B	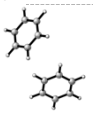	–0.2 –0.2	0.0 0.0	0.1 0.1	0.0 0.0	–0.3 –0.3
$[Ph+Ph]_A$ – ASC_B	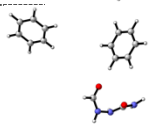	–2.5 –2.6	–3.3 –2.1	4.5 2.3	–1.7 –1.0	–2.0 –1.9
ASC_A – $[Ph+Ph]_B$	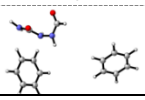	–2.5 –2.7	–1.7 –0.9	3.9 2.0	–1.5 –0.9	–3.2 –2.9
Sum[b]		–14.0 –13.6	–17.8 –11.8	25.1 13.1	–11.0 –5.7	–10.3 –9.3

[a] Computed at a ZORA-BLYP-D3(BJ)/TZ2P (ADF) // ZORA-BLYP-D3(BJ)/TZP (BAND) level of theory with values obtained using the experimental crystal in gray.

[b] The sum of the total interaction energy and decomposition terms of the substituent-only, ASC-only, and mixed fragmentations.

Cooperativity analysis

When studying the interactions for the two distinctive patterns found in PhASCPh crystals, it is found that the hydrogen bond accounts for 50% of the total dimer interaction through favorable orbital interactions and electrostatics. Previous work on hydrogen bonds in supramolecular systems has shown that highly structured, chain-like hydrogen bonds exhibit cooperativity: the phenomenon that the hydrogen-bond strength of chains with n monomers is substantially higher than (n−1) times the hydrogen-bond strength of a dimer. This means that adding monomers to the chain becomes more favorable.[9,11,12]

Given that the structural patterns in the PhASCPh crystal are chain-like (bifurcated and single HB, see Figure S23), the degree of cooperativity was examined by elongating the chain for both patterns, from a dimer (1+1) to a pentamer (4+1). The results presented in Table S7, indicate significant cooperativity for both patterns. As the chain lengthens, the interaction energy (ΔE_{int}) becomes more stabilizing, meaning that there is a stronger interaction between a longer chain and a monomer. For example, the bifurcated chain's interaction strength increases from –20.2 (1+1) to –24.5 (4+1) kcal mol^{-1}. The increase or the longer chains is smaller and goes to an asymptotic value. Additionally, charge transfer between a longer chain and an additional monomer increases, as shown by the VDD charges (ΔQ_n^{VDD}, see Theoretical Methods), which originates from stronger orbital interactions: +54 to +63 milli-electrons for the bifurcated HB pattern and +39 to +45 milli-electrons for the single HB pattern. Note that the VDD charges obtained using the experimental crystal are smaller because the hydrogen bonds are longer, and the donor–acceptor interactions are weaker.

Table S7: Cooperativity analysis of hydrogen-bonded PhASCPh chains. The interaction energy, ΔE_{int} (in kcal mol^{-1}) and associated VDD charges (in milli-electrons) are tabulated.[a]

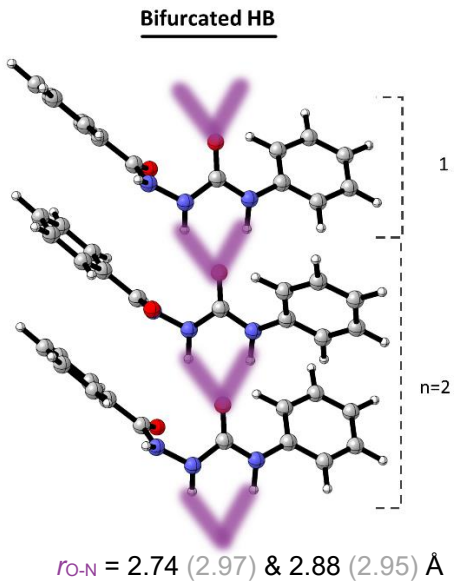

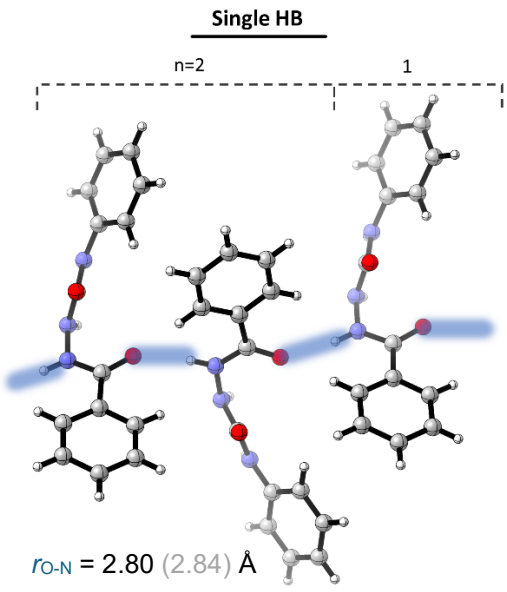

n+1[b]	ΔE_{int}		n+1[b]		ΔE_{int}	n+1[b]		ΔE_{int}	
1+1	–20.2	1+1	–20.2	1+1	–20.2	1+1	–20.2	1+1	–20.2
2+1	–23.4	2+1	–23.4	2+1	–23.4	2+1	–23.4	2+1	–23.4
3+1	–24.2	3+1	–24.2	3+1	–24.2	3+1	–24.2	3+1	–24.2
4+1	–24.5	4+1	–24.5	4+1	–24.5	4+1	–24.5	4+1	–24.5

[a] computed at a ZORA-BLYP-D3(BJ)/TZ2P level of theory with values obtained with experimental structures in gray.

[b] The elongation direction is from bottom to top. Note that trends remain the same regardless of the elongation direction (except that the sign of charge transfer is inverted).

IR studies

Finally, the experimental and theoretical IR spectra of PhASCPh are reported to further understand the impact of the hydrogen bonds on the IR spectra (see Figure S24). These include spectra for the PhASCPh crystal (both experimental and theoretical) and the PhASCPh monomeric structure (theoretical). Peaks from bonds involving in hydrogen bonding are highlighted, including three N–H stretch vibrations between 3200 and 3500 cm^{-1} and two C=O stretch vibrations around 1670 cm^{-1}.

Comparing the monomer IR spectrum (no hydrogen bonding) with the crystal IR spectrum (involving hydrogen bonding) reveals that the stretch vibrations corresponding to the orange and purple N–H bonds (See Figure S24 for the color scheme) undergo a redshift of 268 and 158 cm^{-1}, respectively. This originates from the hydrogen bond-induced weakening of the N–H bonds. Upon hydrogen-bond formation, electrons are transferred from the HB acceptor to the anti-bonding σ* of the N–H bond, which induces and elongation of the N–H by 0.01 Å, as observed in the crystal geometry. The N–H stretch vibration denoted with the color blue in Figure S24, on the other hand, remains nearly unchanged, because the hydrogen bond comprising this N–H bond is significantly longer and weaker with respect to the hydrogen bonds with the prior discussed orange and purple N–H bonds (Figure S24).

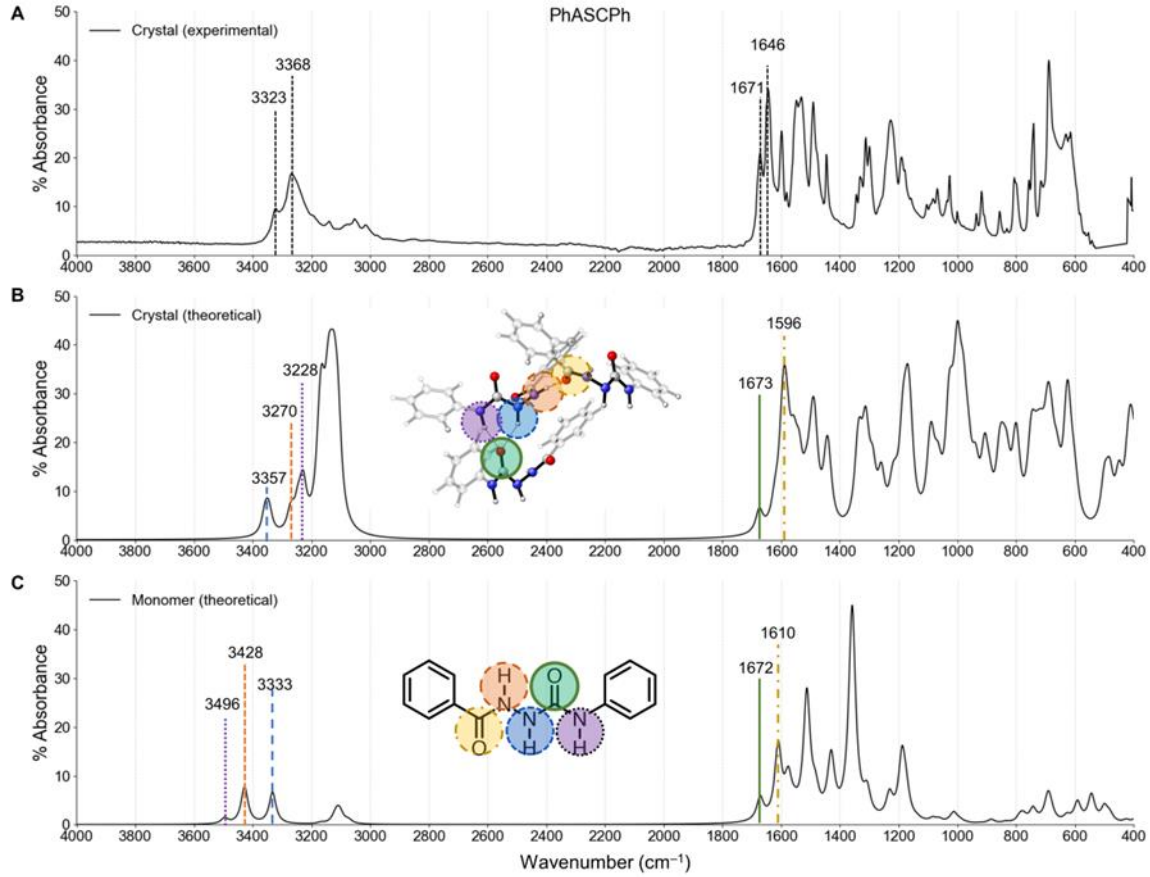

Figure S24: IR spectra comparison of PhASCPh between the experimental crystal (A) with computed spectra of the crystal (B) and monomer (C). Highlighted peaks are associated with stretching modes.

5.2 PhASCBz

Crystal Structure

A procedure similar to that used for PhASCPh was applied to obtain the theoretical crystal structure of PhASCBz (R_1 = Phenyl, R_2 = Benzoyl; CIF ID: l1349a). DFT calculations were conducted at the ZORA-BLYP-D3(BJ)/TZP level of theory, starting from the experimental structure. Unlike PhASCPh, the PhASCBz monomer exhibits multiple conformers within the crystal structure that are not energetically equivalent: monomers in the repeating unit cell adopt distinct geometries with an energy difference of 15 kcal mol^{-1} (see main text Figure 2). Furthermore, the hydrogen-bonding patterns form a stairs-like structure in both the theoretical and experimental structures (Figure S25).

Three distinct hydrogen-bond patterns contribute to this structure. The “Double HB” pattern (Figure S25, purple) comprises two hydrogen bonds oriented in opposite directions, connecting two ASC motifs to form each “step” of the stairway. These steps are linked perpendicularly by the “σ HB” pattern (blue), where a hydrogen bond forms between the C=O group of one step and the H–N group of an adjacent step, both lying in the same plane. The third pattern, “π HB” (green), involves hydrogen bonds between orthogonal C=O and H–N groups. This occurs when the H–N group of one step points towards a C=O group of an adjacent stairway step involved in a double HB, locking two stairs together. Thus, the double HB and σ HB patterns contribute to forming stairways and two stairways bind together through π HBs. Note that within a double stairway, one has the σ HBs in one direction and the other in the opposite direction (blue arrows in the schematic representation, Figure S25A). All these patterns combined describe a repeating, three-dimensional network of “double stairways.”

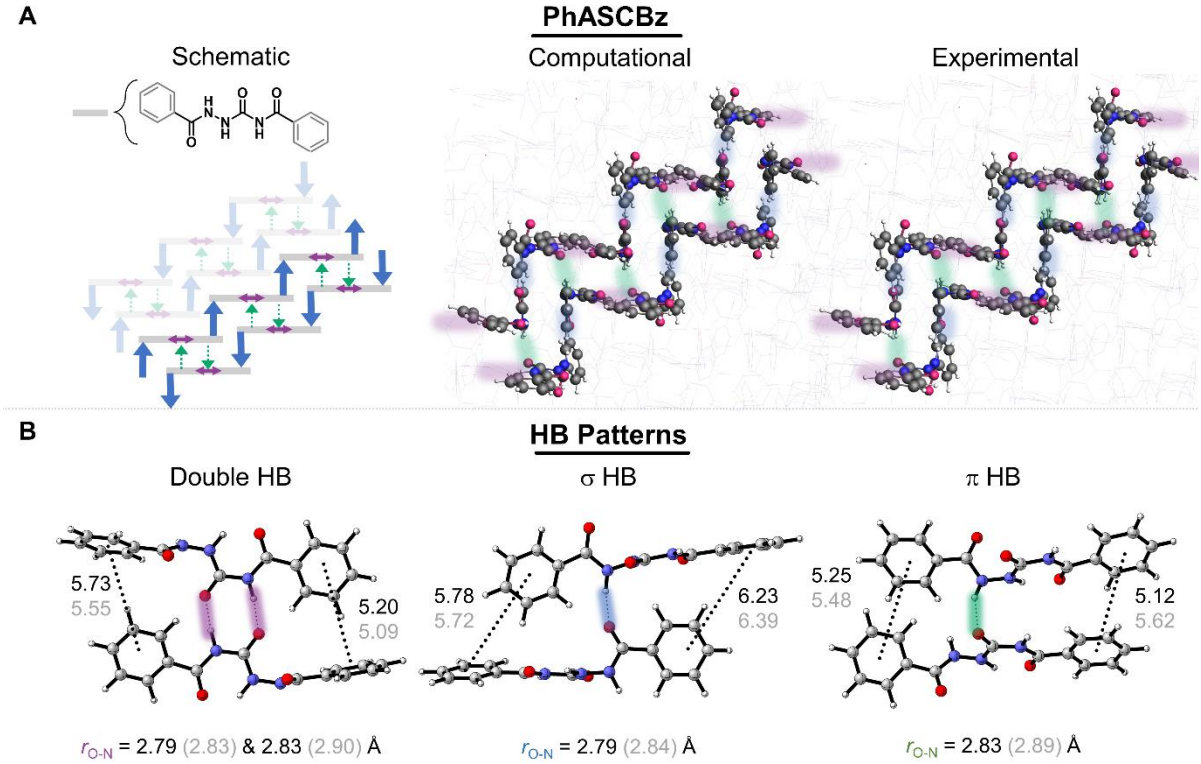

Figure S25: Experimental and optimized crystal structure of PhASCBz including a schematic representation (A) and structural HB patterns, being “double HB”, “σ HB”, and “π HB” (B). Values in parenthesis depict experimental bond lengths in Å. Optimized at a ZORA-BLYP-D3(BJ)/TZP level of theory.

Interaction decomposition

The contributions stemming from the hydrogen-bond interaction for each pattern can be isolated through the same fragmentation scheme used for PhASCPh (see Scheme S2). Dimers of PhASCBz were made for each of the three hydrogen-bond patterns and the results are tabulated in Table S8. The interaction energy (ΔE_{int}) summed over all fragmentations has a maximum difference of 1.4 kcal mol^{-1} compared to the interaction energy of the complete dimer which validates this approach.

The hydrogen-bond component in the double HB and σ HB dimers is strong, accounting for more than half of the total interaction energy. In the π HB dimer, this interaction accounts for less than half of the total interaction energy. The origin of this difference lies in the nature of the hydrogen bonds. In the double HB and s HB dimers, strong electrostatic interactions (ΔV_{elstat}) are present between the negatively charged HB acceptor (C=O$^{\delta-}$) and positively charged HB donor (N–H$^{\delta+}$), alongside significant donor-acceptor interactions (ΔE_{oi}), where the lone pair on the C=O donates electrons to the σ* orbital of the H–N. The hydrogen bond in the π HB dimer deviates because the involved lone pair is less favorable aligned with the σ* orbital of the H–N, resulting in less donor-acceptor interactions. The remaining interaction energy in the PhASCBz dimers arises from phenyl–benzoyl and mixed ASC–phenyl interactions, each making a relatively smaller contribution to the overall interaction.

Table S8: Gas–phase decomposition of the interaction energy ΔE_{int} (in kcal mol^{-1}) of **PhASCBz** dimers decomposed into components defined in Figure S25.

Double Hydrogen Bond						
System	**Structure**	ΔE_{int}	ΔV_{elstat}	ΔE_{Pauli}	ΔE_{oi}	ΔE_{disp}
$[PhASCBz]_A$ – $[BzASCPh]_B$	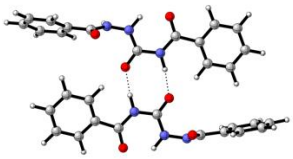	–26.6 –23.0	–35.8 –24.1	45.0 25.6	–22.7 –11.1	–13.1 –13.3
ASC_A – ASC_B	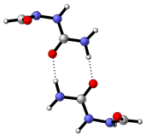	–14.8 –10.6	–24.9 –16.3	29.4 16.2	–15.8 –7.2	–3.5 –3.3
Ph_A – Bz_B	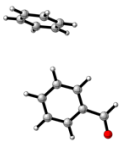	–1.6 –1.9	–0.5 –0.6	1.0 1.0	–0.3 –0.3	–1.8 –2.0
Bz_A – Ph_B	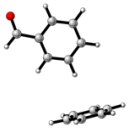	–2.9 –3.4	–1.6 –1.3	3.0 2.1	–1.0 –0.8	–3.4 –3.6
$[Ph+Bz]_A$ – ASC_B	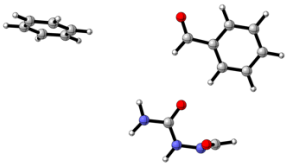	–3.7 –4.7	–5.2 –3.9	6.7 3.9	–2.6 –1.4	–2.6 –3.3
ASC_A – $[Bz+Ph]_B$	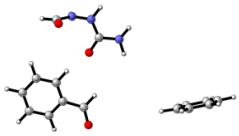	–4.6 –3.9	–5.0 –3.5	5.8 3.7	–2.2 –1.5	–3.2 –2.5
Sum[b]		–27.6 –24.9	–37.1 –25.9	45.7 26.8	–21.8 –11.2	–14.4 –14.6

σ Hydrogen Bond						
$[PhASCBz]_A$ – $[BzASCPh]_B$	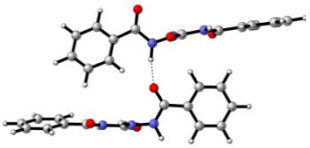	–14.2 –14.6	–17.2 –11.0	26.8 13.7	–10.3 –5.1	–13.5 –12.3
ASC_A – ASC_B	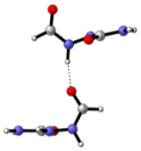	–7.7 –7.3	–12.0 –8.6	13.2 6.6	–6.7 –3.2	–2.1 –2.1
Ph_A – Bz_B	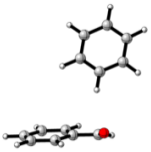	–2.3 –2.7	–2.3 –1.4	4.4 2.5	–1.1 –0.6	–3.3 –3.2
Bz_A – Ph_B	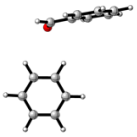	–2.4 –2.5	–1.7 –1.1	3.4 1.7	–0.9 –0.5	–3.1 –2.6
$[Ph+Bz]_A$ – ASC_B	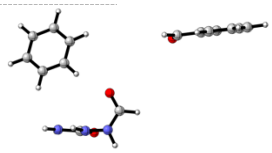	–1.1 –1.2	–0.5 0.2	3.9 2.1	–1.5 –0.9	–3.0 –2.6
ASC_A – $[Bz +Ph]_B$	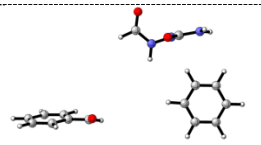	–1.0 –1.4	–0.4 0.3	4.1 2.3	–1.3 –0.8	–3.4 –3.1
Sum[b]		–14.4 –15.0	–17.0 –10.6	28.9 15.1	–11.5 –6.1	–14.9 –13.5
π Hydrogen Bond						
$[PhASCBz]_A$ – $[PhASCBz]_B$	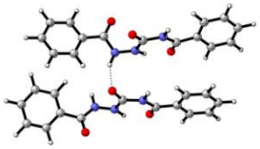	–15.3 –13.4	–14.2 –9.1	22.7 12.0	–8.1 –4.3	–15.7 –12.0
ASC_A – ASC_B	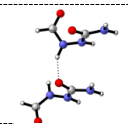	–6.1 –6.2	–9.4 –5.9	13.3 7.2	–5.9 –3.7	–4.2 –3.8
Bz_A – Bz_B	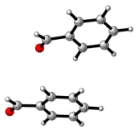	–2.8 –2.3	–1.2 –1.2	4.2 2.3	–0.8 –0.5	–5.0 –3.0
Ph_A – Ph_B	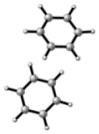	–2.1 –2.1	–1.8 –0.2	4.2 1.5	–0.8 –0.4	–3.6 –3.1
$[Ph+Bz]_A$ – ASC_B	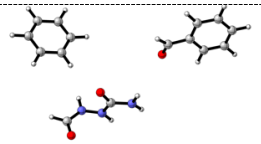	–3.8 –3.4	–2.6 –2.1	1.8 1.3	–0.9 –0.7	–2.2 –1.9

ASC_A – $[Ph+Bz]_B$ 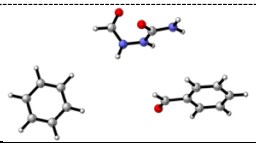	–1.8 –1.4	–0.2 –0.1	1.0 0.6	–0.4 –0.3	–2.1 –1.6
Sum[b]	–16.7 –15.4	–15.3 –9.5	24.5 13.0	–8.8 –5.6	–17.1 –13.4

[a] Computed at a ZORA-BLYP-D3(BJ)/TZ2P (ADF) // ZORA-BLYP-D3(BJ)/TZP (BAND) level of theory with values obtained using the experimental crystal in gray.
[b] The sum of the total interaction energy and decomposition terms of the substituent-only, ASC-only, and mixed fragmentations.

Cooperativity analysis

Since the stair-like chains are composed of steps connected by σ HB, the degree of cooperativity was assessed using two approaches. In the first approach, ASC-wise, the chain is elongated by adding ASC motives one at a time (Table S9), alternating between double and σ HBs. The second approach called "stepwise" forms the stairs using steps, *i.e.*, two ASC motives linked together by a double HB. The results show that both approaches indicate a lack of cooperativity, as the interaction energy (ΔE_{int}) and charge transfer (ΔQ_n^{VDD}) do not significantly increase as the stairs become longer. Instead, an oscillating pattern emerges in the ASC-wise approach with interaction energies alternating between –14.3 and –28.3 kcal mol^{-1}, corresponding to the addition of a monomer via a σ HB or double HB. In addition, the stepwise approach shows a constant value of around –16.0 kcal mol^{-1}, and the charge transfer remains the same (+33 milli-electrons). The lack of cooperativity is due to charge not being able to be transferred in one direction; the opposing charge flow in double HBs cancels out, and the distance between adjacent σ HBs is too large to facilitate significant charge transfer.

Table S9: Cooperativity analysis of two hydrogen-bonded PhASCBz chains termed ASC-wise and stepwise. The interaction energy, ΔE_{int} (in kcal mol^{-1}) and associated VDD charges (in milli-electrons) are tabulated.[a]

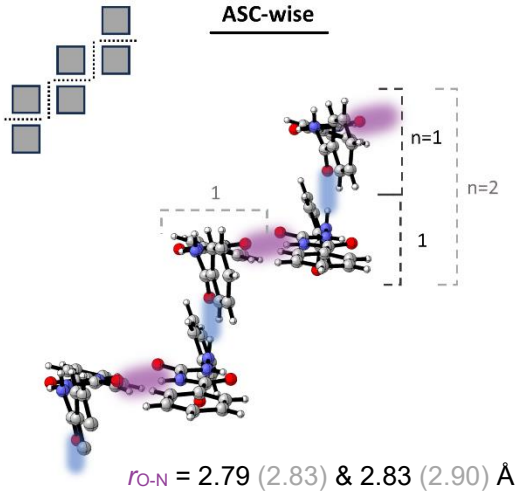

$r_{O\text{-}N}$ = 2.79 (2.83) & 2.83 (2.90) Å

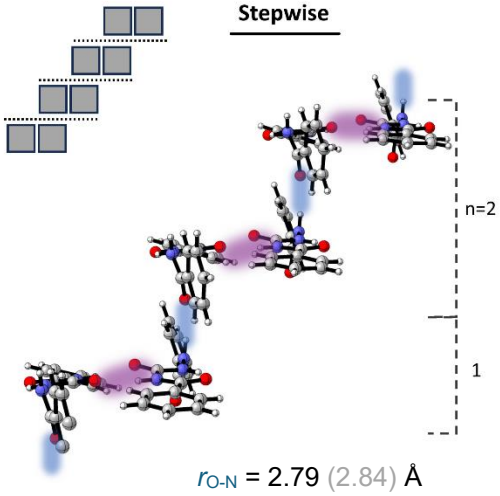

$r_{O\text{-}N}$ = 2.79 (2.84) Å

n+1[b]	ΔE_{int}		ΔQ_n^{VDD}	
1+1	–14.3	–14.6	+32	+15
2+1	–28.0	–24.2	–3	–1
3+1	–14.2	–14.9	+30	+14
4+1	–28.3	–24.5	–3	–1
5+1	–14.1	–14.8	+30	+14

n+1[b]	ΔE_{int}		ΔQ_n^{VDD}	
1+1	–15.9	–16.2	+33	+15
2+1	–16.0	–16.4	+33	+15
3+1	–16.1	–16.5	+33	+16

[a] computed at a ZORA-BLYP-D3(BJ)/TZ2P level of theory with values obtained with experimental structures in gray.
[b] The elongation direction is from top to bottom. Note that trends remain the same regardless of the elongation direction (except that the sign of charge transfer is inverted).

IR studies

The experimental IR spectrum of the PhASCBz crystal was measured, and the spectra of the optimized crystal and monomeric structures were calculated (see Figure S26). Highlighted in the spectra are the stretch vibrations of bonds involved in hydrogen bonding, including three N–H stretches between 3200 and 3500 cm^{-1} and three C=O stretches between 1600 and 1670 cm^{-1}. Comparing the monomeric spectrum (no hydrogen bonds) with the theoretical crystal spectrum (involving hydrogen bonds) reveals redshifts attributed to hydrogen bonding. Specifically, the N–H bond denoted with orange shows two distinct shifts: 133 cm^{-1} for the σ HB with the yellow C=O bond and 201 cm^{-1} for the π HB with the green C=O bond. The purple N–H bond, which participates in a bifurcated HB, exhibits a shift of 326 cm^{-1}. Meanwhile, the blue N–H bond, involved in an intramolecular hydrogen bond with the dark blue C=O bond, shifts by 45 cm^{-1}. These redshifts correlate with elongations of the N–H bonds by 0.02 Å (purple) and 0.01 Å (orange) reflecting the bond-weakening effects of hydrogen bonding. The blue N–H bond remains the same length up to two decimals, showing that the strength of the internal hydrogen bond changes less significantly upon complexation.

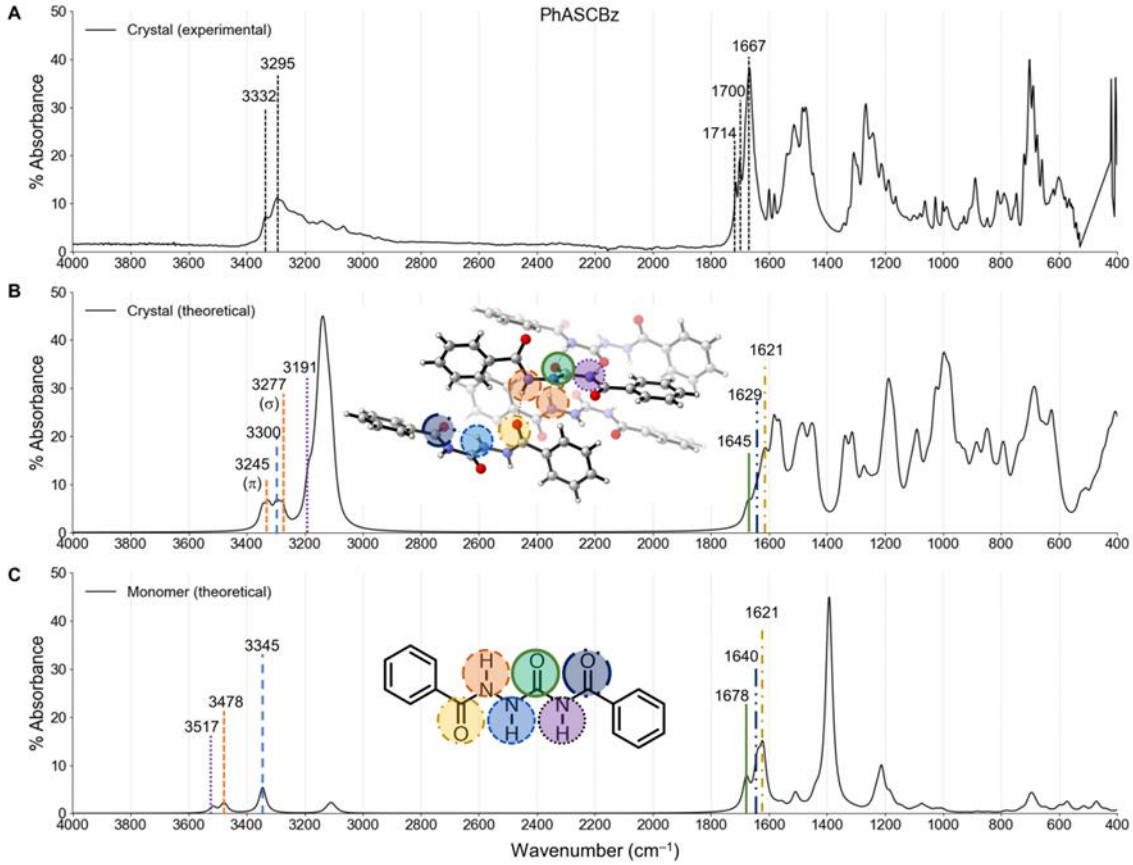

Figure S26: IR spectra comparison of PhASCBz between the experimental crystal (A) with computed spectra of the crystal (B) and monomer (C). Highlighted peaks are associated with stretching modes.

5.3 Theoretical methods

Computational details

Calculations were carried out using the periodic DFT module BAND[13,14] and the DFT module ADF[15-17] of the Amsterdam Modeling Suite 2023.104. The exchange-correlation function used is BLYP-D3(BJ), that is, a BLYP level of the generalized gradient approximation (GGA); exchange functional developed by Becke (B[18]), and the GGA correlation functional developed by Lee, Yang, and Parr (LYP[19]). The DFT-D3(BJ) method developed by Grimme and coworkers,[20] which contains the damping function proposed by Becke and Johnson,[21] is used to describe non-local dispersion interactions. An uncontracted relativistically optimized Slater type orbitals (STOs) basis set was used containing diffuse function with either one set of diffuse functions (TZP, BAND calculations), or two sets of diffuse functions (TZ2P, ADF calculations). The smaller basis set for BAND calculations were chosen because of the unit cell's size (~260 atoms). However, the TZP performs sufficiently well for hydrogen bonds in large supramolecular systems.[22] The 1*s* orbitals on carbon, nitrogen, and oxygen atoms were frozen within each basis set. Hydrogen-bonded systems have shown that the employed level of theory, *i.e.*, BLYP-D3(BJ)/TZ2P, gives a basis set superposition error (BSSE) of only a few tenths of a kcal mol^{-1} and hence this will not affect the computed trends in hydrogen-bond strength.[23] Moreover, the employed level of theory has shown to give accurate results for describing hydrogen-bonded systems.[24] The zeroth-order regular approximation (ZORA[25]) method was applied to account for relativistic effects. The molecular density was fitted by the systematically improvable Zlm fitting scheme; a numerical quality of "normal" was used for BAND calculations and "VeryGood" for ADF calculations.[26] The k-space grid for BAND calculations was set to "normal", that is, 3 k-space points for lattice vectors between 10 and 20 Bohr and 1 point for lattice vectors greater than 20 Bohr. The computational settings are summarized in Table S8.

Table S10: Computational settings used for optimizing crystal structures (BAND) and for fragment calculations (ADF) for determining the interaction strength.

	Functional	**Basis set**	**Numerical Quality**	**Frozen Core**
BAND2023.104	BLYP-D3(BJ)	TZP	Normal	1s on C, O, N
ADF2023.104	BLYP-D3(BJ)	TZ2P	VeryGood	None

Both the unit cell and molecular geometry were optimized with periodic DFT and verified through frequency analyses with zero imaginary frequencies for the equilibrium geometries.[27, 28] Geometries were visualized using the CYLview2.0 software.[29] Most of the calculations were automated using the application programming interface PLAMS.[30]

Energy decomposition analysis

To understand the different components that determine the hydrogen-bond strength, ΔE can be partitioned as formulated by eqn(S3) according to the activation strain model (ASM) of reactivity and bonding.[31-34] In this model, ΔE comprises two components, ΔE_{strain} and ΔE_{int}. Here, the strain energy (ΔE_{strain}) is the energy required to deform the equilibrium geometry of each fragment, to the geometry it acquires when it interacts in the hydrogen-bonded chain. The interaction energy (ΔE_{int}) accounts for the stabilizing interaction between the two deformed fragments.

$$\Delta E = \Delta E_{\text{strain}} + \Delta E_{\text{int}} \qquad (S3)$$

In the framework of the Kohn-Sham molecular orbital model using quantitative canonical energy decomposition analysis (EDA),[35, 36] the latter term, ΔE_{int}, can be further decomposed

into electrostatic interaction (ΔV_{elstat}), Pauli repulsion (ΔE_{Pauli}), orbital interaction (ΔE_{oi}), and an additional term that accounts for dispersion interactions ΔE_{disp} (eqn(S4)).

$$\Delta E_{\text{int}} = \Delta V_{\text{elstat}} + \Delta E_{\text{Pauli}} + \Delta E_{\text{oi}} + \Delta E_{\text{disp}} \tag{S4}$$

The term ΔV_{elstat} represents the usually attractive classical Coulomb interaction between the unperturbed charge distributions of the deformed fragments ΔE_{Pauli} comprises destabilizing interactions between occupied orbitals of the fragments and is responsible for steric repulsion. The orbital interaction energy (ΔE_{oi}) accounts for charge transfer and polarization effects, including interactions between the highest occupied and lowest unoccupied MOs (HOMO–LUMO). Finally, ΔE_{disp} accounts for dispersion corrections as introduced by Grimme *et al*.[20]

Voronoi deformation density charge analysis

For computing the charge transfer between molecular fragment that form a bond, the Voronoi deformation density (VDD) method was used.[37] In this method, Voronoi cells are considered for describing the spatial extent of an atom, which is defined as the compartment of space bounded by the bond midplanes on and perpendicular to all bond axes between one nucleus and its neighboring nuclei. Here, the charge rearrangement ΔQ_A^{VDD} compared to the initial density of the polyatomic fragments (ρ_i) is measured and gives insight into the change in electronic density upon interacting (eqn(S5)).

$$\Delta Q_A^{VDD} = -\int_{Voronoi\ cell\ of\ A\ in\ molecule} \left[\rho_{molecule}(\boldsymbol{r}) - \sum_{subsystems,i} \rho_i(\boldsymbol{r})\right] d\boldsymbol{r} \tag{S5}$$

Thus, ΔQ_A^{VDD} is an indication for the number of electrons that flows into ($\Delta Q_A^{VDD} < 0$) or out of ($\Delta Q_A^{VDD} > 0$) the Voronoi cell of a nucleus A as the result of the interaction between the two molecular fragments.

Theoretical IR spectra

Calculating the IR frequencies and normal modes with ADF yields peak heights (intensity) and positions (frequency in wavenumbers cm^{-1}) while BAND only positions; in this case, each vibration has an intensity of 1. The theoretical spectra presented in this work have been created by extracting the frequencies and peaks of ADF/BAND calculations and plotting them with a Lorentzian curve (width of 1) on a grid between 4000- and 400 cm^{-1} (18000 points with a spacing of 0.2). The resulting spectra were scaled to the maximum peak height found in the experimental section. The settings for the spacing and Lorentzian curve width were chosen to resemble the experimental spectrum as closely as possible.

The frequency of a vibration is given by the following formula which can be derived from the quantum harmonic oscillator model:

$$\widetilde{w} = \frac{1}{2\pi\tilde{c}}\sqrt{\frac{k}{u}} \tag{S6}$$

With $\widetilde{w}$ being the wavenumber in cm^{-1}, $\tilde{c}$ the speed of light in cm s^{-1}, u the reduced mass, and k the force constant associated with a quantum harmonic oscillator. Upon forming hydrogen bonds comprised of C=O and H–N, the individual bonds are weakened, lowering their force constants and shifting the peak to the right on a spectrum plotted from high to low wavenumbers (redshift). Upon increasing the temperature, the reverse happens: hydrogen bonds are weakened, and the vibrations of the individual bonds shift to the left (blueshift).

6. Molecular characterization data

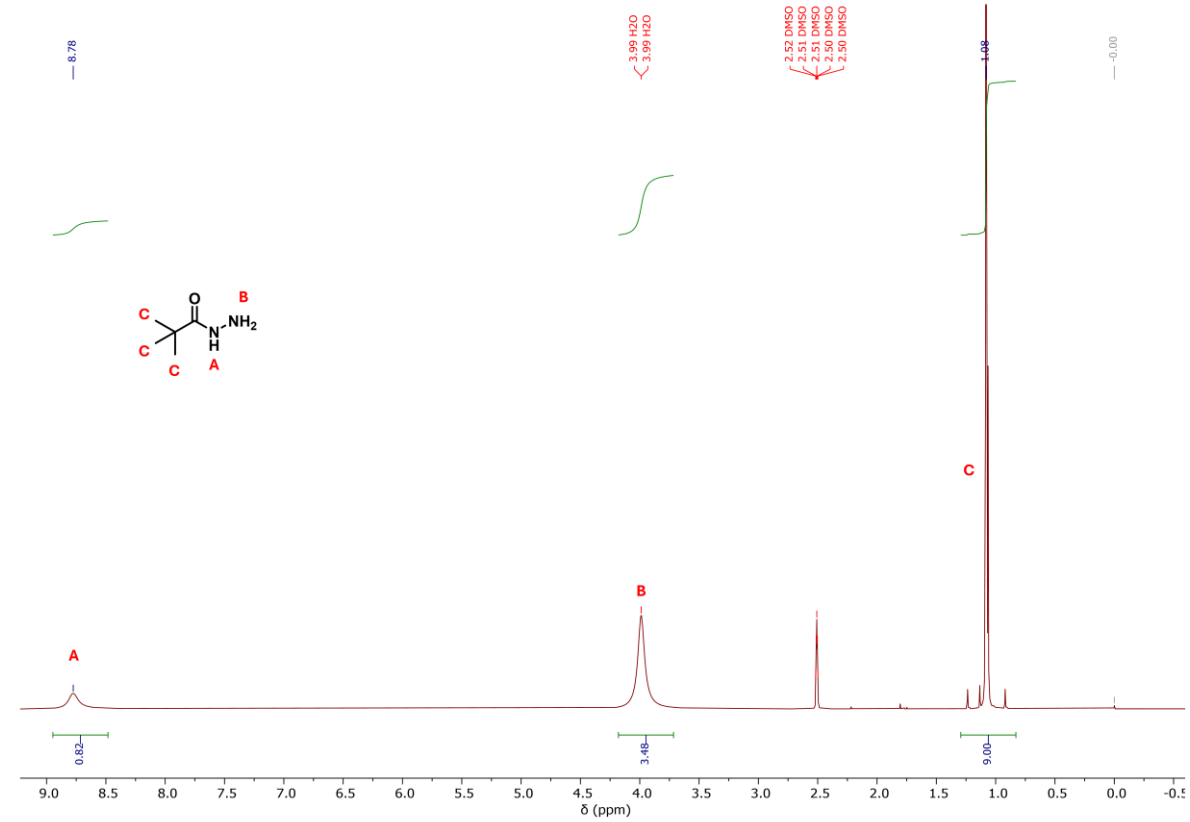

Figure S27: ^{1}H NMR spectrum of *tert*-butyl hydrazide in DMSO-d_6.

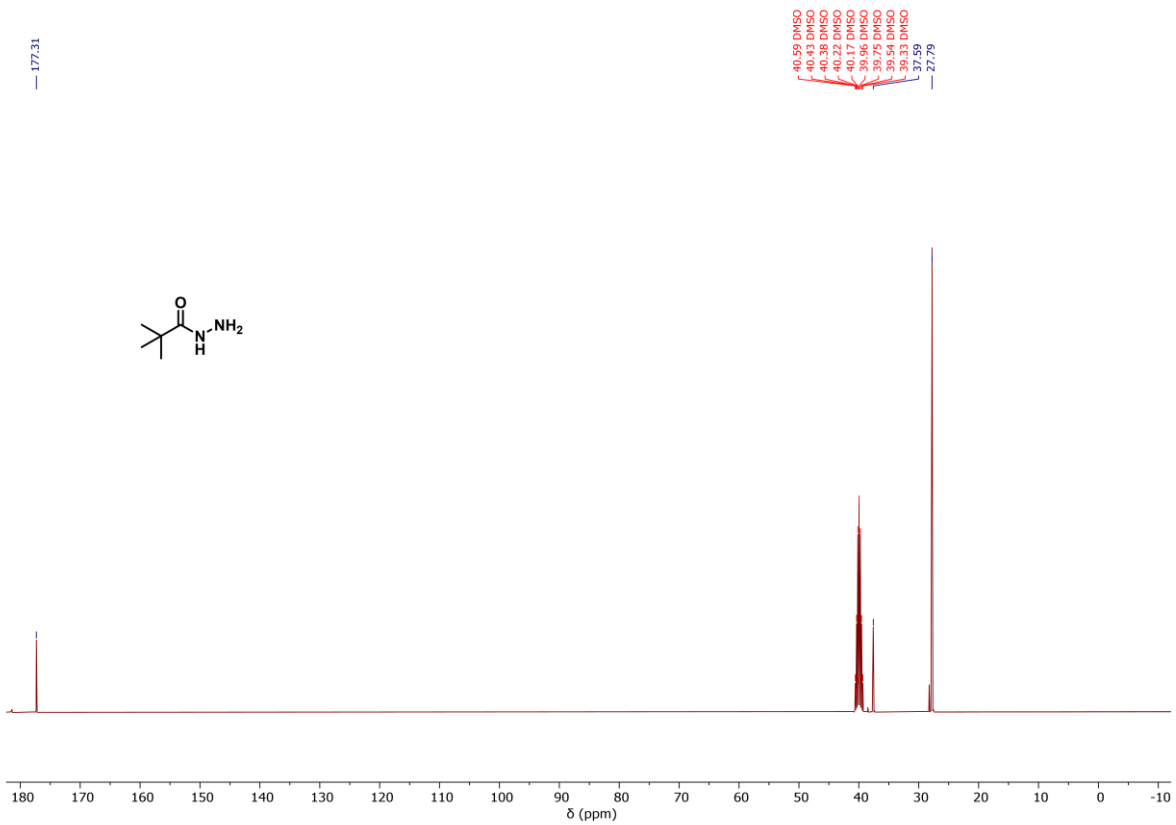

Figure S28: ^{13}C NMR spectrum of *tert*-butyl hydrazide in DMSO-d_6.

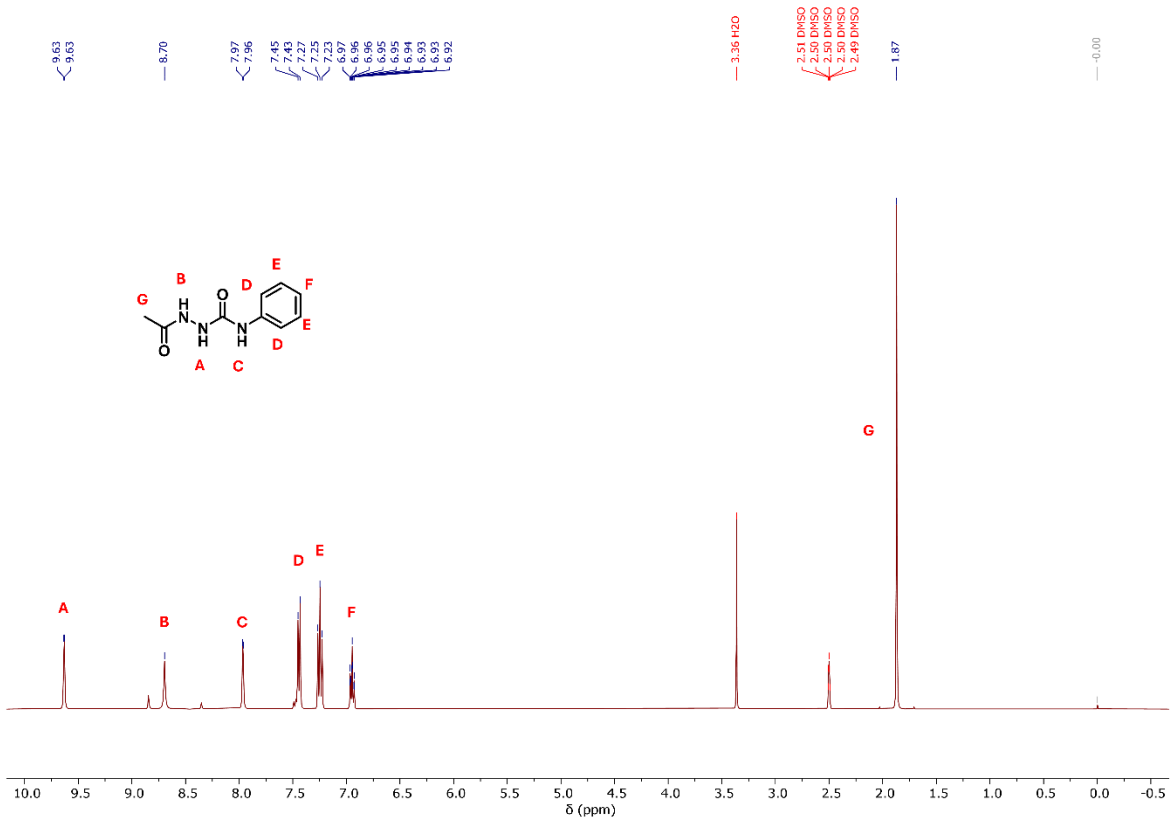

Figure S29: ^{1}H NMR spectrum of MeASCPh in DMSO-d_6.

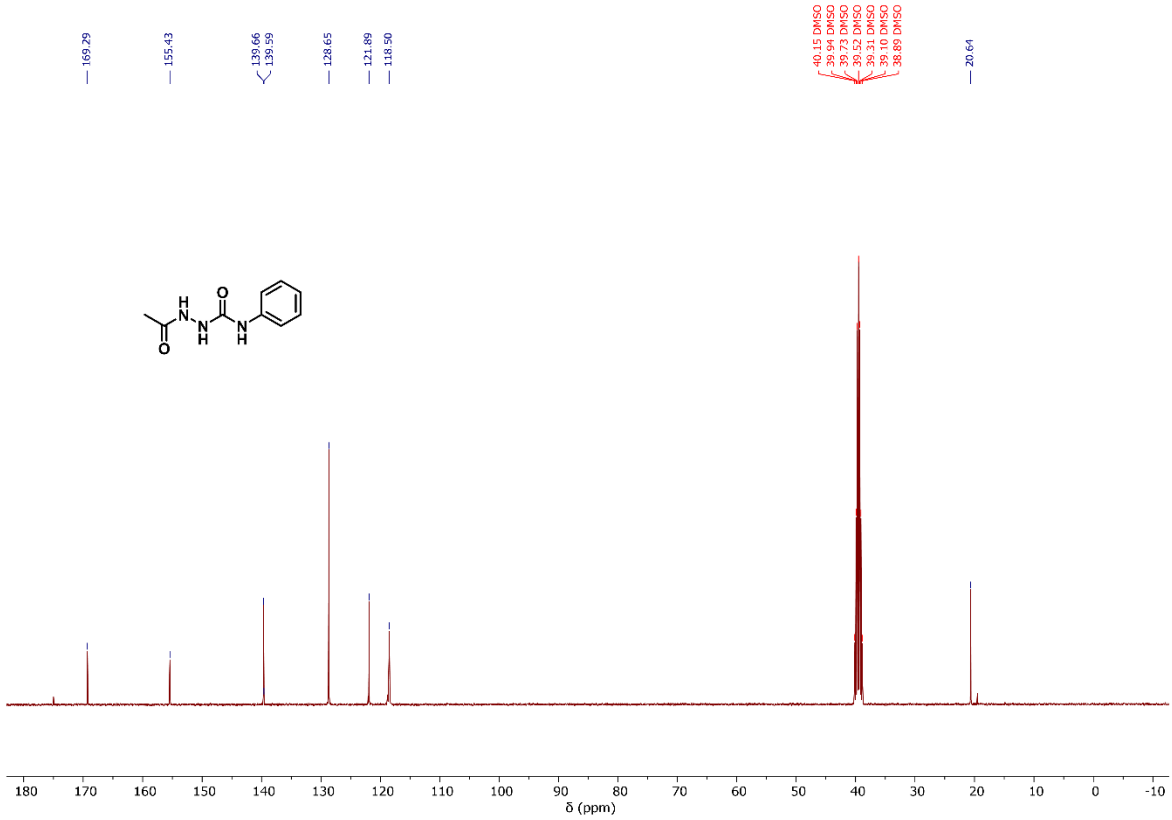

Figure S30: ^{13}C NMR spectrum of MeASCPh in DMSO-d_6.

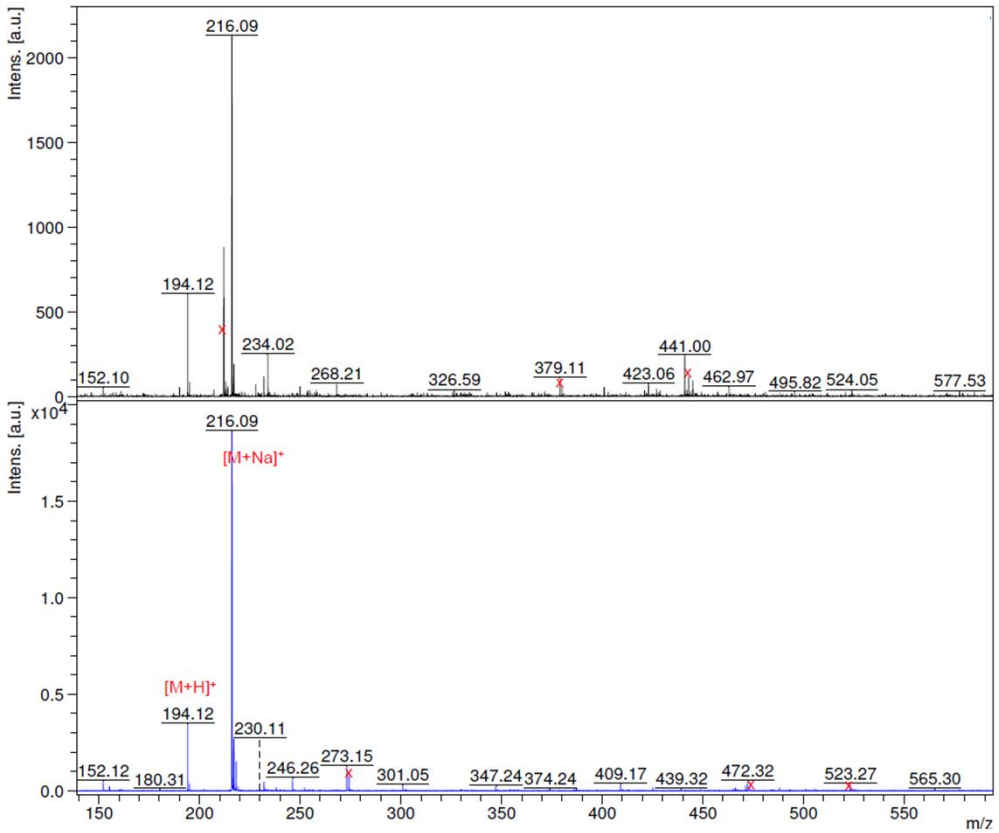

Figure S31: MALDI-ToF-MS spectra of MeASCPh (black: CHCA, blue: DCTB maxtrix). Known matrix peaks indicated with x.

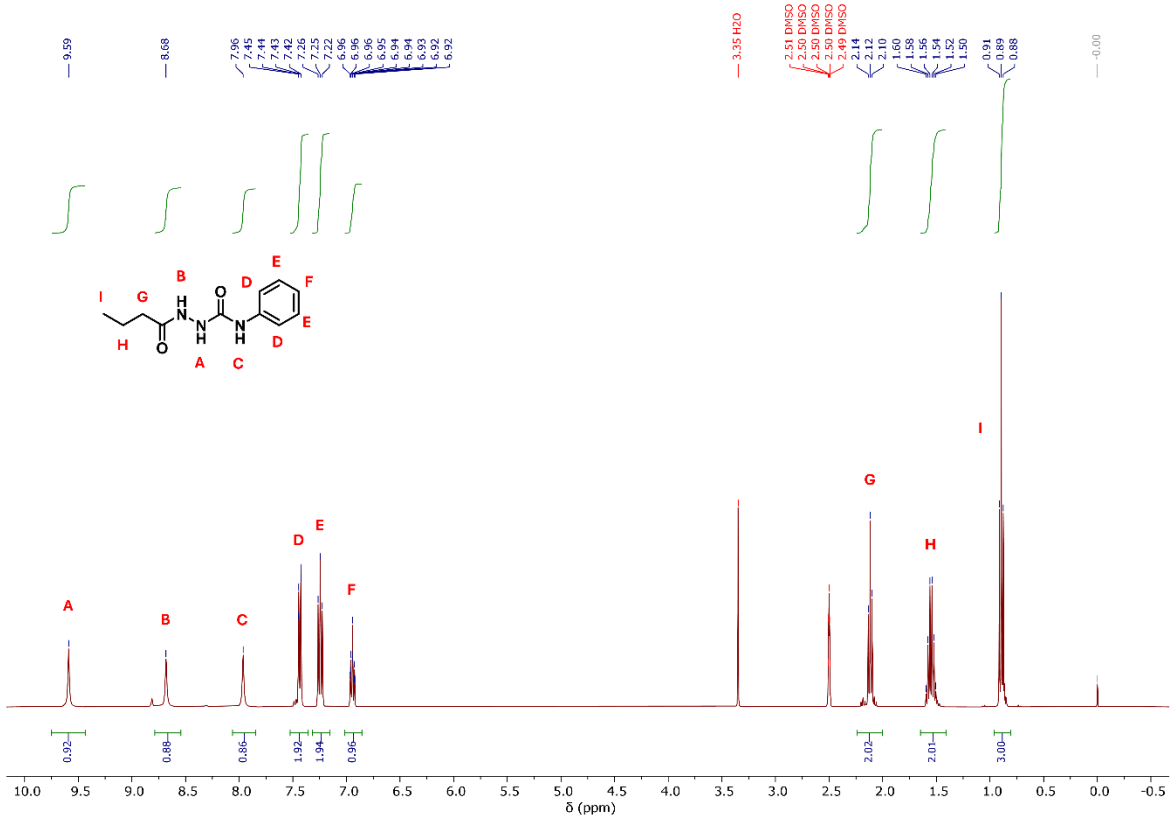

Figure S32: ^{1}H NMR spectrum of BuASCPh in DMSO-d_6.

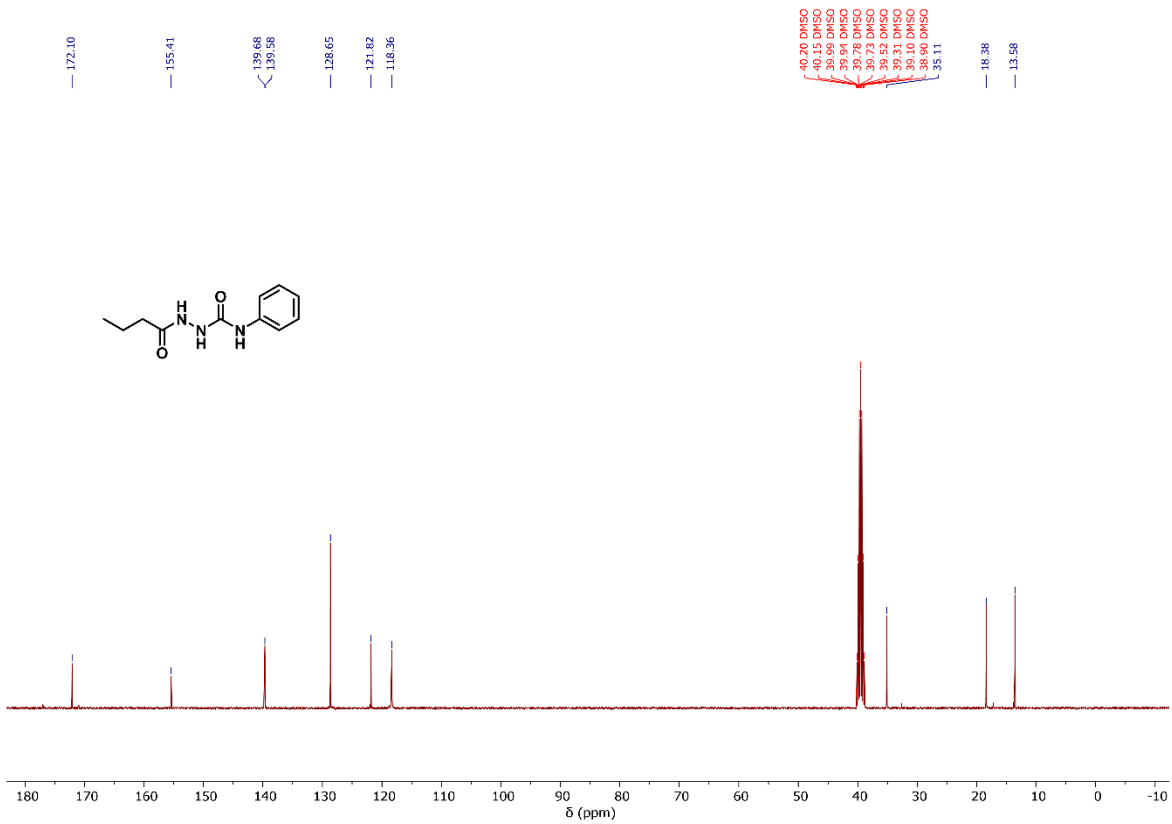

Figure S33*:* ^{13}C NMR spectrum of BuASCPh in DMSO-d_6.

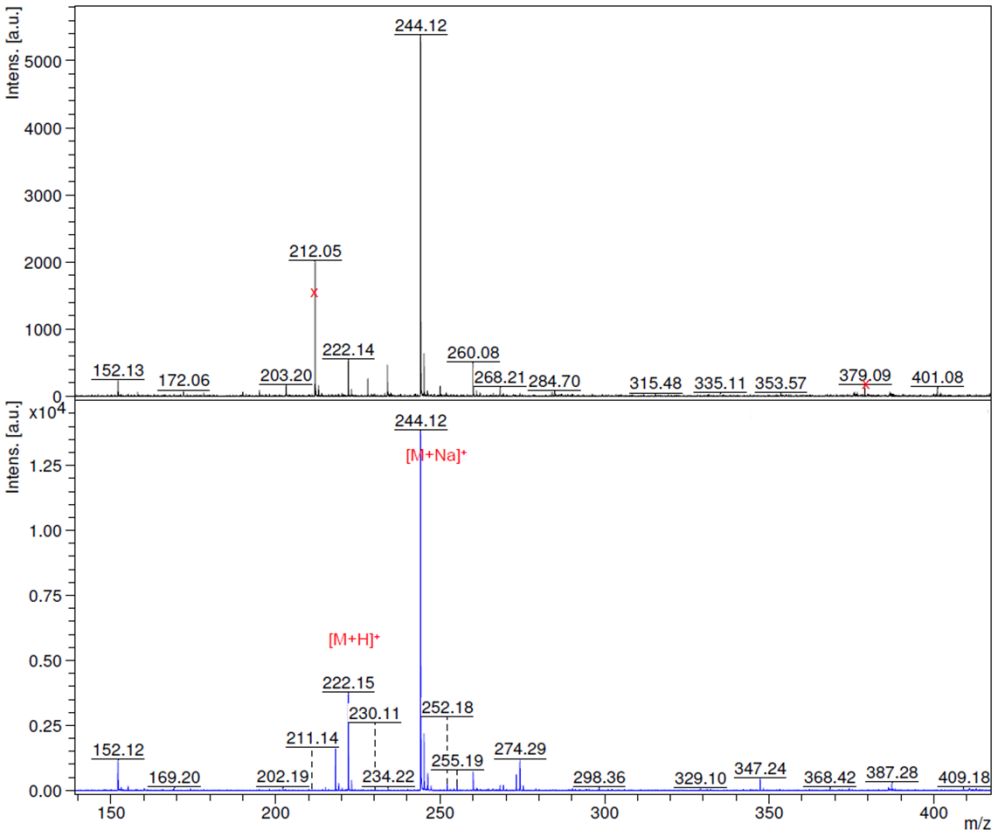

Figure S34: MALDI-ToF-MS spectra of BuASCPh (black: CHCA, blue: DCTB maxtrix). Known matrix peaks indicated with x.

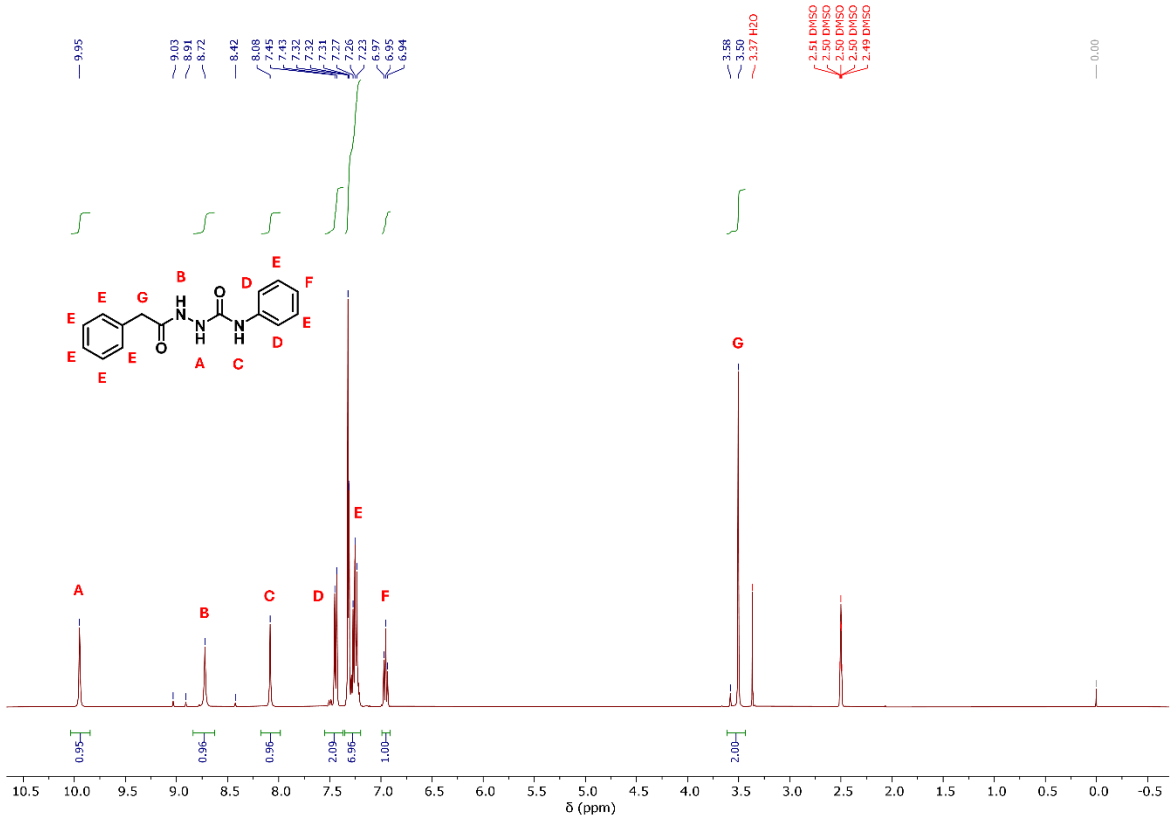

Figure S35*:* ^{1}H NMR spectrum of BnASCPh in DMSO-d_6.

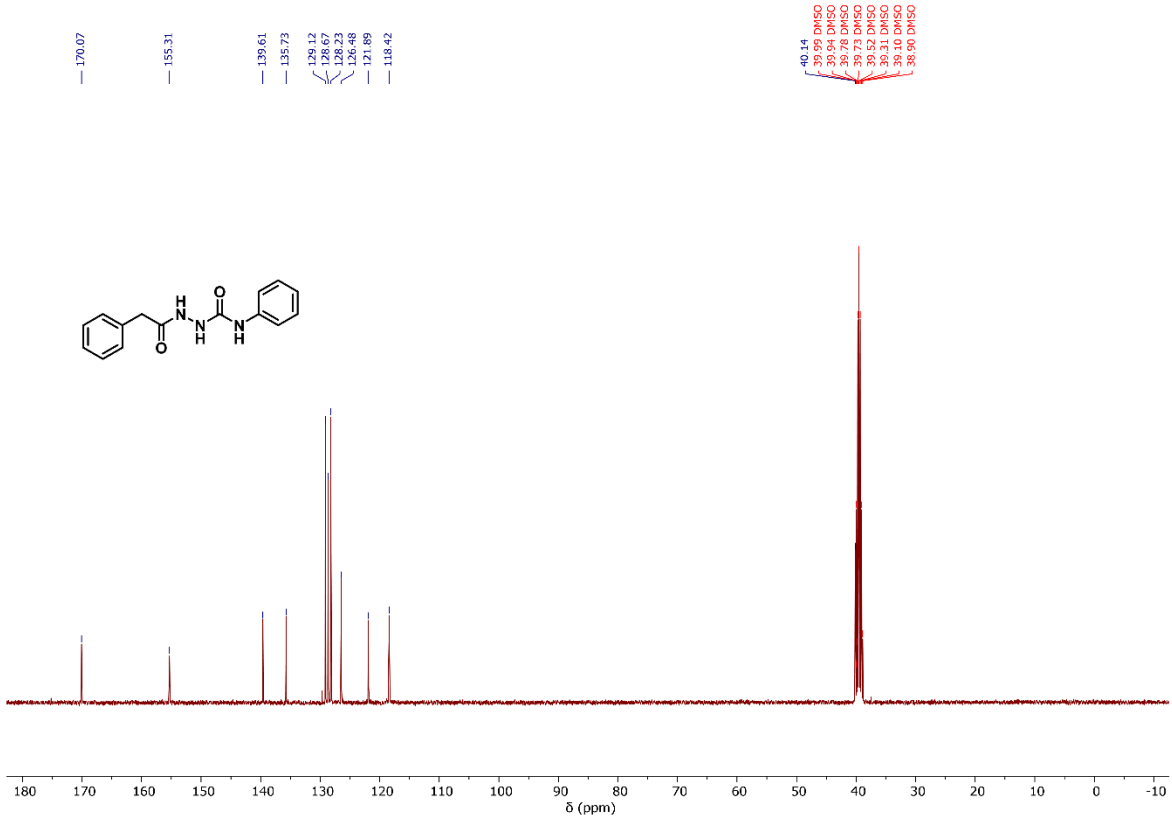

Figure S36: ^{13}C NMR spectrum of BnASCPh in DMSO-d_6.

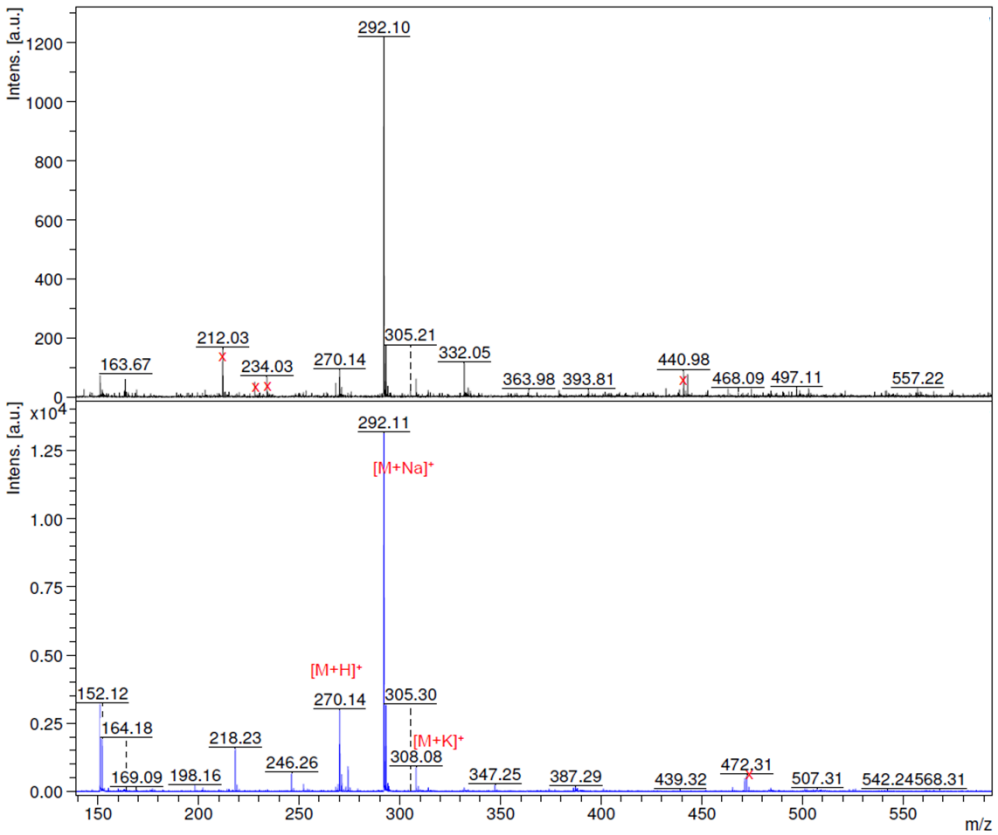

Figure S37: MALDI-ToF-MS spectra of BnASCPh (black: CHCA, blue: DCTB maxtrix). Known matrix peaks indicated with x.

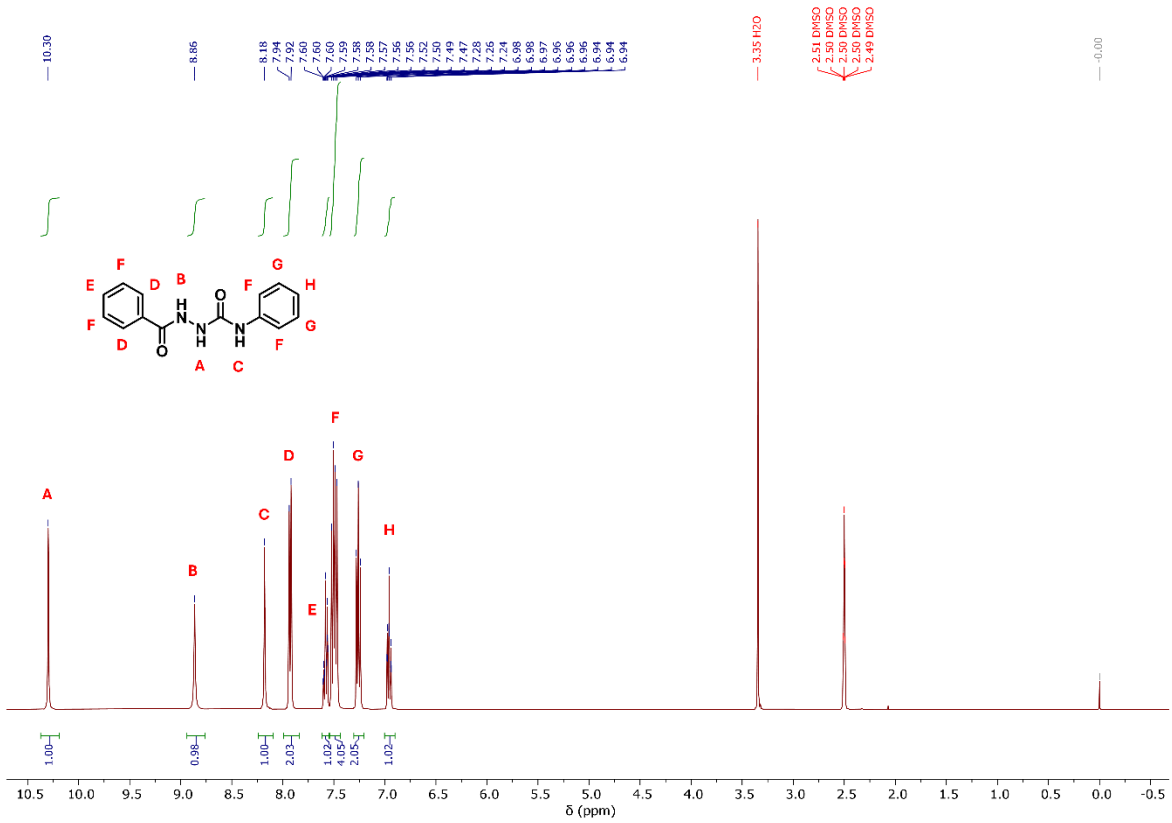

Figure S38: ^{1}H NMR spectrum of PhASCPh in DMSO-d_6.

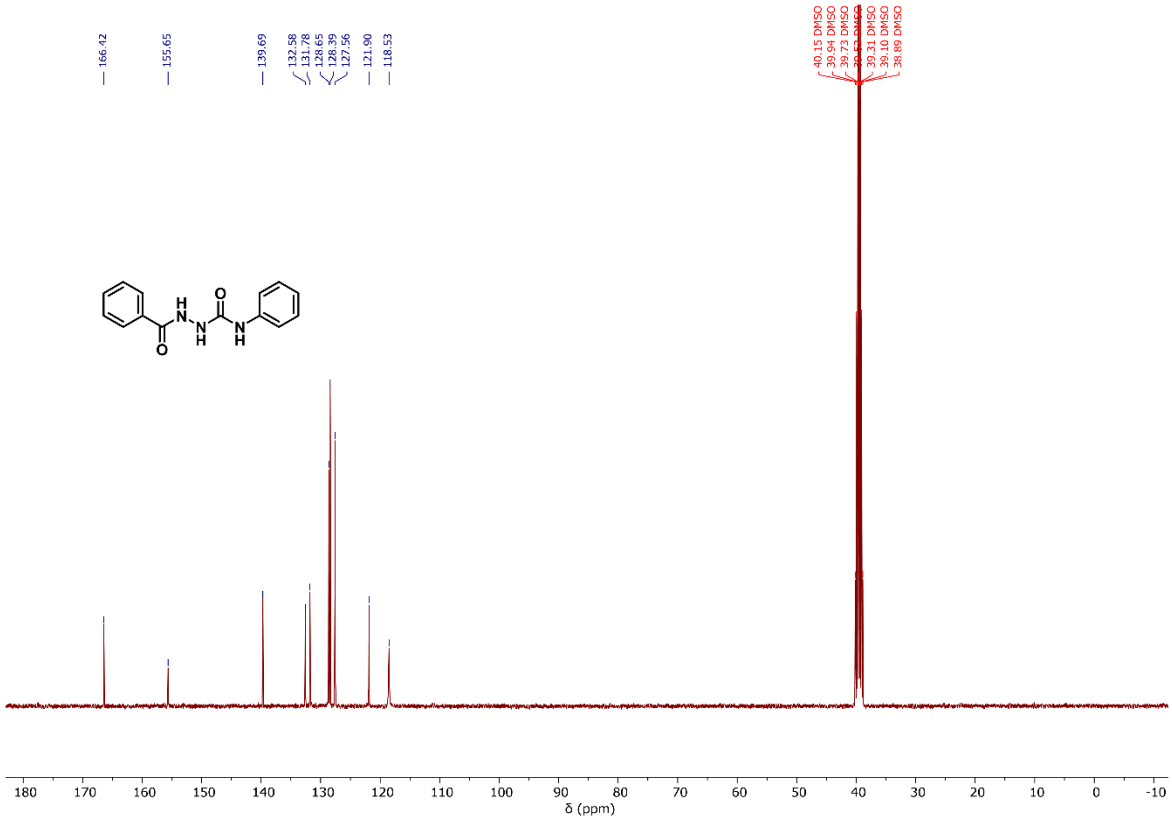

Figure S39: ^{13}C NMR spectrum of PhASCPh in DMSO-d_6.

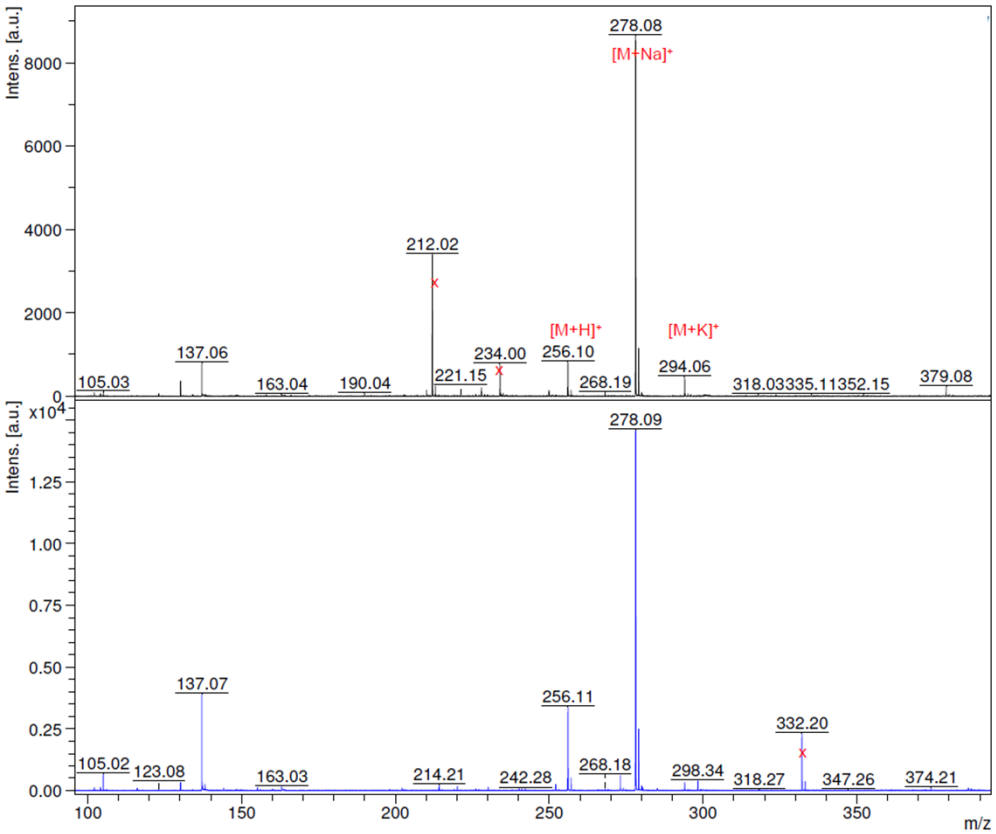

Figure S40: MALDI-ToF-MS spectra of PhASCPh (black: CHCA, blue: DCTB maxtrix). Known matrix peaks indicated with x.

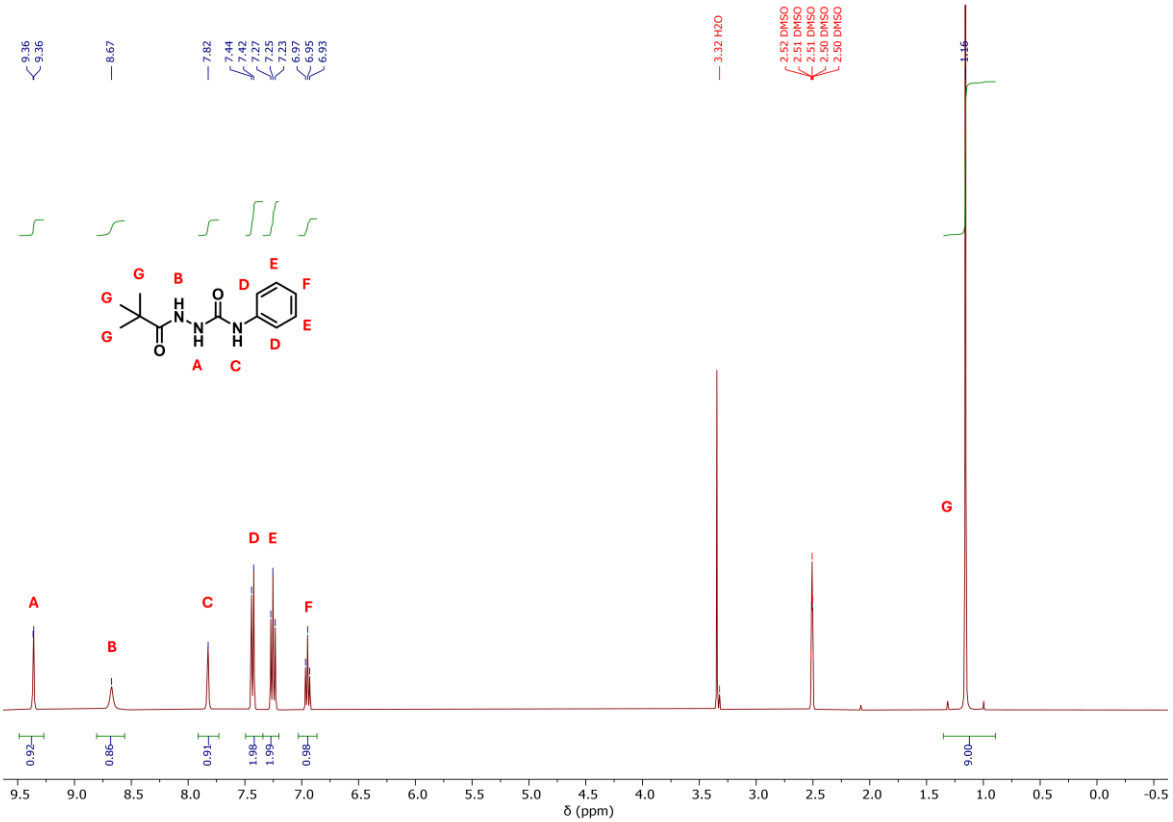

Figure S41: ^{1}H NMR spectrum of *t*-BuASCPh in DMSO-d_6.

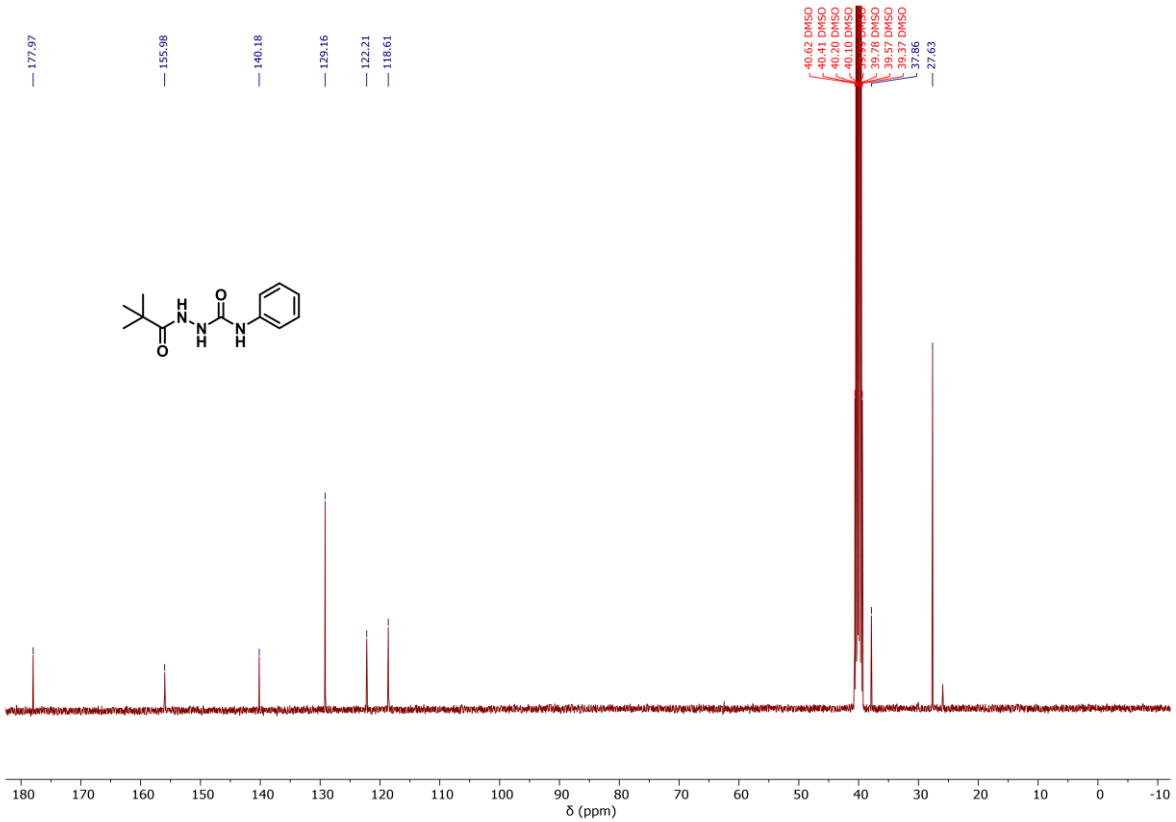

Figure S42: ^{13}C NMR spectrum of *t*-BuASCPh in DMSO-d_6.

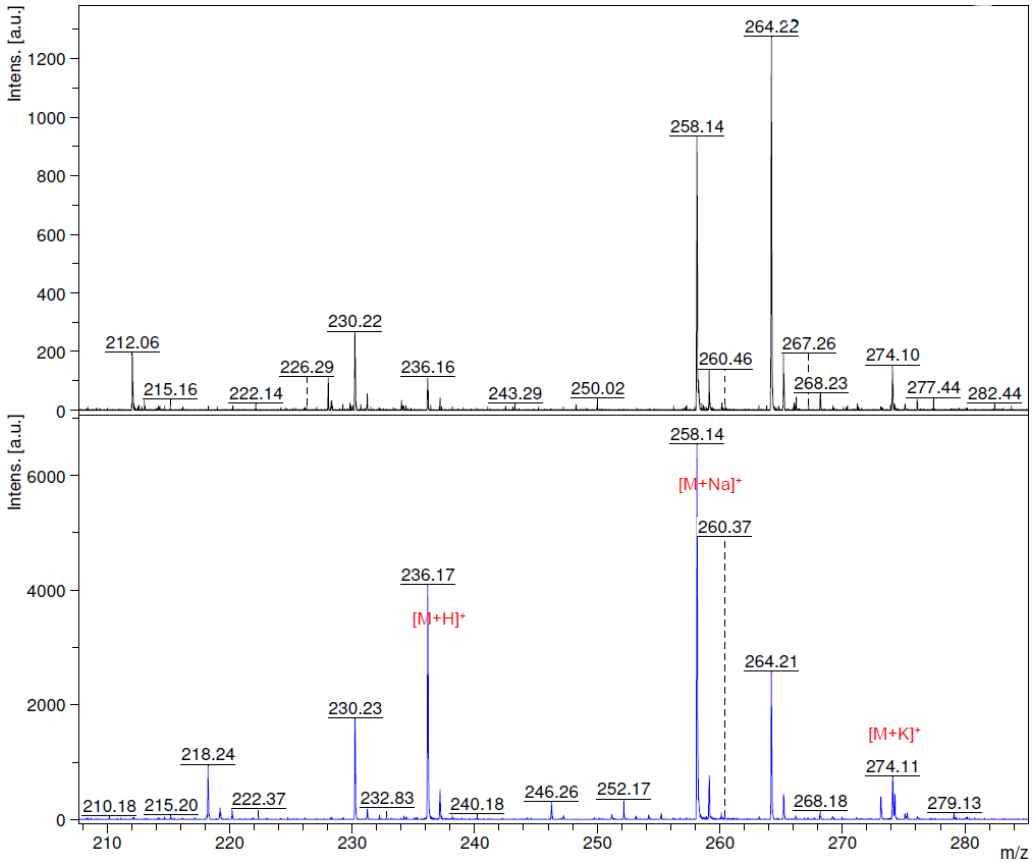

Figure S43: MALDI-ToF-MS spectra of PhASCPh (black: CHCA, blue: DCTB maxtrix). Known matrix peaks indicated with x.

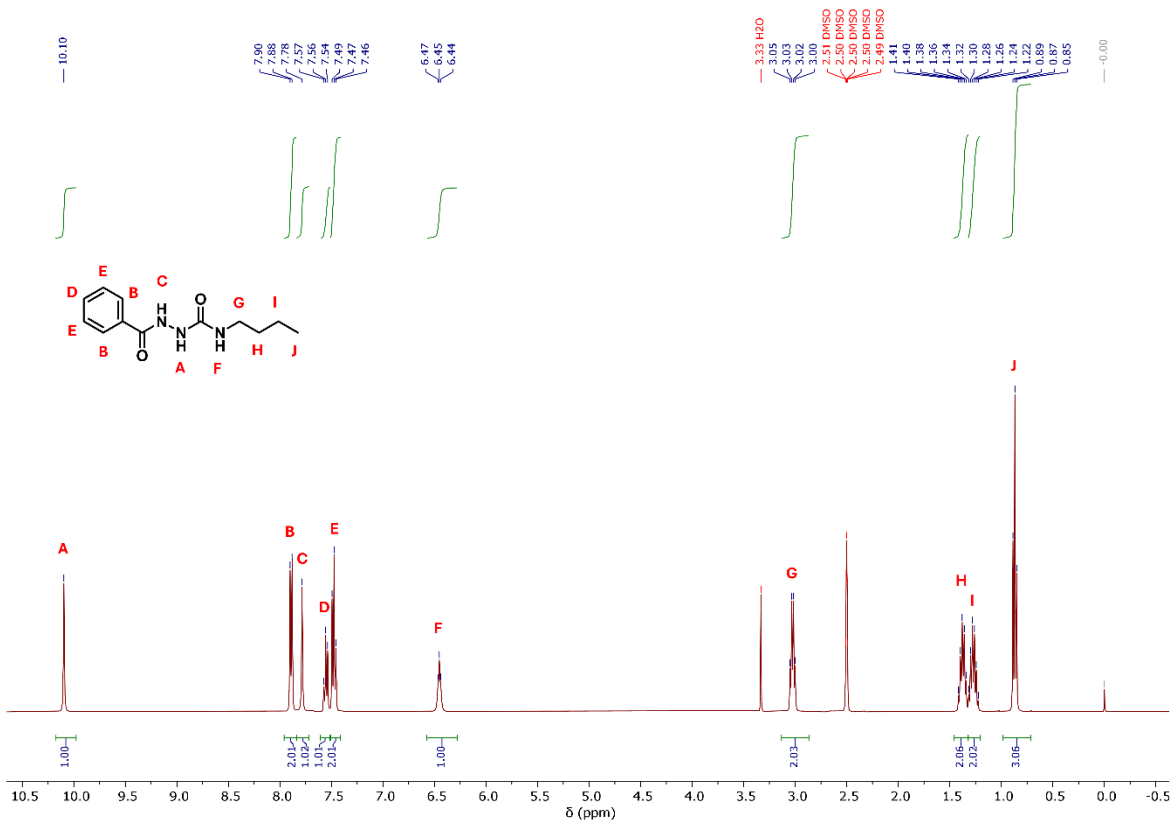

Figure S44: ^{1}H NMR spectrum of PhASCBu in DMSO-d_6.

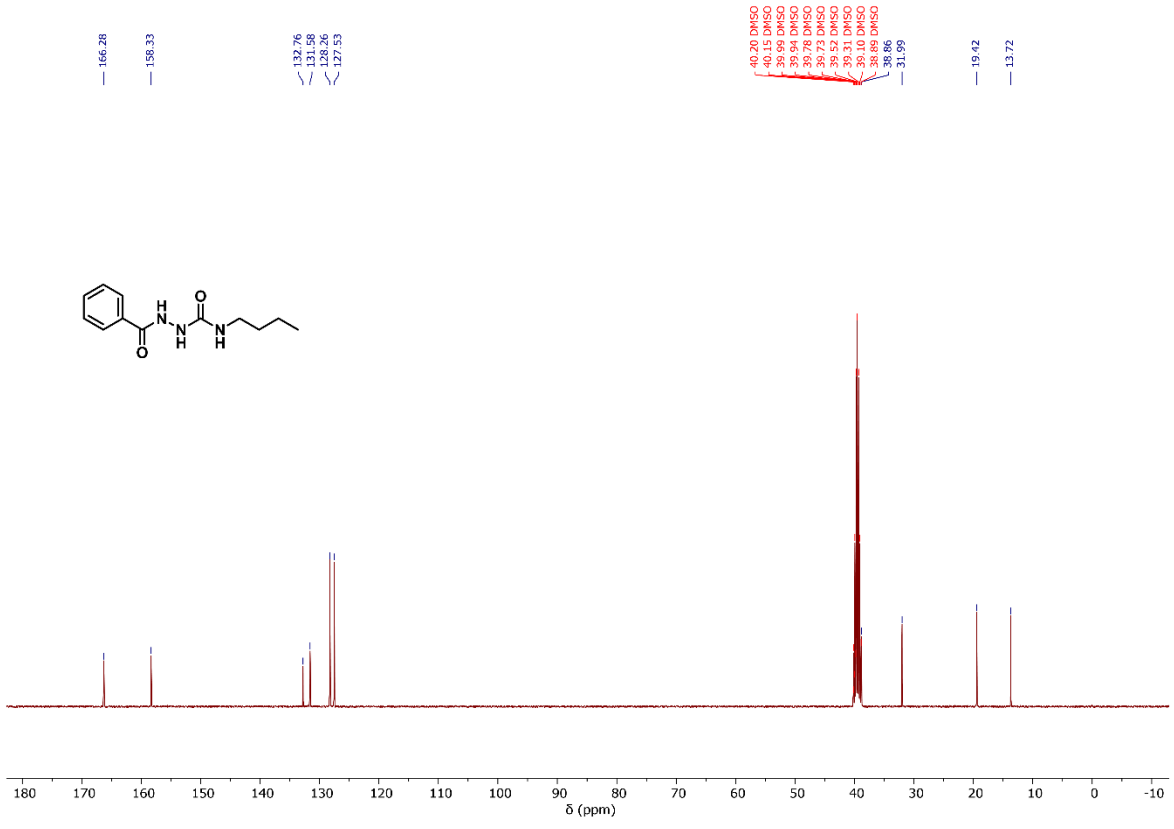

Figure S45: ^{13}C NMR spectrum of PhASCBu in DMSO-d_6.

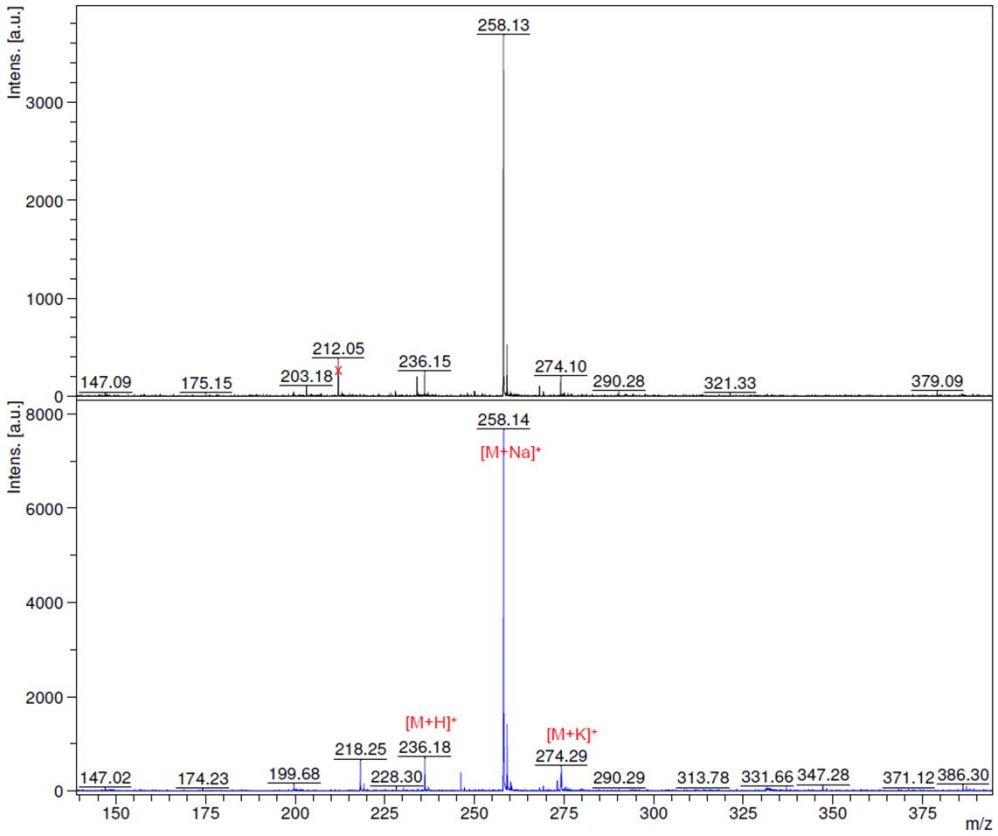

Figure S46: MALDI-ToF-MS spectra of PhASCBu (black: CHCA, blue: DCTB maxtrix). Known matrix peaks indicated with x.

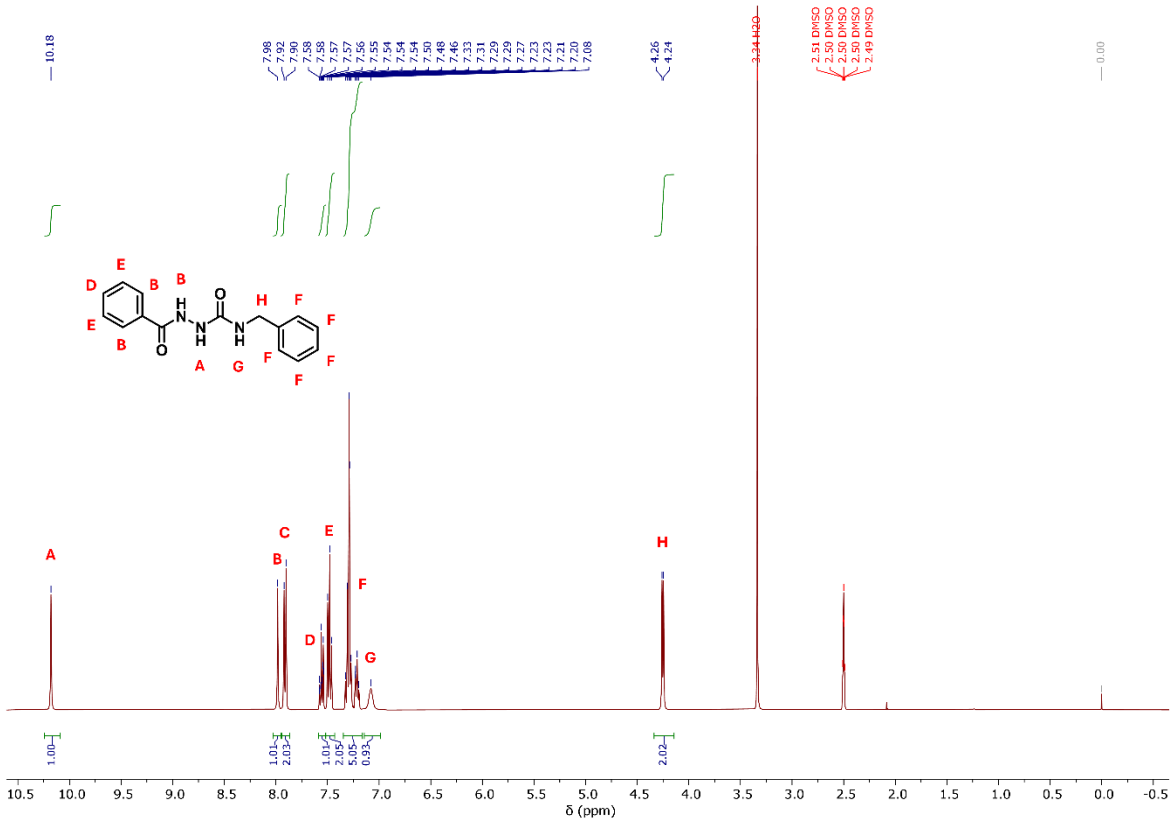

Figure S47: ^{1}H NMR spectrum of PhASCBn in DMSO-d_6.

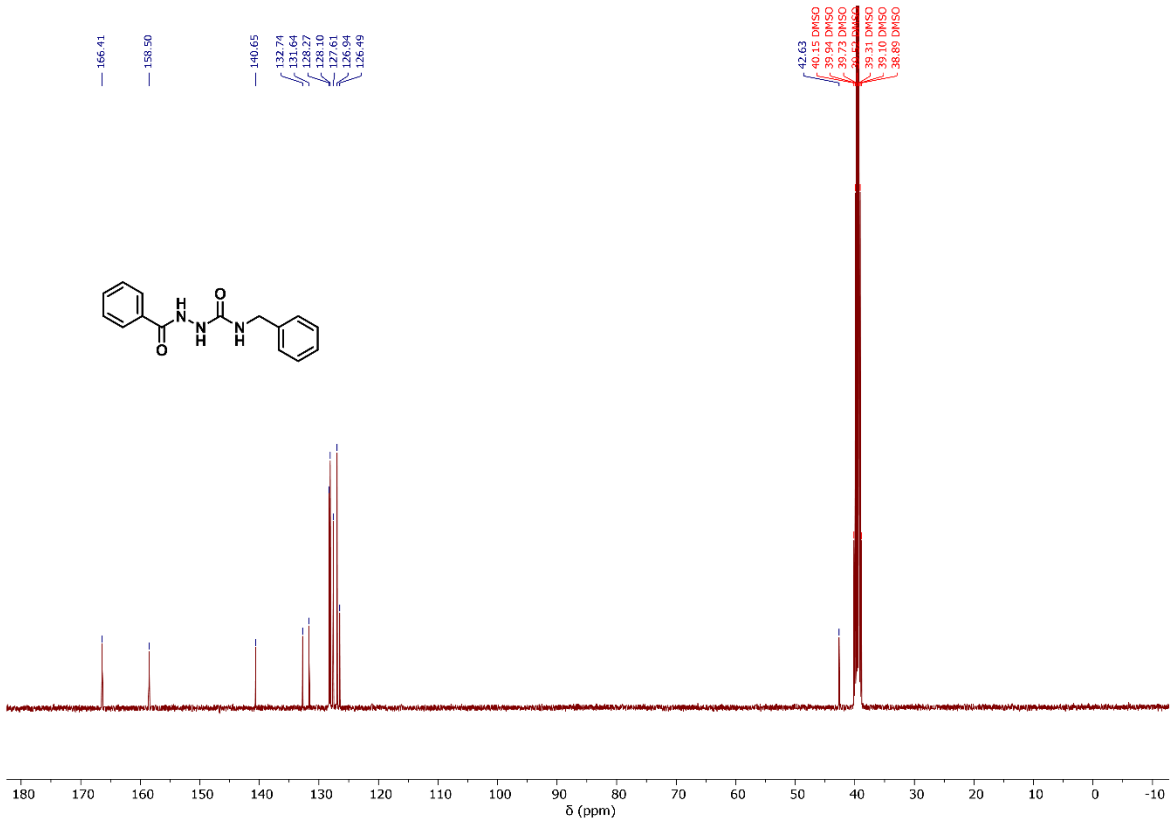

Figure S48: ^{13}C NMR spectrum of PhASCBn in DMSO-d_6.

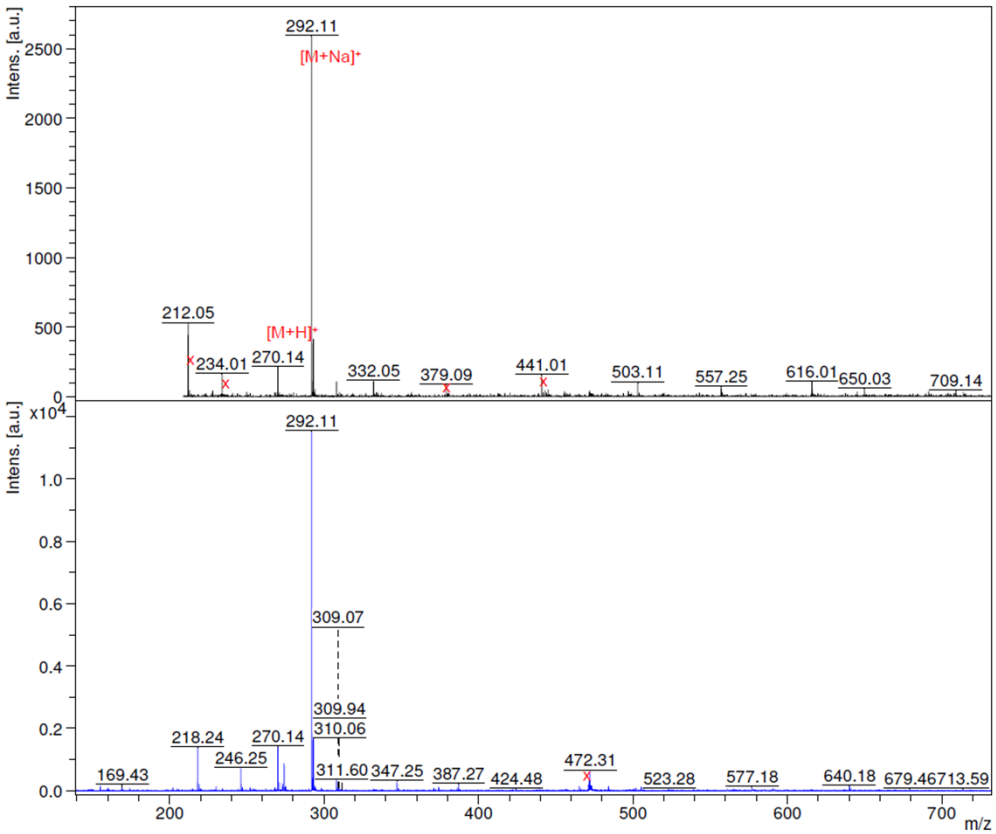

Figure S49: MALDI-ToF-MS spectra of PhASCBn (black: CHCA, blue: DCTB maxtrix). Known matrix peaks indicated with x.

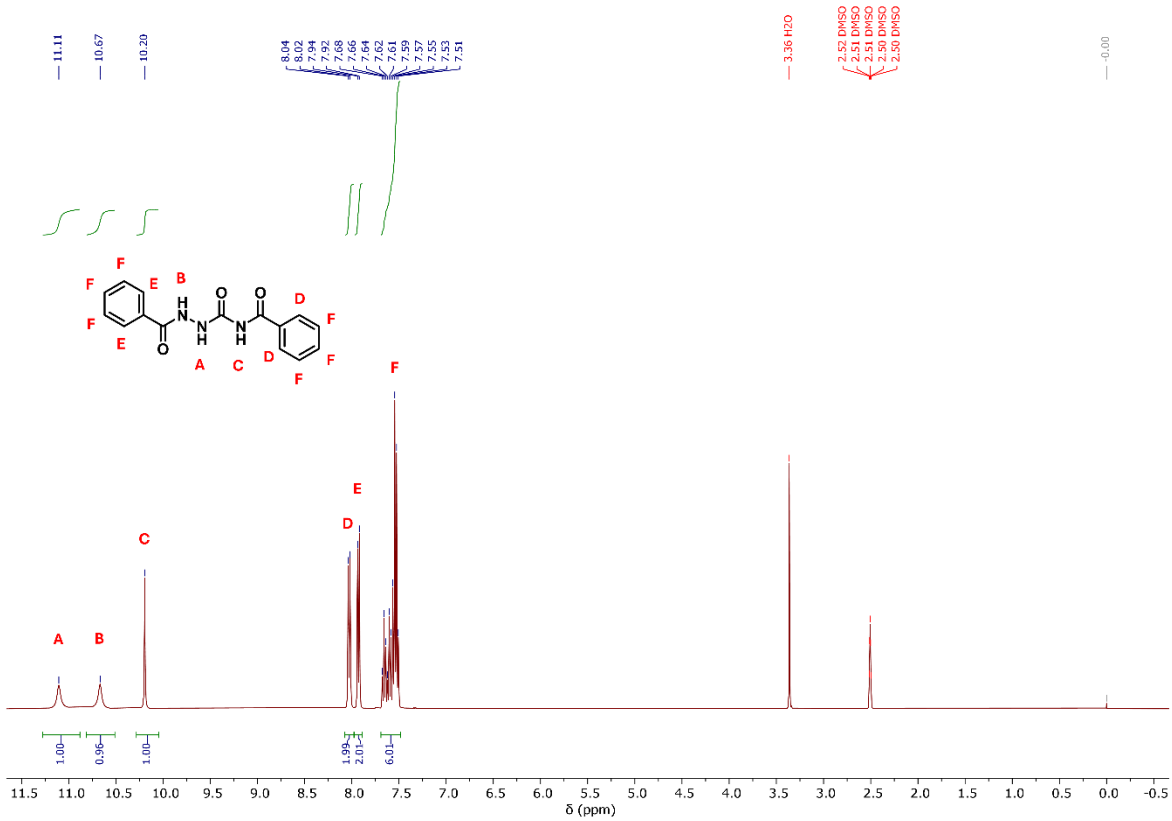

Figure S50: ^{1}H NMR spectrum of PhASCBz in DMSO-d_6.

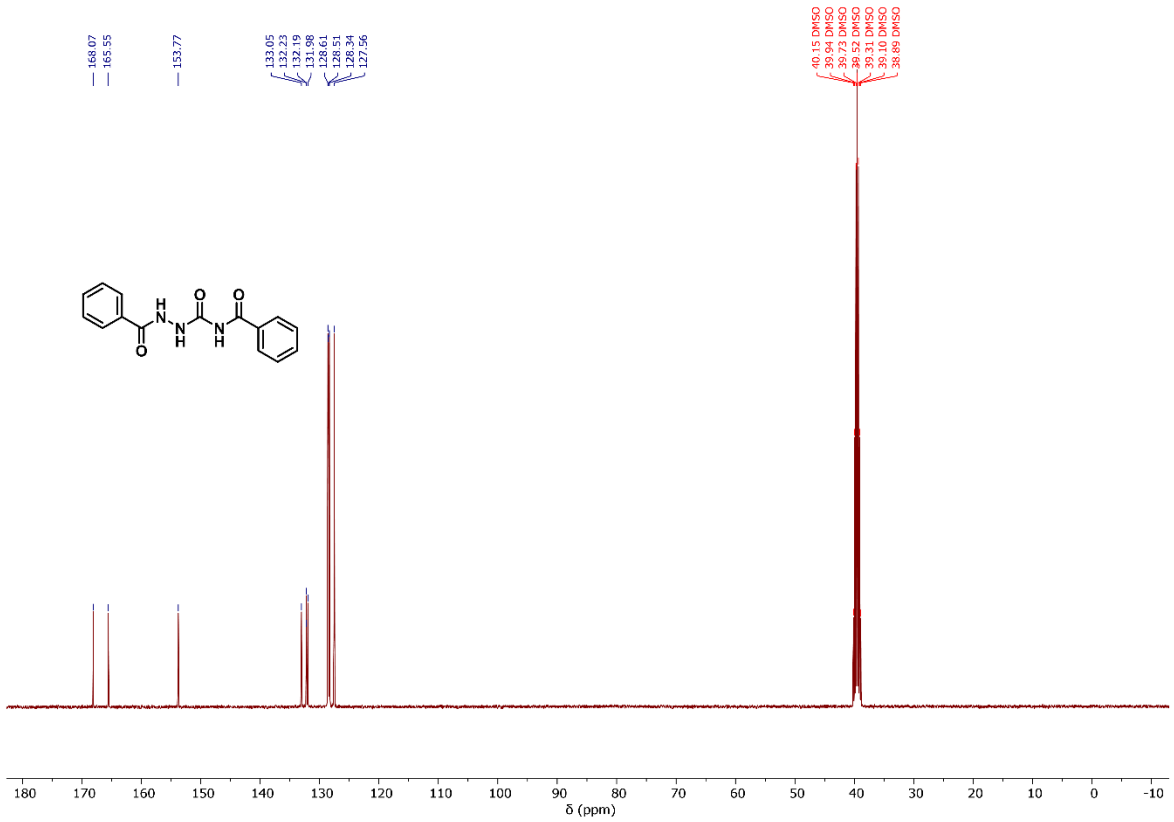

Figure S51: ^{13}C NMR spectrum of PhASCBz in DMSO-d_6.

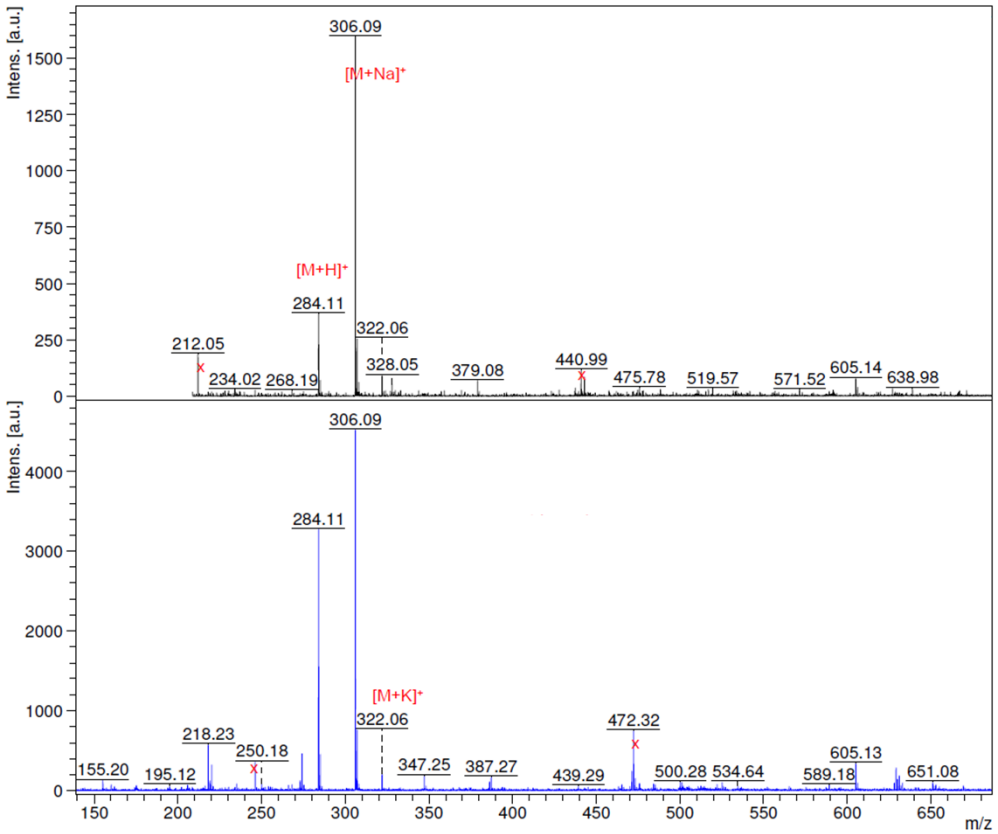

Figure S52: MALDI-ToF-MS spectra of PhASCBz (black: CHCA, blue: DCTB maxtrix). Known matrix peaks indicated with x.

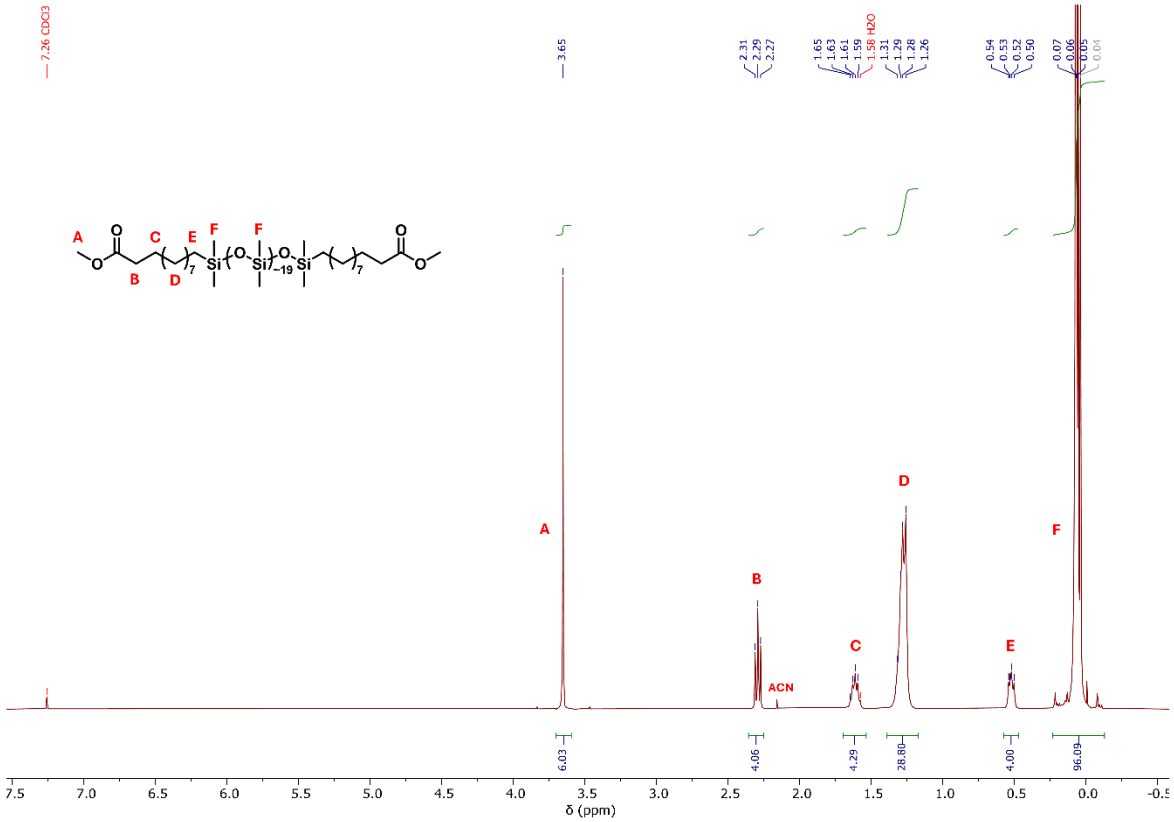

Figure S53: ^{1}H NMR spectrum of methyl ester terminated pDMS in $CDCl_3$.

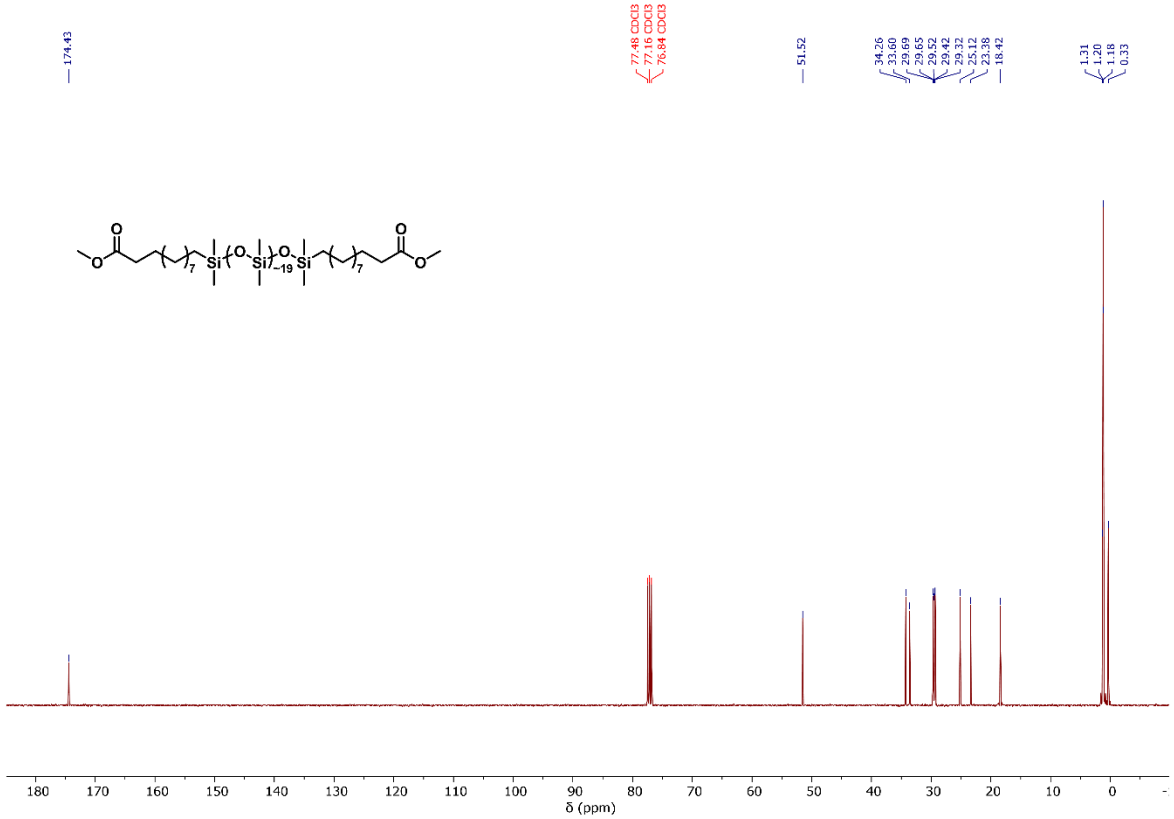

Figure S54: ^{13}C NMR spectrum of methyl ester terminated pDMS in $CDCl_3$.

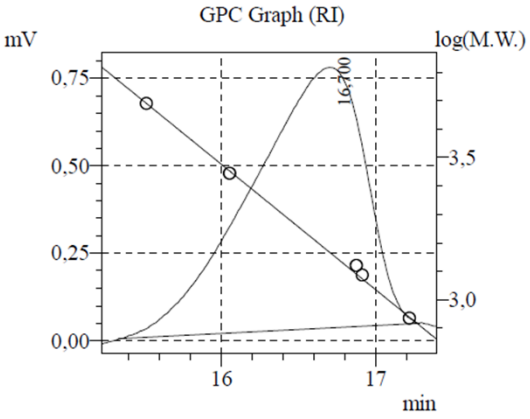

Total Average(RI)

Chromatogram Detector 2 Ch1

#	Mn	Mw	Mw/Mn
1	1714	1938	1,13035
	1714	1938	1,13035

Figure S55: SEC chromatogram (RI detector) of methyl ester terminated pDMS.

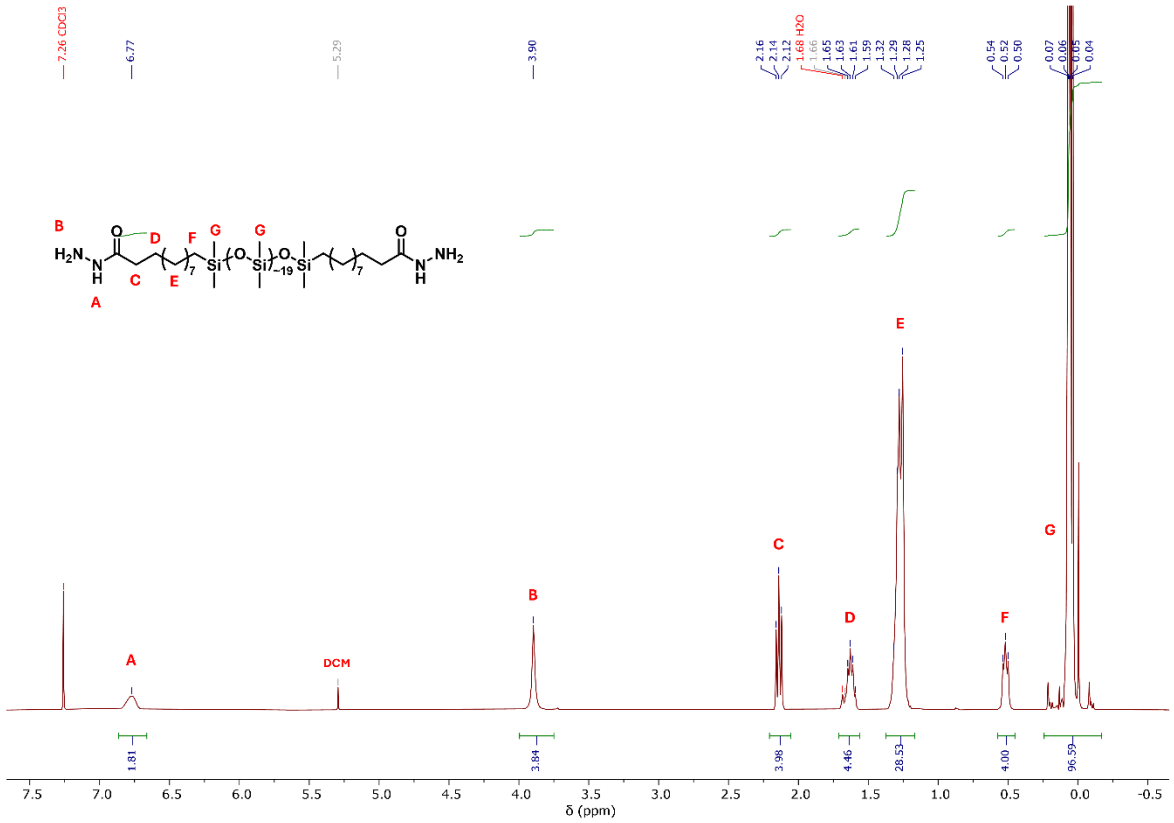

Figure S56: ^{1}H NMR spectrum of acyl hydrazide terminated pDMS in $CDCl_3$.

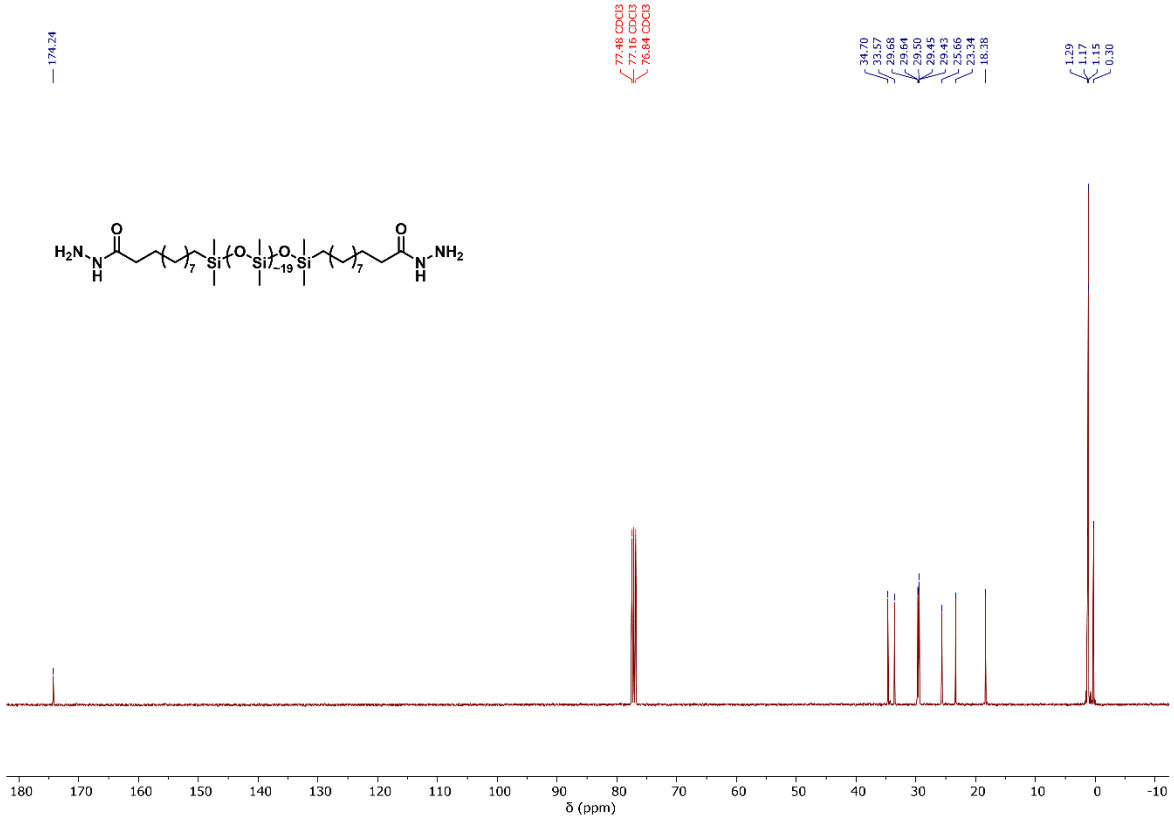

Figure S57: ^{13}C NMR spectrum of acyl hydrazide terminated pDMS in $CDCl_3$.

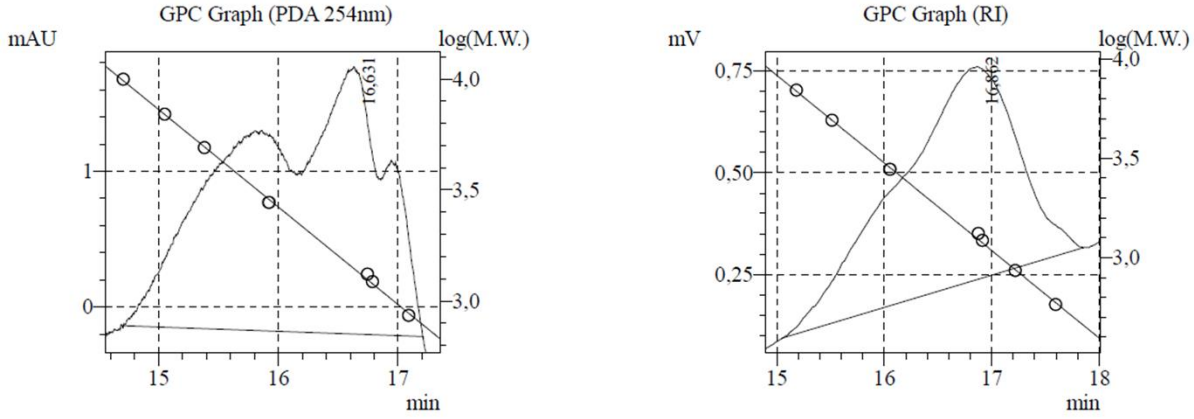

Total Average (PDA 254 nm)

Chromatogram PDA Ch1

#	Mn	Mw	Mz	Mw/Mn
1	1982	2775	3822	1,39976
	1982	2775	3822	1,39976

Total Average(RI)

Chromatogram Detector 2 Ch1

#	Mn	Mw	Mw/Mn
1	1446	1935	1,33847
	1446	1935	1,33847

Figure S58: SEC chromatogram (left: UV detector, right: RI detector) of acyl hydrazide terminated pDMS. Note: There are interactions of the molecule with the column which gives rise to the tailing in the SEC trace.

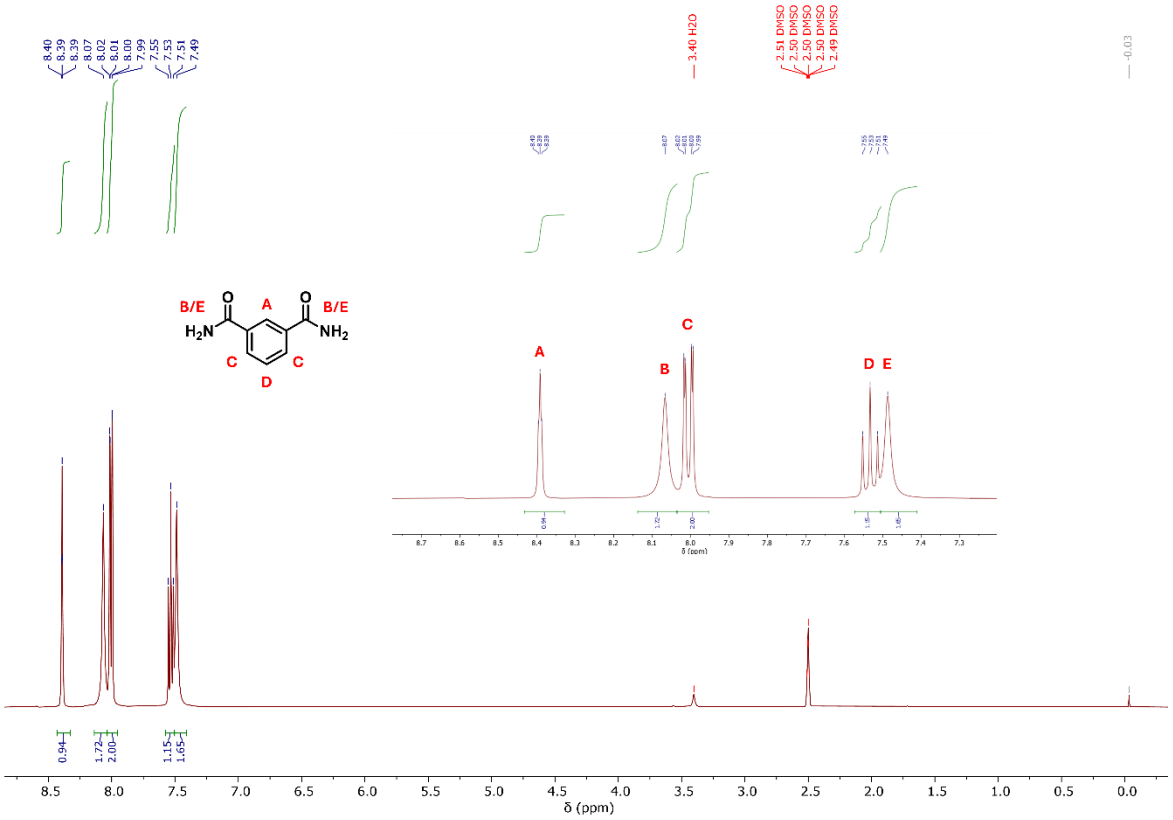

Figure S59: ^{1}H NMR spectrum of isophthalamide in DMSO-d_6.

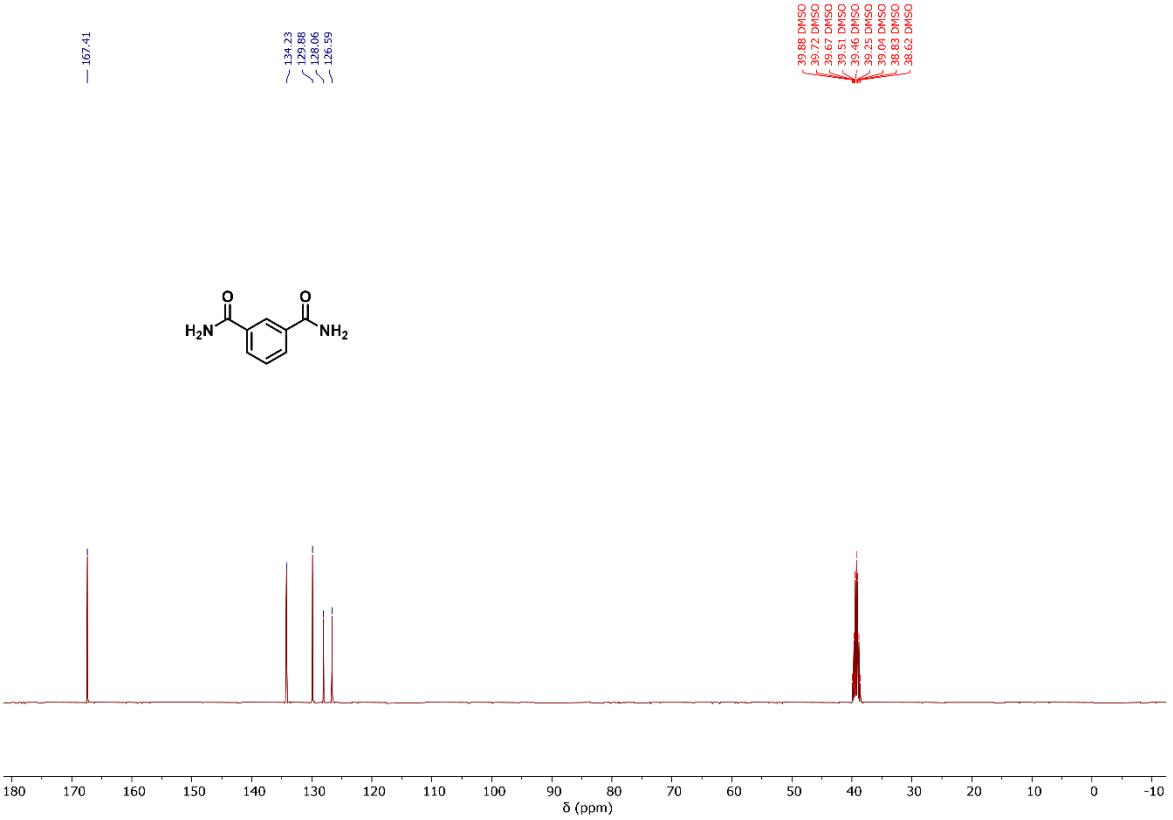

Figure S60: ^{13}C NMR spectrum of isophthalamide in DMSO-d_6.

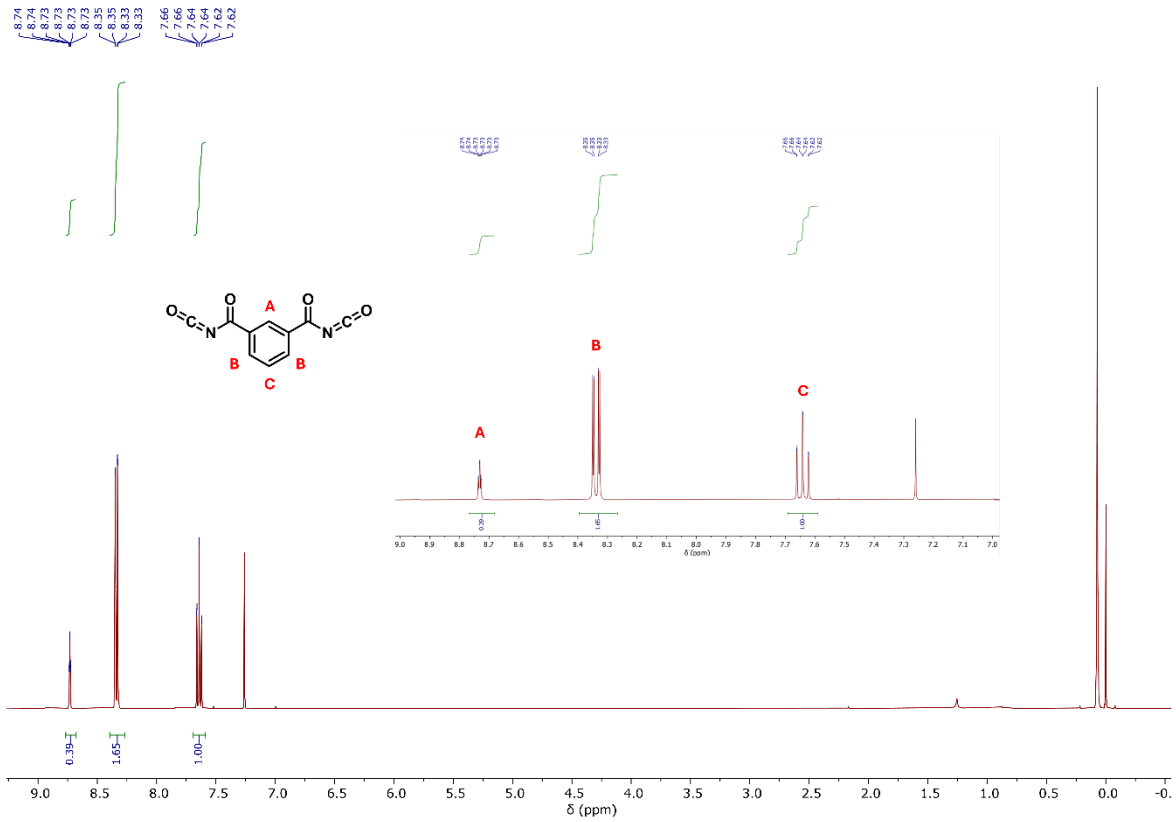

Figure S61: ^{1}H NMR spectrum of isophthaloyl diisocyanate in $CDCl_3$.

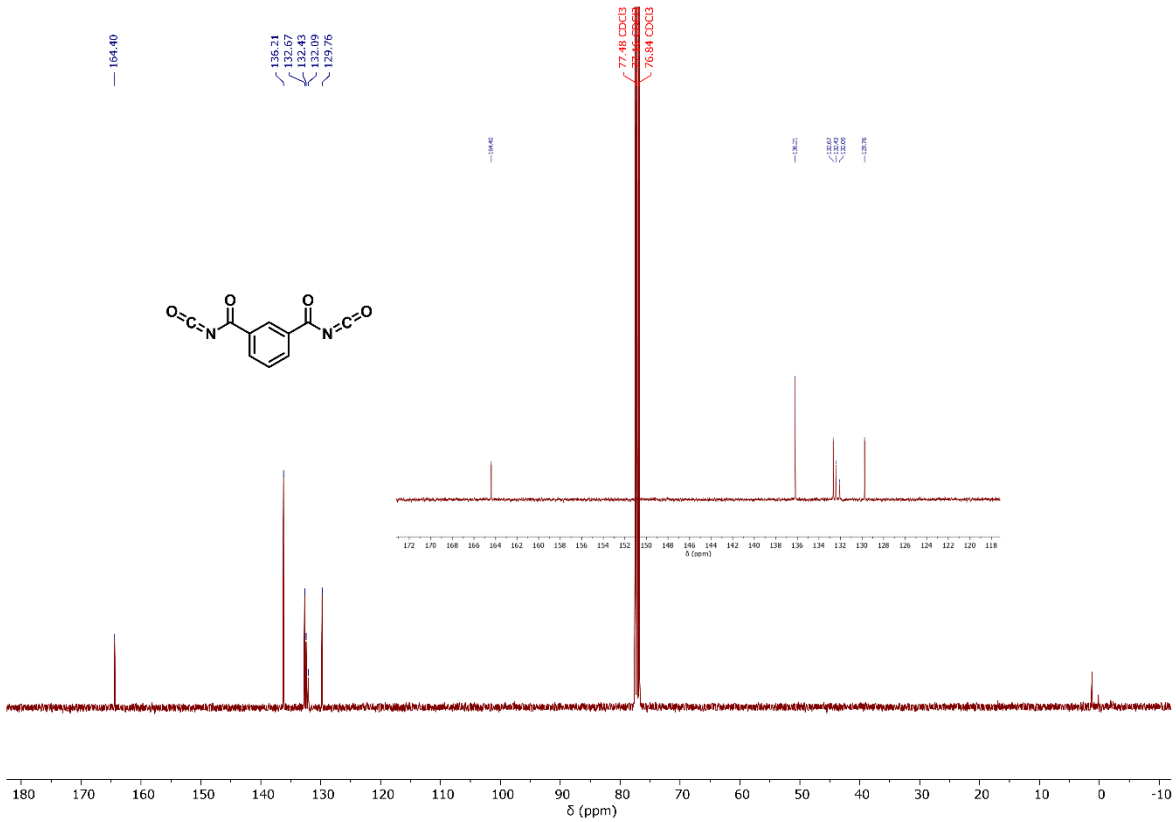

Figure S62: ^{13}C NMR spectrum of isophthaloyl diisocyanate in $CDCl_3$.

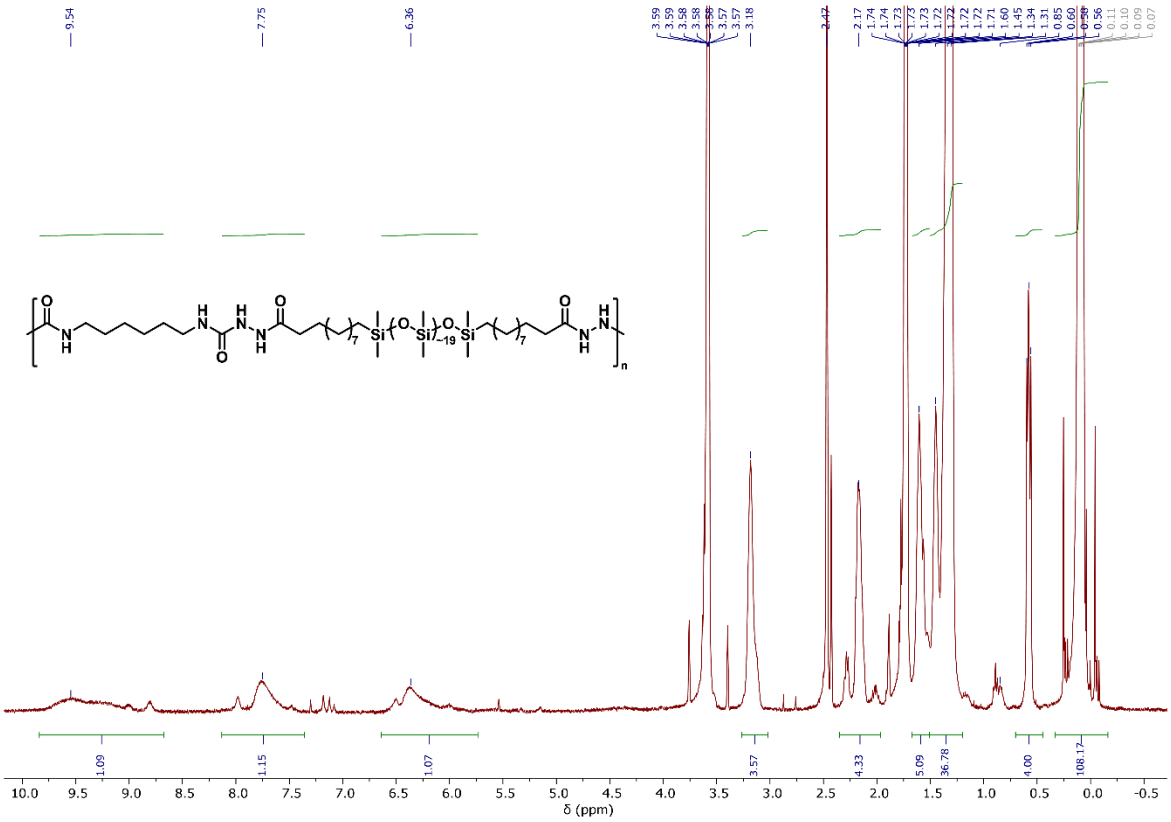

Figure S63: ^{1}H NMR spectrum of ASC-HDI in THF-d_8.

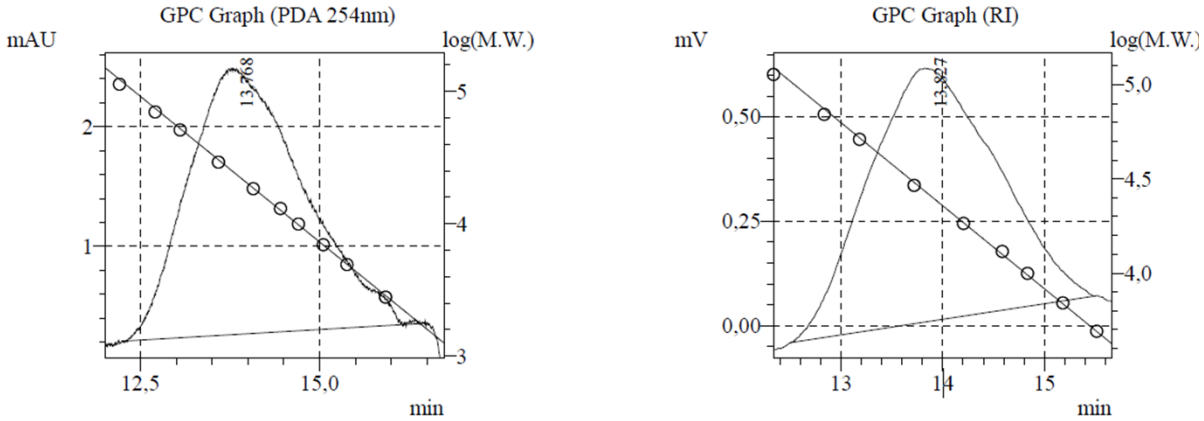

Total Average (PDA 254 nm)

Chromatogram PDA Ch1

#	Mn	Mw	Mz	Mw/Mn
1	13922	24239	36052	1,74108
	13922	24239	36052	1,74108

Total Average(RI)

Chromatogram Detector 2 Ch1

#	Mn	Mw	Mw/Mn
1	20854	28677	1,37509
	20854	28677	1,37509

Figure S64: SEC chromatogram (left: UV detector, right: RI detector) of ASC-HDI.

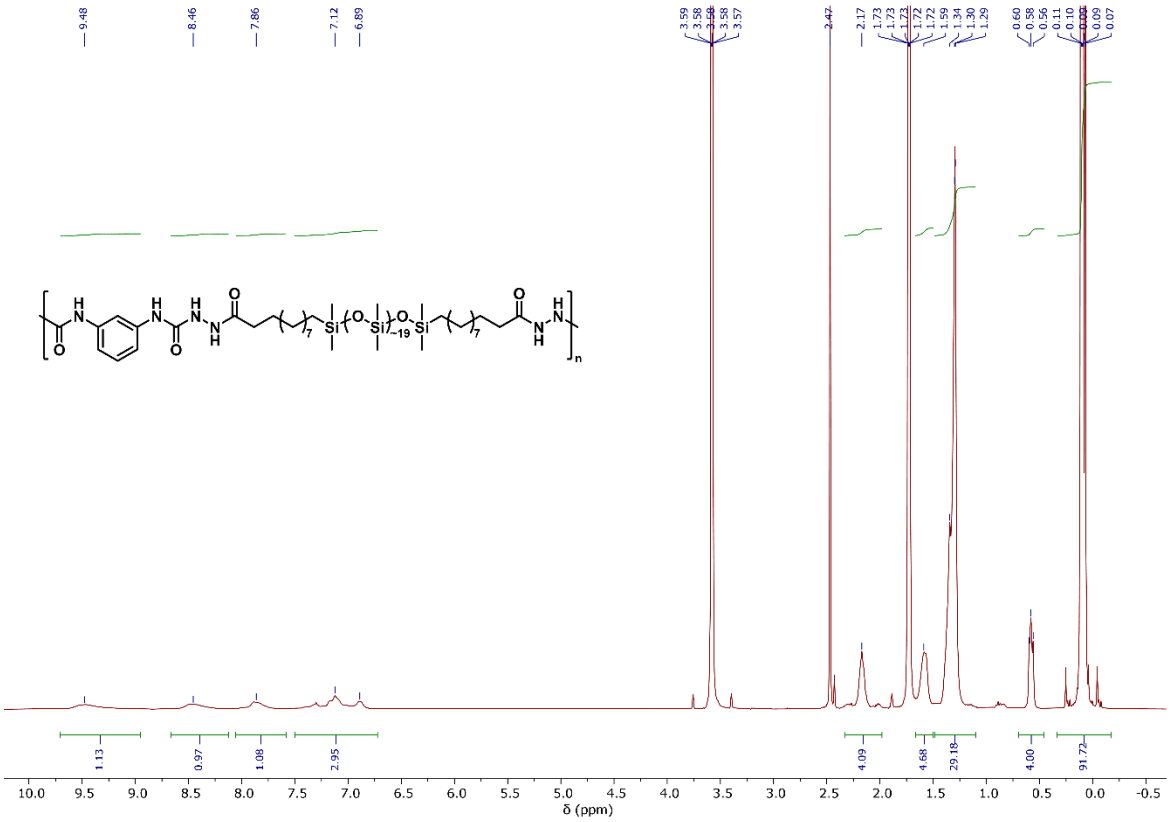

Figure S65: ^{1}H NMR spectrum of ASC-PDI in THF-d_8.

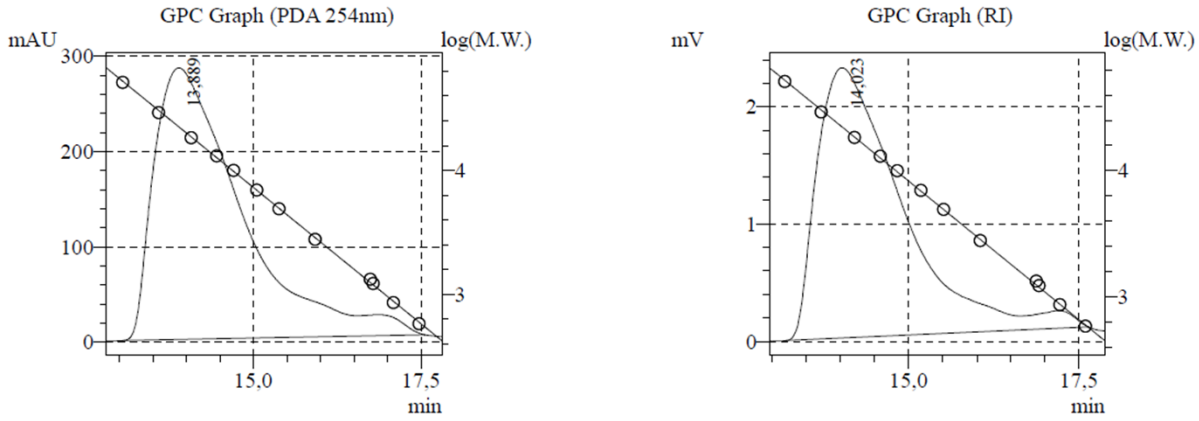

Total Average (PDA 254 nm)

Chromatogram PDA Ch1

#	Mn	Mw	Mz	Mw/Mn
1	7756	16531	22286	2,13139
	7756	16531	22286	2,13139

Total Average(RI)

Chromatogram Detector 2 Ch1

#	Mn	Mw	Mw/Mn
1	8190	16843	2,05647
	8190	16843	2,05647

Figure S66: SEC chromatogram (left: UV detector, right: RI detector) of ASC-PDI.

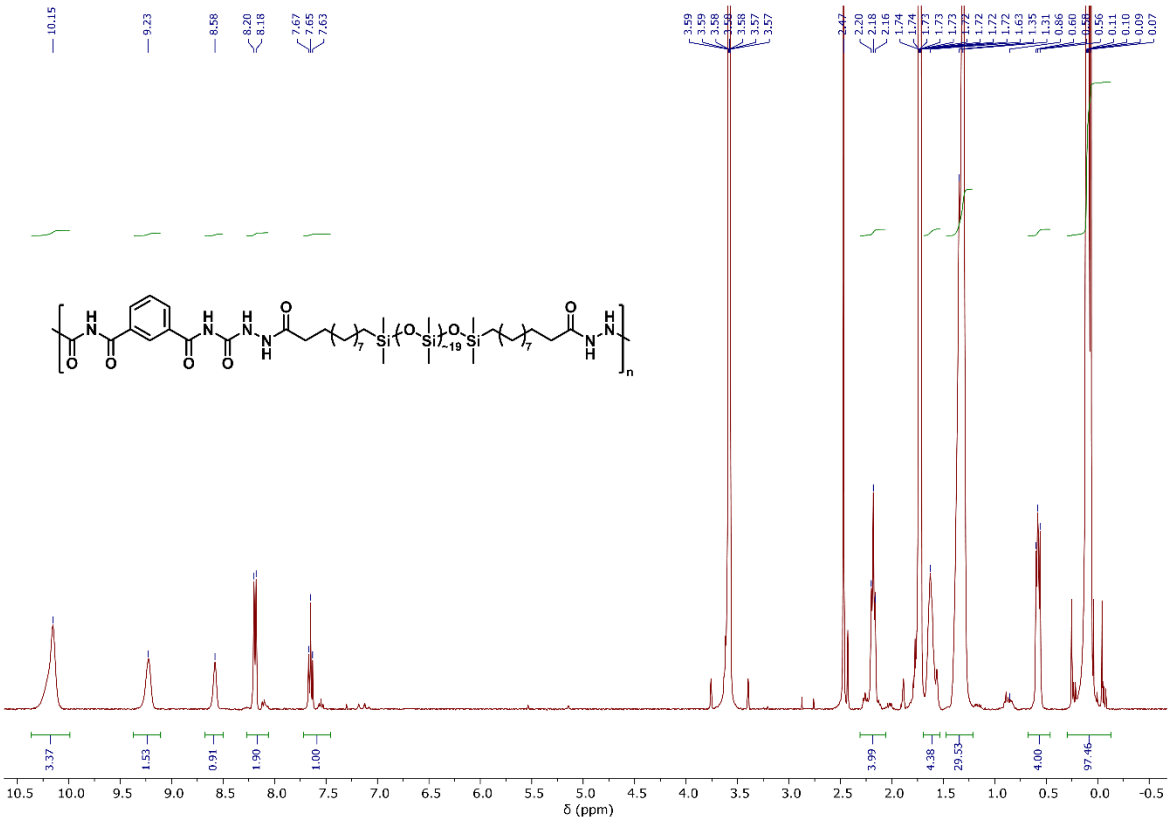

Figure S67: ^{1}H NMR spectrum of ASC-BDI in THF-d_8.

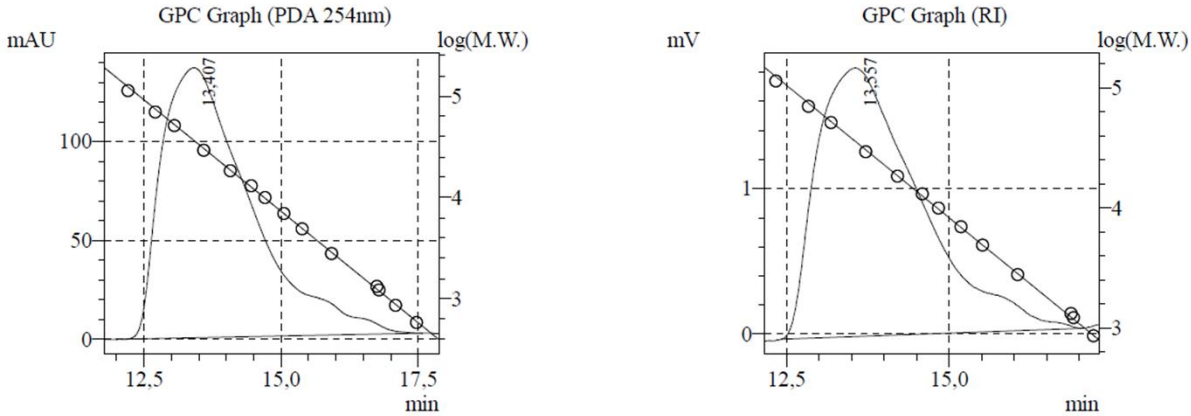

Total Average (PDA 254 nm)

Chromatogram PDA Ch1

#	Mn	Mw	Mz	Mw/Mn
1	13505	31354	45546	2,32168
	13505	31354	45546	2,32168

Total Average(RI)

Chromatogram Detector 2 Ch1

#	Mn	Mw	Mw/Mn
1	15850	31670	1,99816
	15850	31670	1,99816

Figure S68: SEC (left: UV detector, right: RI detector) chromatogram of ASC-BDI.

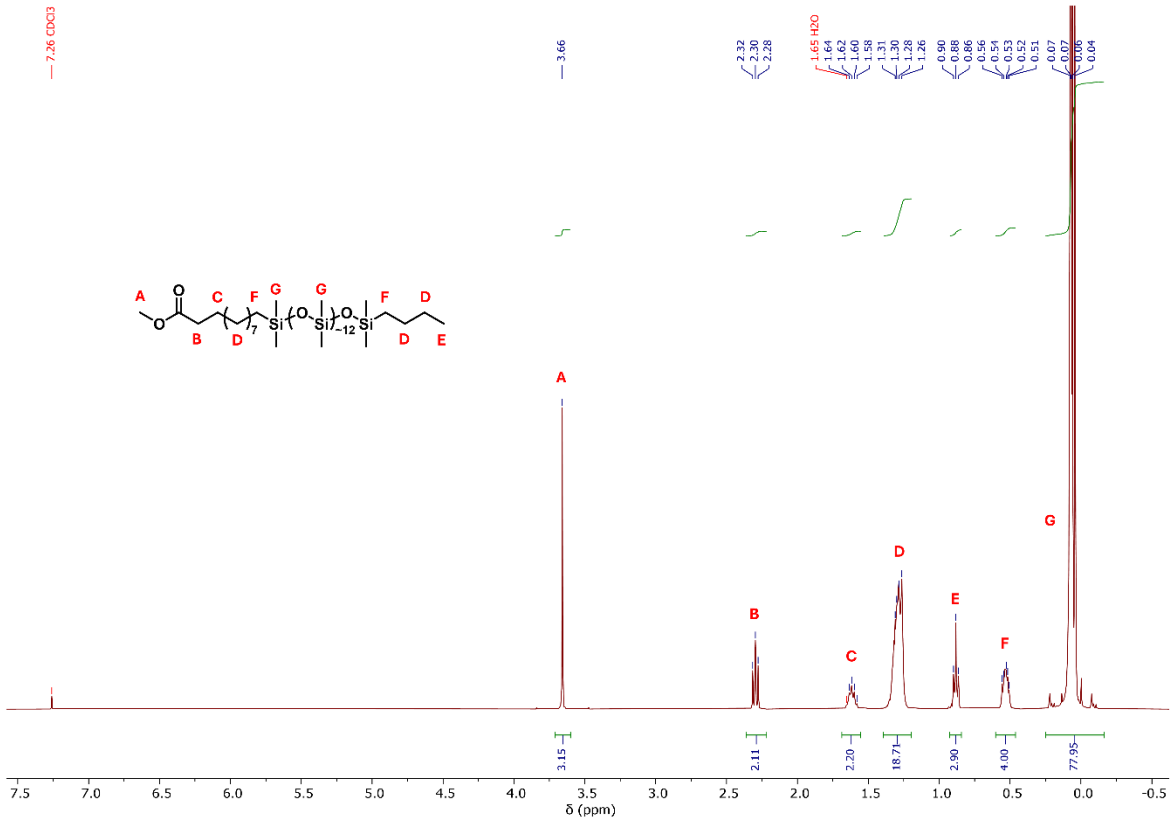

Figure S69: ^{1}H NMR spectrum of monofunctional methyl ester terminated pDMS in $CDCl_3$.

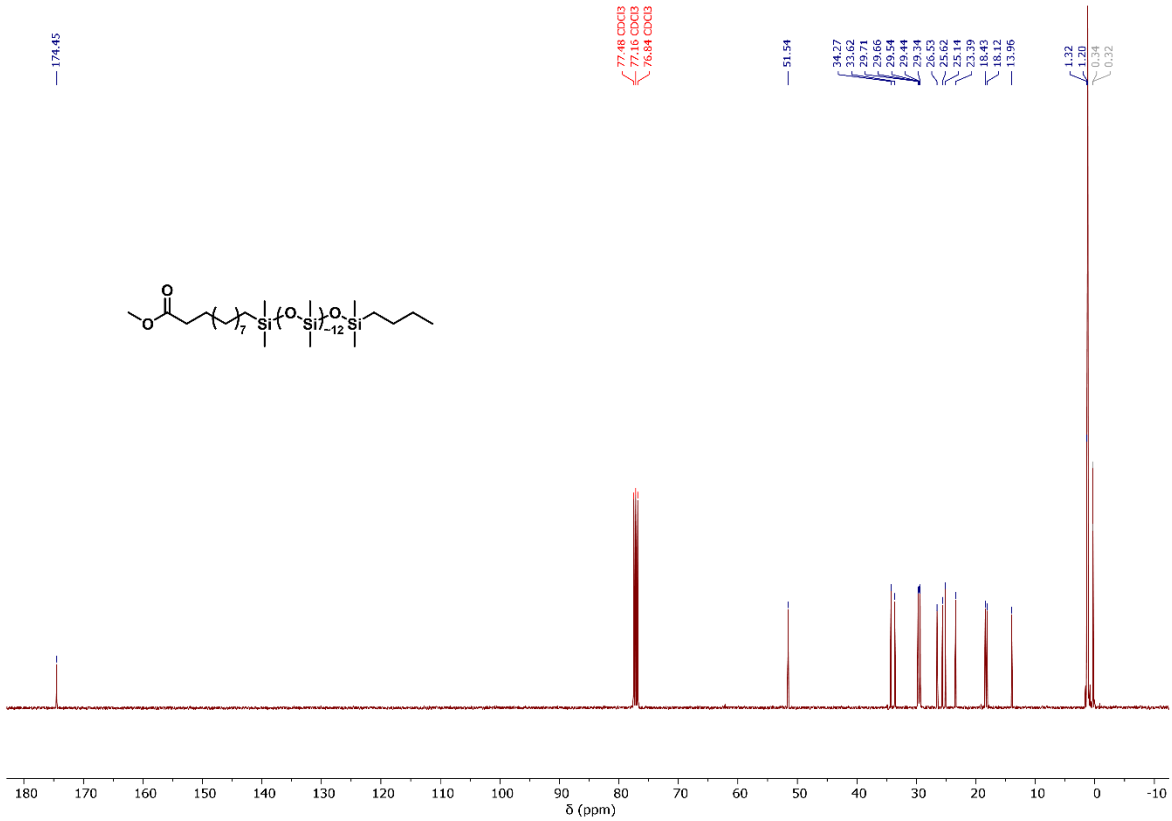

Figure S70: ^{13}C NMR spectrum of monofunctional methyl ester terminated pDMS in $CDCl_3$.

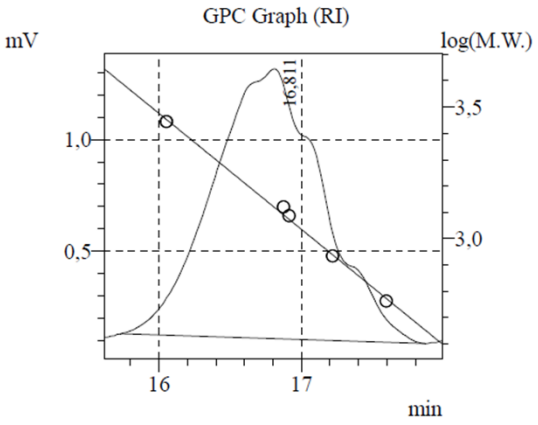

Total Average(RI)

Chromatogram Detector 2 Ch1

#	Mn	Mw	Mw/Mn
1	1284	1462	1,13858
	1284	1462	1,13858

Figure S71: SEC chromatogram (RI detector) of monofunctional methyl ester terminated pDMS.

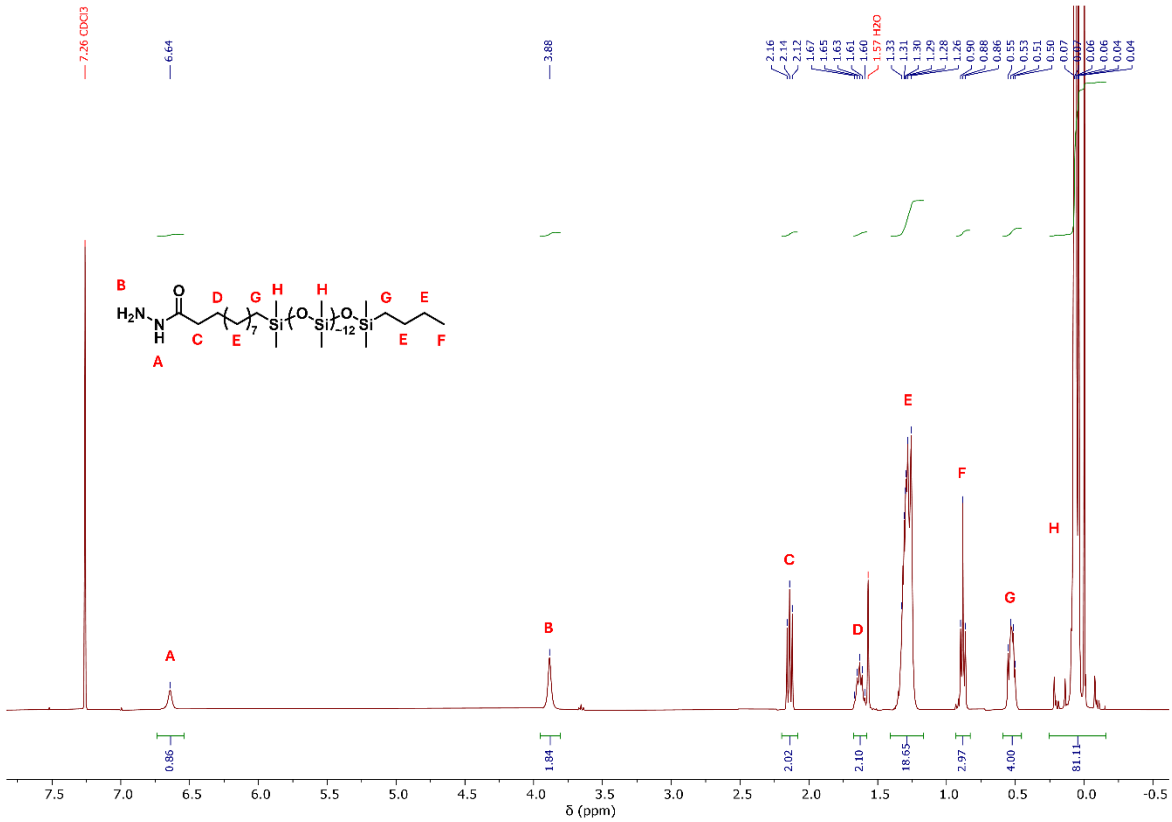

Figure S72: ^{1}H NMR spectrum of monofunctional acyl hydrazide terminated pDMS in $CDCl_3$.

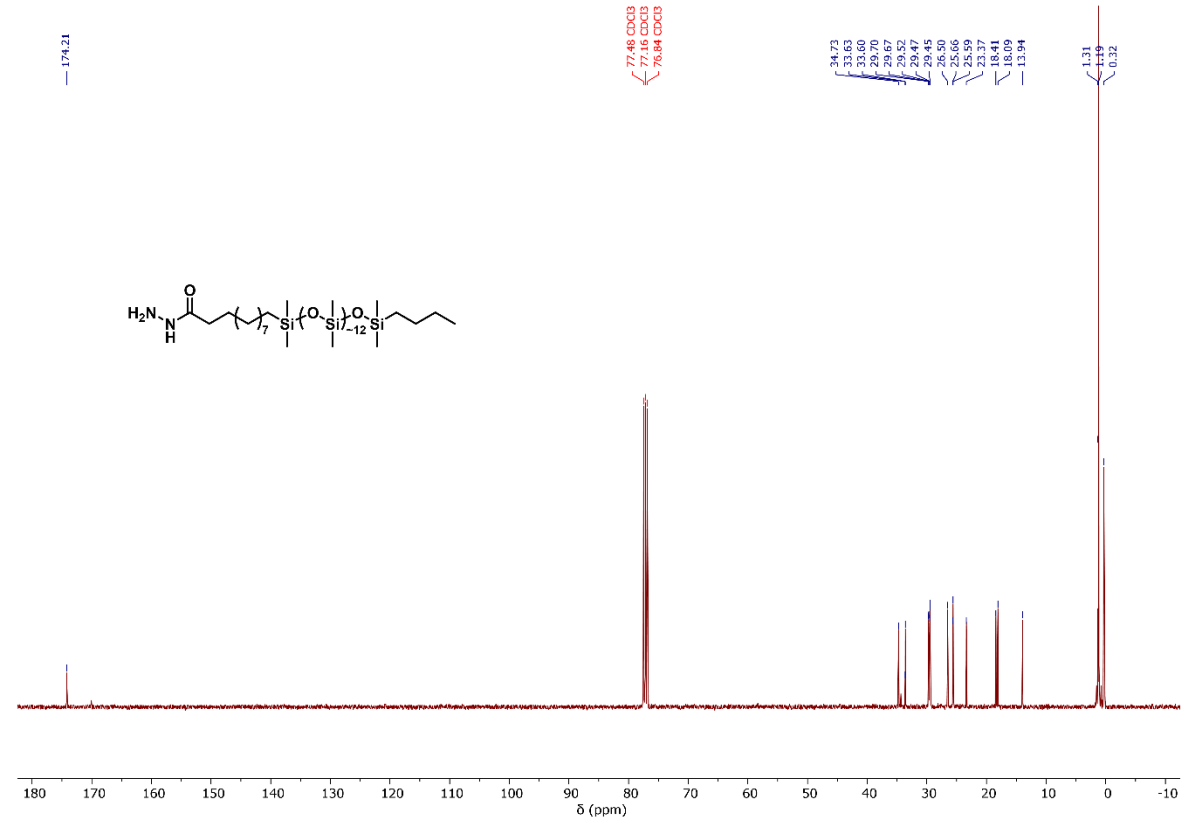

Figure S73: ^{13}C NMR spectrum of monofunctional acyl hydrazide terminated pDMS in $CDCl_3$.

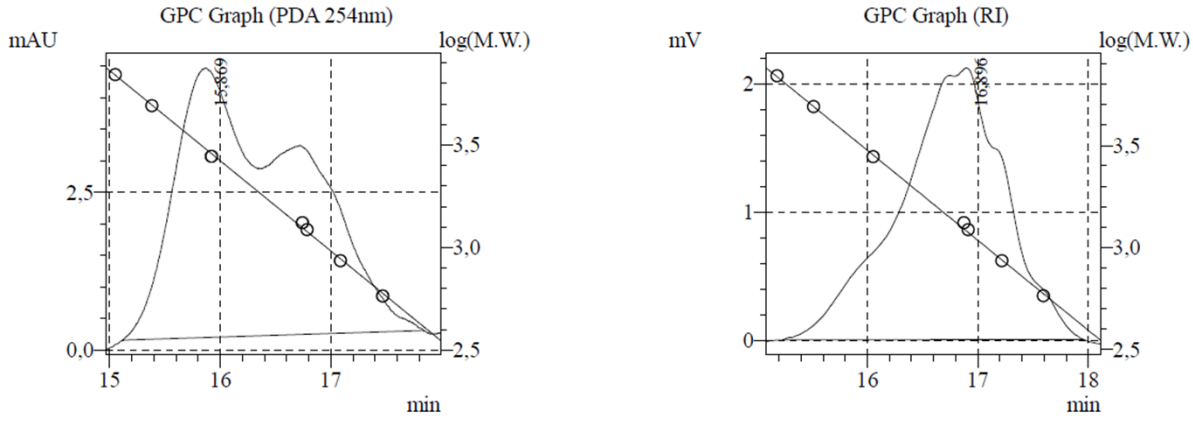

Total Average (PDA 254 nm)

Chromatogram PDA Ch1

#	Mn	Mw	Mz	Mw/Mn
1	1660	2240	2823	1,34944
	1660	2240	2823	1,34944

Total Average(RI)

Chromatogram Detector 2 Ch1

#	Mn	Mw	Mw/Mn
1	1287	1618	1,25783
	1287	1618	1,25783

Figure S74: SEC chromatogram (left: UV detector, right: RI detector) of monofunctional acyl hydrazide terminated pDMS. Note: There are interactions of the molecule with the column which gives rise to the tailing in the SEC trace.

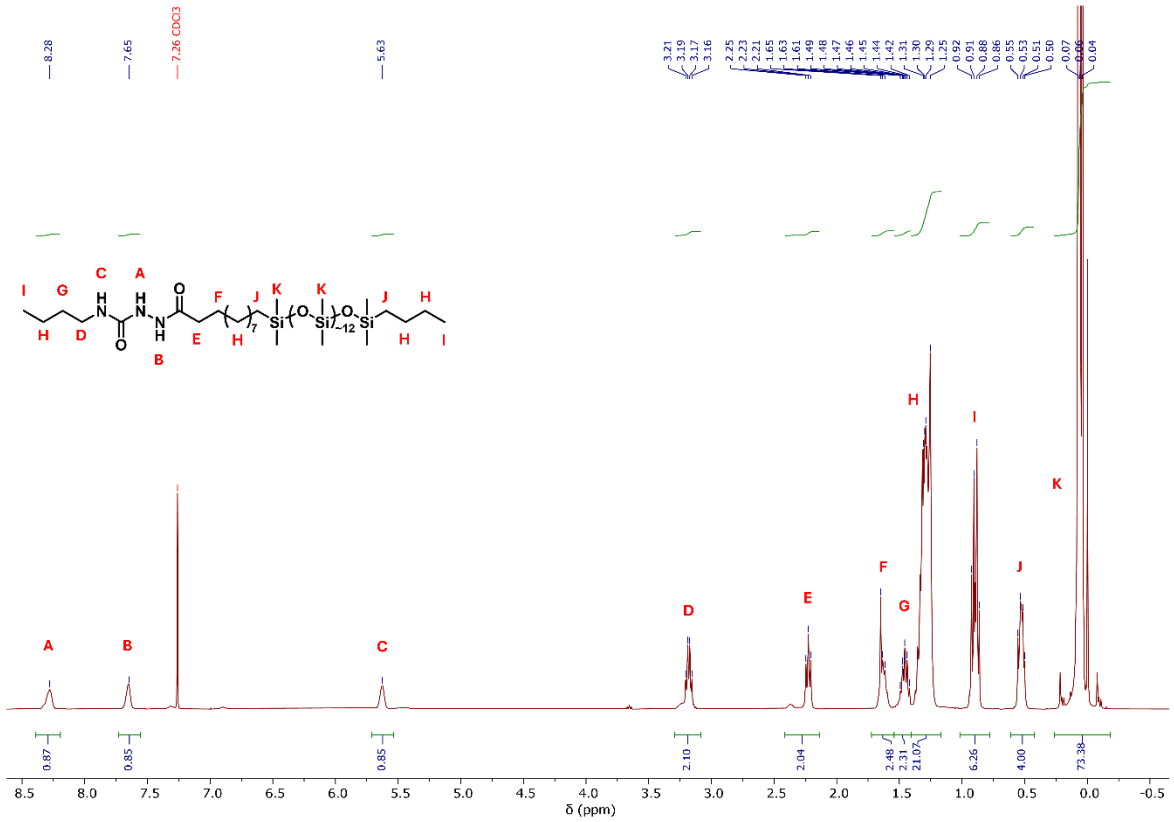

Figure S75: ^{1}H NMR spectrum of H-monoASC in $CDCl_3$.

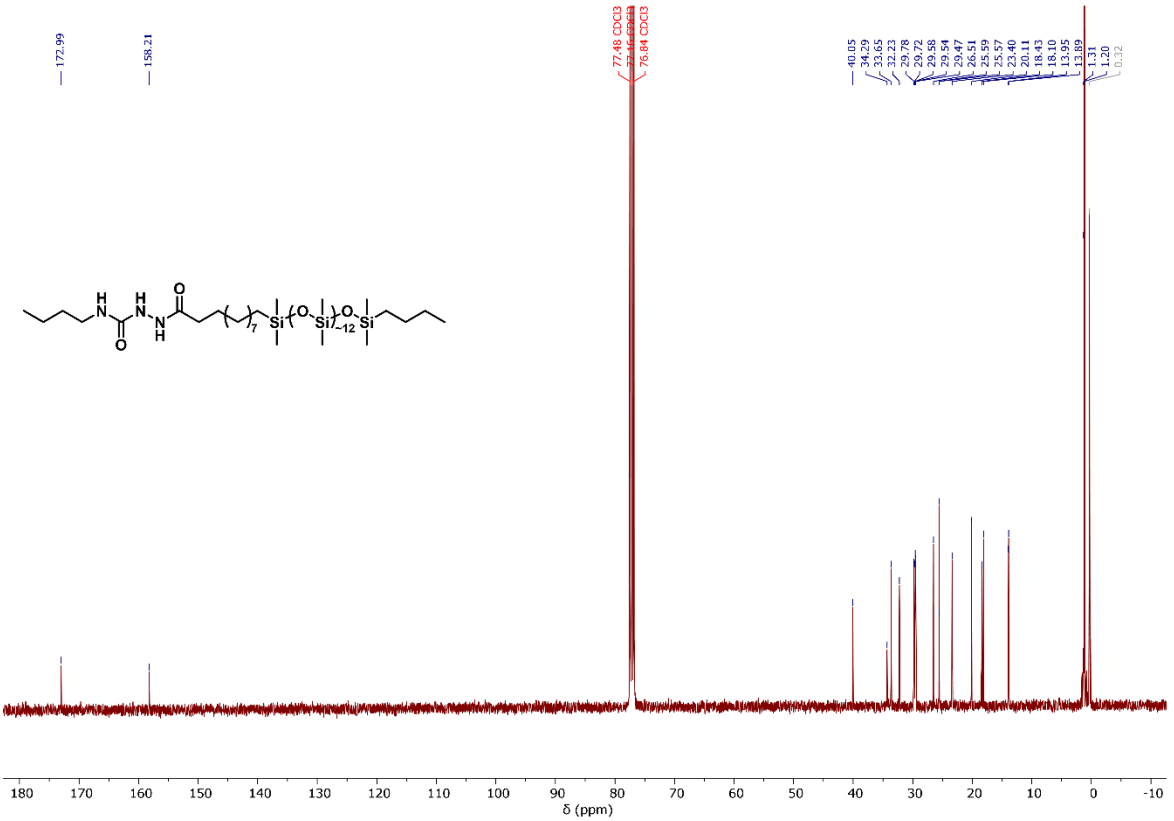

Figure S76: ^{13}C NMR spectrum of H-monoASC in $CDCl_3$.

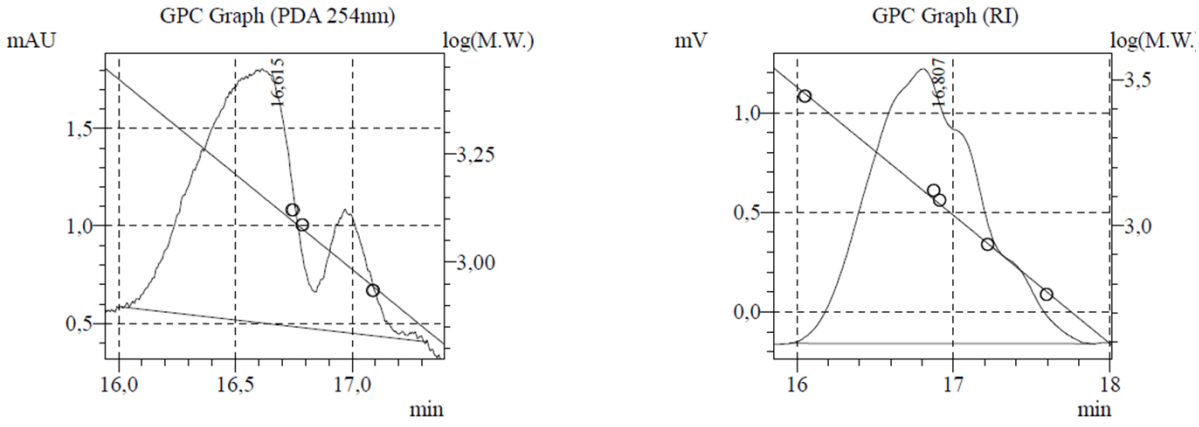

Total Average (PDA 254 nm)

Chromatogram PDA Ch1

#	Mn	Mw	Mz	Mw/Mn
1	1408	1492	1572	1,05972
	1408	1492	1572	1,05972

Total Average(RI)

Chromatogram Detector 2 Ch1

#	Mn	Mw	Mw/Mn
1	1211	1352	1,11678
	1211	1352	1,11678

Figure S77: SEC chromatogram (left: UV detector, right: RI detector) of H-monoASC. Note: There are interactions of the molecule with the column which gives rise to the tailing in the SEC trace.

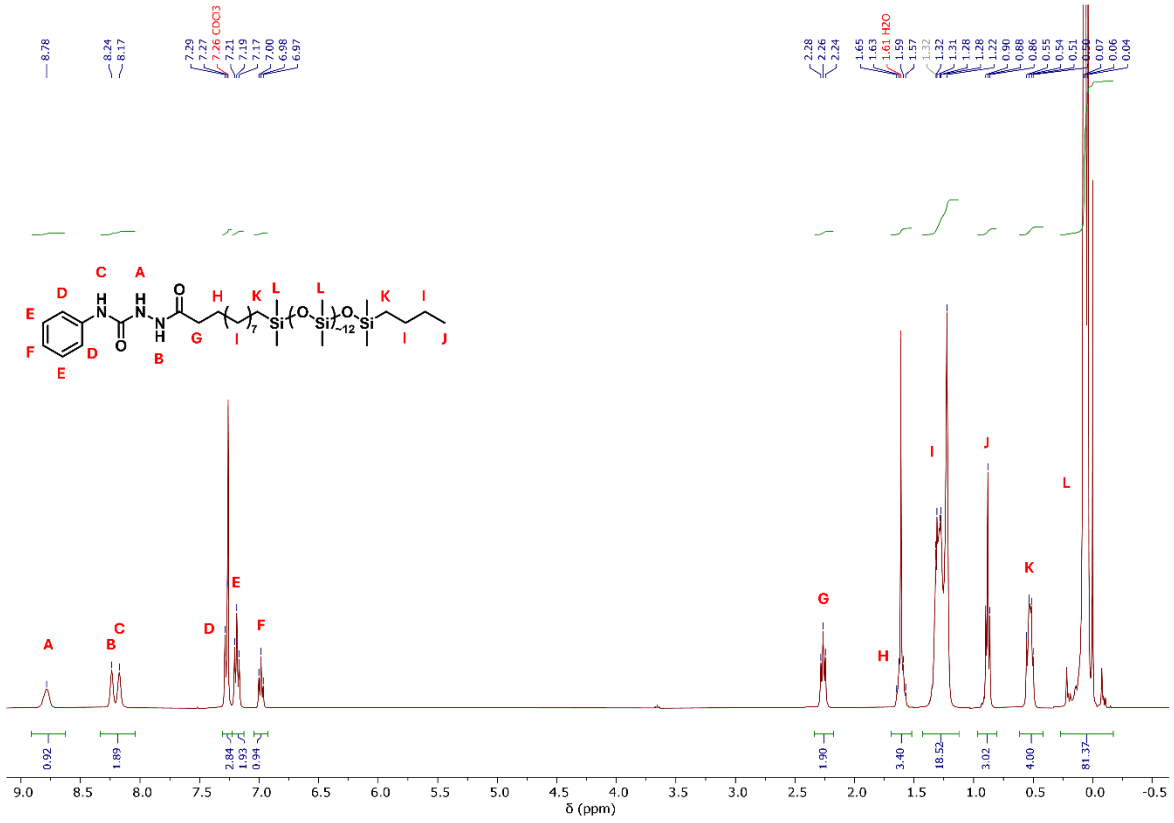

Figure S78: ^{1}H NMR spectrum of P-monoASC in $CDCl_3$.

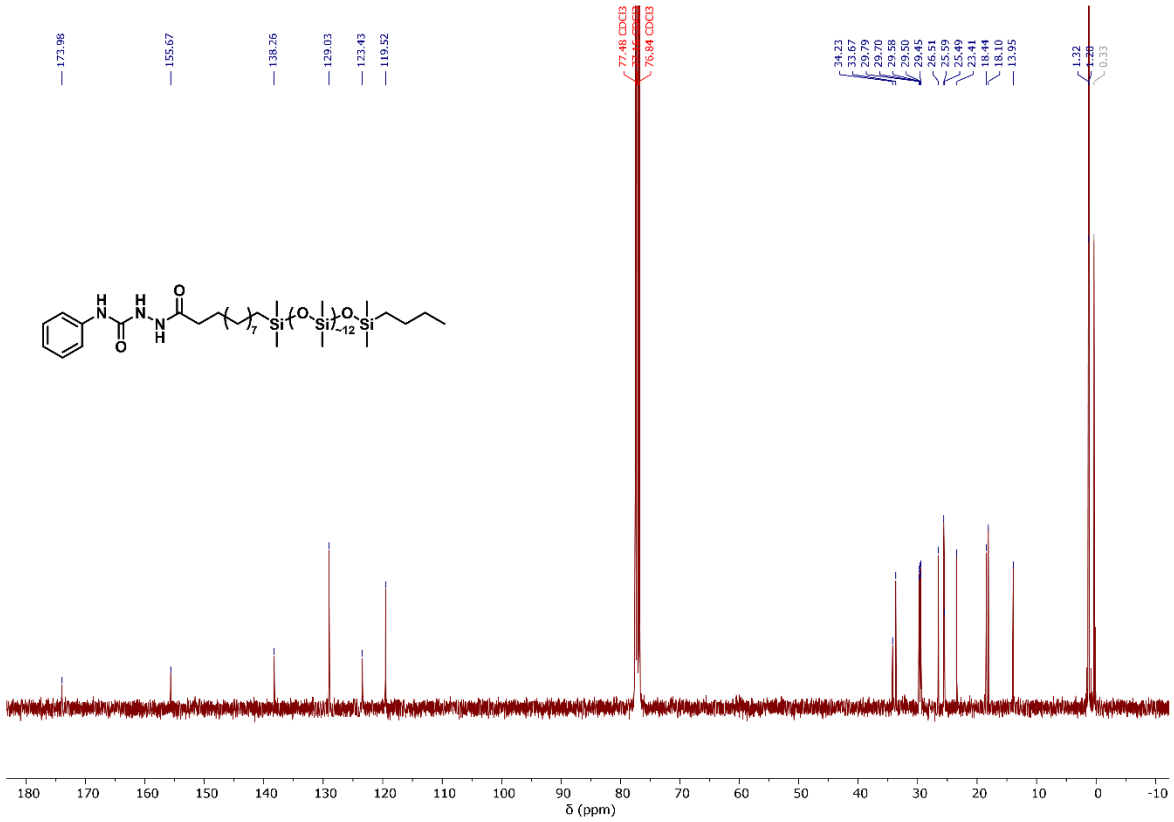

Figure S79: ^{13}C NMR spectrum of P-monoASC in $CDCl_3$.

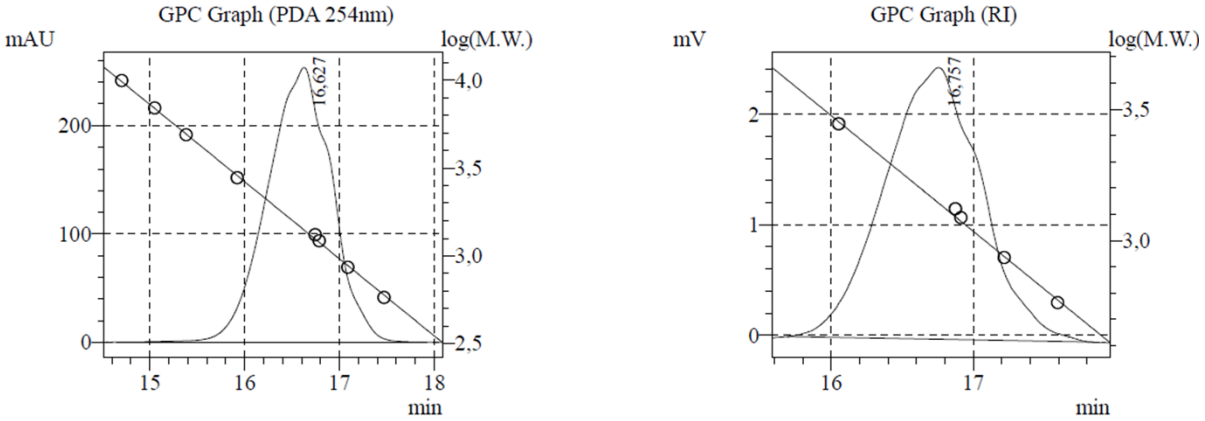

Total Average (PDA 254 nm)

Chromatogram PDA Ch1

#	Mn	Mw	Mz	Mw/Mn
1	1415	1575	1772	1,11259
	1415	1575	1772	1,11259

Total Average(RI)

Chromatogram Detector 2 Ch1

#	Mn	Mw	Mw/Mn
1	1379	1532	1,11089
	1379	1532	1,11089

Figure S80: SEC chromatogram (left: UV detector, right: RI detector) of P-monoASC.

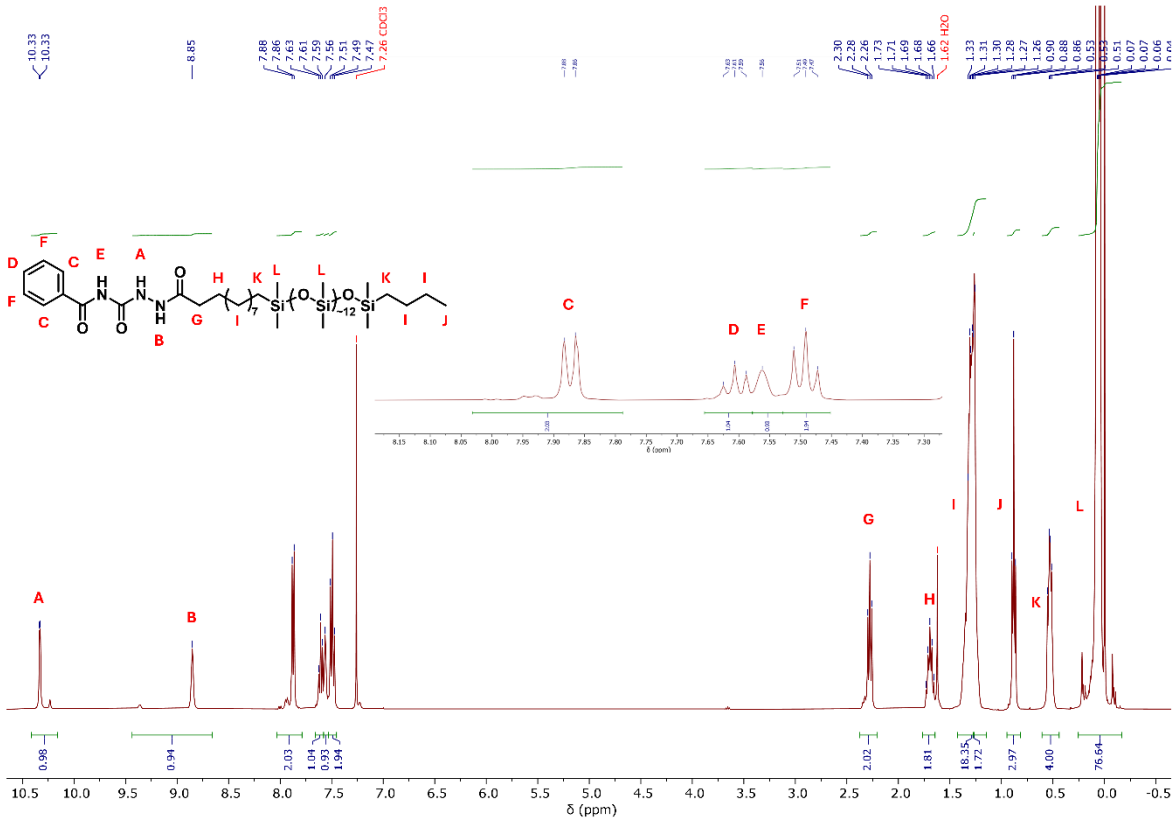

Figure S81: ^{1}H NMR spectrum of B-monoASC in $CDCl_3$.

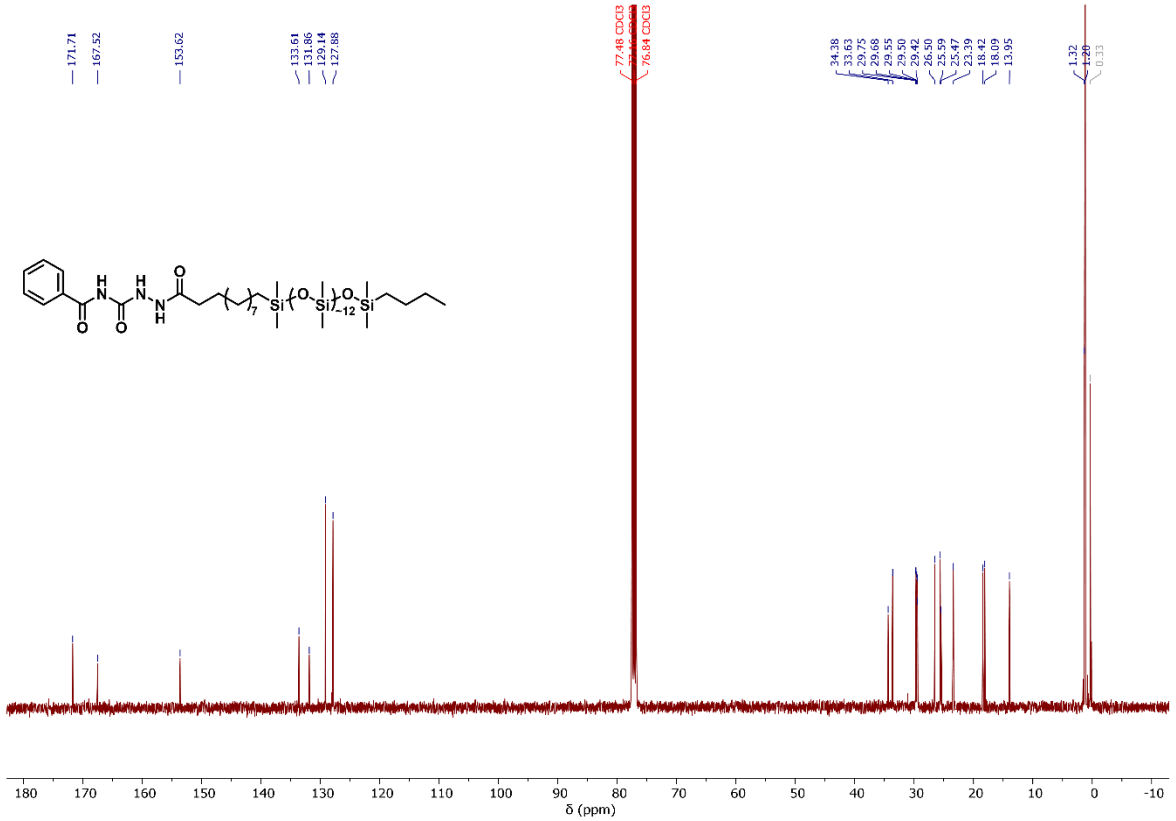

Figure S82: ^{13}C NMR spectrum of B-monoASC in $CDCl_3$.

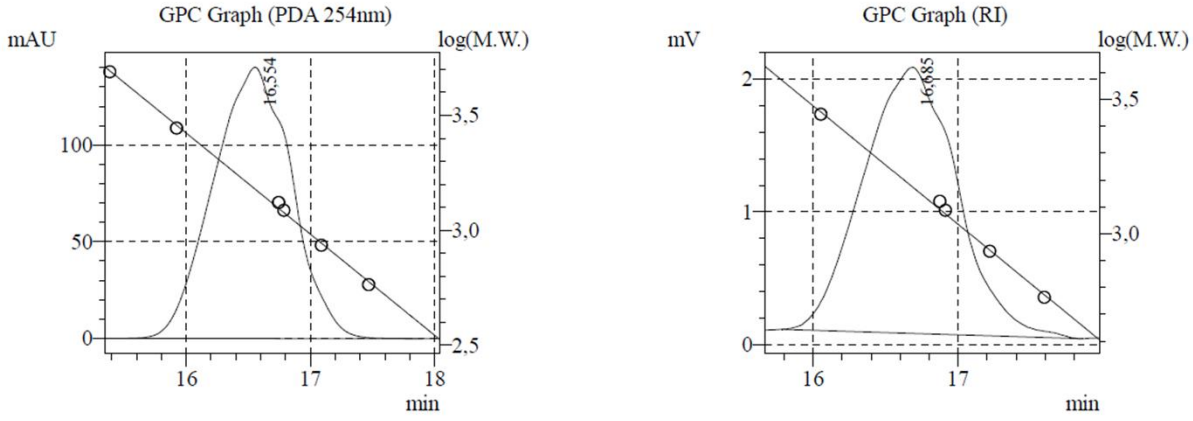

Total Average (PDA 254 nm)

Chromatogram PDA Ch1

#	Mn	Mw	Mz	Mw/Mn
1	1484	1613	1751	1,08739
	1484	1613	1751	1,08739

Total Average(RI)

Chromatogram Detector 2 Ch1

#	Mn	Mw	Mw/Mn
1	1440	1580	1,09724
	1440	1580	1,09724

Figure S83: SEC chromatogram (left: UV detector, right: RI detector) of B-monoASC.

7. Cartesian Coordinates

Table S11: Cartesian coordinates (in Å) of the experimentally-measured crystal structures PhASCPh and PhASCBz.

PhASCPh (experimental)

O	2.35220280	1.47991915	4.27059457
O	2.62684720	7.69048085	18.09934457
O	7.33125280	3.10528085	23.38690542
O	7.60589720	6.06511915	9.55815543
O	7.60589720	7.69048085	23.38690542
O	7.33125280	1.47991915	9.55815543
O	2.62684720	6.06511915	4.27059457
O	2.35220280	3.10528085	18.09934457
O	4.03044139	2.44904702	6.64222520
O	0.94860861	6.72135298	20.47097520
O	9.00949139	2.13615298	21.01527480
O	5.92765861	7.03424702	7.18652480
O	5.92765861	6.72135298	21.01527480
O	9.00949139	2.44904702	7.18652480
O	0.94860861	7.03424702	6.64222520
O	4.03044139	2.13615298	20.47097520
N	2.67345111	3.48163406	3.21297178
N	2.30559889	5.68876594	17.04172177
N	7.65250111	1.10356594	24.44452822
N	7.28464889	8.06683406	10.61577822
N	7.28464889	5.68876594	24.44452822
N	7.65250111	3.48163406	10.61577822
N	2.30559889	8.06683406	3.21297178
N	2.67345111	1.10356594	17.04172177
N	1.90368998	3.42752870	5.37108650

N	3.07536002	5.74287130	19.19983650
N	6.88273998	1.15767130	22.28641350
N	8.05441002	8.01272870	8.45766350
N	8.05441002	5.74287130	22.28641350
N	6.88273998	3.42752870	8.45766350
N	3.07536002	8.01272870	5.37108650
N	1.90368998	1.15767130	19.19983650
N	1.80500521	2.72415902	6.56589050
N	3.17404479	6.44624098	20.39464050
N	6.78405521	1.86104098	21.09160950
N	8.15309479	7.30935902	7.26285950
N	8.15309479	6.44624098	21.09160950
N	6.78405521	2.72415902	7.26285950
N	3.17404479	7.30935902	6.56589050
N	1.80500521	1.86104098	20.39464050
C	3.31793934	3.02091317	2.03559200
C	1.66111066	6.14948683	15.86434200
C	8.29698934	1.56428683	25.62190800
C	6.64016066	7.60611317	11.79315800
C	6.64016066	6.14948683	25.62190800
C	8.29698934	3.02091317	11.79315800
C	1.66111066	7.60611317	2.03559200
C	3.31793934	1.56428683	15.86434200
C	3.08352566	3.68191560	0.85019155
C	1.89552433	5.48848440	14.67894155
C	8.06257567	0.90328440	26.80730845
C	6.87457434	8.26711560	12.97855845
C	6.87457434	5.48848440	26.80730845
C	8.06257567	3.68191560	12.97855845
C	1.89552433	8.26711560	0.85019155
C	3.08352566	0.90328440	14.67894155
C	3.75221208	3.29950992	27.35437380
C	1.22683792	5.87089008	13.52562380
C	8.73126208	1.28569008	0.30312620
C	6.20588792	7.88470992	14.13187620
C	6.20588792	5.87089008	0.30312620
C	8.73126208	3.29950992	14.13187620
C	1.22683792	7.88470992	27.35437380
C	3.75221208	1.28569008	13.52562380
C	4.65839918	2.26692288	27.38120157
C	0.32065082	6.90347712	13.55245157
C	9.63744918	2.31827712	0.27629843
C	5.29970082	6.85212288	14.10504842
C	5.29970082	6.90347712	0.27629843
C	9.63744918	2.26692288	14.10504842
C	0.32065082	6.85212288	27.38120157
C	4.65839918	2.31827712	13.55245157
C	4.90406551	1.62132672	0.90550655
C	0.07498449	7.54907328	14.73425655
C	9.88311551	2.96387328	26.75199345
C	5.05403449	6.20652672	12.92324345
C	5.05403449	7.54907328	26.75199345
C	9.88311551	1.62132672	12.92324345
C	0.07498449	6.20652672	0.90550655
C	4.90406551	2.96387328	14.73425655
C	4.24762756	1.98502478	2.06407922

C	0.73142244	7.18537522	15.89282922
C	9.22667756	2.60017522	25.59342077
C	5.71047244	6.57022478	11.76467078
C	5.71047244	7.18537522	25.59342077
C	9.22667756	1.98502478	11.76467078
C	0.73142244	6.57022478	2.06407922
C	4.24762756	2.60017522	15.89282922
C	2.34503297	2.71022002	4.27280717
C	2.63401703	6.46017998	18.10155717
C	7.32408297	1.87497998	23.38469282
C	7.61306703	7.29542002	9.55594283
C	7.61306703	6.46017998	23.38469282
C	7.32408297	2.71022002	9.55594283
C	2.63401703	7.29542002	4.27280717
C	2.34503297	1.87497998	18.10155717
C	2.92320025	2.18283031	7.10327572
C	2.05584975	6.98756969	20.93202572
C	7.90225026	2.40236969	20.55422427
C	7.03489974	6.76803031	6.72547427
C	7.03489974	6.98756969	20.55422427
C	7.90225026	2.18283031	6.72547427
C	2.05584975	6.76803031	7.10327572
C	2.92320025	2.40236969	20.93202572
C	2.73827834	1.23607822	8.24442418
C	2.24077166	7.93432178	22.07317417
C	7.71732834	3.34912178	19.41307582
C	7.21982166	5.82127822	5.58432582
C	7.21982166	7.93432178	19.41307582
C	7.71732834	1.23607822	5.58432582
C	2.24077166	5.82127822	8.24442418
C	2.73827834	3.34912178	22.07317417
C	1.50526640	0.70639591	8.61614098
C	3.47378360	8.46400409	22.44489097
C	6.48431640	3.87880409	19.04135902
C	8.45283360	5.29159591	5.21260902
C	8.45283360	8.46400409	19.04135902
C	6.48431640	0.70639591	5.21260902
C	3.47378360	5.29159591	8.61614098
C	1.50526640	3.87880409	22.44489097
C	1.42281333	8.96681712	9.65744585
C	3.55623667	0.20358288	23.48619585
C	6.40186333	4.78878288	18.00005415
C	8.53528667	4.38161712	4.17130415
C	8.53528667	0.20358288	18.00005415
C	6.40186333	8.96681712	4.17130415
C	3.55623667	4.38161712	9.65744585
C	1.42281333	4.78878288	23.48619585
C	2.55923170	8.57432400	10.33947980
C	2.41981830	0.59607600	24.16822980
C	7.53828170	5.18127600	17.31802020
C	7.39886830	3.98912400	3.48927020
C	7.39886830	0.59607600	17.31802020
C	7.53828170	8.57432400	3.48927020
C	2.41981830	3.98912400	10.33947980
C	2.55923170	5.18127600	24.16822980
C	3.78597004	9.09795384	9.97218820

C	1.19307996	0.07244616	23.80093820
C	8.76502004	4.65764616	17.68531180
C	6.17212996	4.51275384	3.85656180
C	6.17212996	0.07244616	17.68531180
C	8.76502004	9.09795384	3.85656180
C	1.19307996	4.51275384	9.97218820
C	3.78597004	4.65764616	23.80093820
C	3.87867995	0.83111335	8.93254277
C	1.10037005	8.33928665	22.76129278
C	8.85772995	3.75408665	18.72495723
C	6.07942005	5.41631335	4.89620723
C	6.07942005	8.33928665	18.72495723
C	8.85772995	0.83111335	4.89620723
C	1.10037005	5.41631335	8.93254277
C	3.87867995	3.75408665	22.76129278
H	2.58213533	4.33759920	3.32996300
H	2.39691467	4.83280080	17.15871300
H	7.56118533	0.24760080	24.32753700
H	7.37596467	8.92279920	10.49878700
H	7.37596467	4.83280080	24.32753700
H	7.56118533	4.33759920	10.49878700
H	2.39691467	8.92279920	3.32996300
H	2.58213533	0.24760080	17.15871300
H	2.46313603	4.40115007	0.82281063
H	2.51591397	4.76924993	14.65156063
H	7.44218603	0.18404993	26.83468937
H	7.49496397	8.98635007	13.00593938
H	7.49496397	4.76924993	26.83468937
H	7.44218603	4.40115007	13.00593938
H	2.51591397	8.98635007	0.82281063
H	2.46313603	0.18404993	14.65156063
H	2.20671496	4.24589520	5.42087000
H	2.77233504	4.92450480	19.24962000
H	7.18576496	0.33930480	22.23663000
H	7.75138504	8.83109520	8.40788000
H	7.75138504	4.92450480	22.23663000
H	7.18576496	4.24589520	8.40788000
H	2.77233504	8.83109520	5.42087000
H	2.20671496	0.33930480	19.24962000
H	3.58212773	3.75592073	26.53847755
H	1.39692227	5.41447927	12.70972755
H	8.56117773	0.82927927	1.11902245
H	6.37597227	8.34112073	14.94777245
H	6.37597227	5.41447927	1.11902245
H	8.56117773	3.75592073	14.94777245
H	1.39692227	8.34112073	26.53847755
H	3.58212773	0.82927927	12.70972755
H	0.98286447	2.53744968	6.83969975
H	3.99618553	6.63295032	20.66844975
H	5.96191447	2.04775032	20.81780025
H	8.97523553	7.12264968	6.98905025
H	8.97523553	6.63295032	20.81780025
H	5.96191447	2.53744968	6.98905025
H	3.99618553	7.12264968	6.83969975
H	0.98286447	2.04775032	20.66844975
H	5.10920237	2.00409922	26.58743133

H	9.82794763	7.16630078	12.75868132
H	0.13015237	2.58110078	1.07006867
H	4.84889763	6.58929922	14.89881867
H	4.84889763	7.16630078	1.07006867
H	0.13015237	2.00409922	14.89881867
H	9.82794763	6.58929922	26.58743133
H	5.10920237	2.58110078	12.75868132
H	5.53580737	0.91190458	0.92846228
H	9.40134263	8.25849542	14.75721228
H	0.55675737	3.67329542	26.72903773
H	4.42229263	5.49710458	12.90028773
H	4.42229263	8.25849542	26.72903773
H	0.55675737	0.91190458	12.90028773
H	9.40134263	5.49710458	0.92846228
H	5.53580737	3.67329542	14.75721228
H	4.42966162	1.53017294	2.87803945
H	0.54938838	7.64022706	16.70678945
H	9.40871162	3.05502706	24.77946055
H	5.52843838	6.11537294	10.95071055
H	5.52843838	7.64022706	24.77946055
H	9.40871162	1.53017294	10.95071055
H	0.54938838	6.11537294	2.87803945
H	4.42966162	3.05502706	16.70678945
H	0.71807859	0.96995321	8.15426073
H	4.26097141	8.20044679	21.98301072
H	5.69712859	3.61524679	19.50323927
H	9.24002141	5.55515321	5.67448927
H	9.24002141	8.20044679	19.50323927
H	5.69712859	0.96995321	5.67448927
H	4.26097141	5.55515321	8.15426073
H	0.71807859	3.61524679	21.98301072
H	0.57806771	8.60944663	9.90498048
H	4.40098230	0.56095337	23.73373048
H	5.55711770	5.14615337	17.75251953
H	9.38003229	4.02424663	3.92376952
H	9.38003229	0.56095337	17.75251953
H	5.55711770	8.60944663	3.92376952
H	4.40098230	4.02424663	9.90498048
H	0.57806771	5.14615337	23.73373048
H	2.49838771	7.95128702	11.05387302
H	2.48066229	1.21911298	24.88262303
H	7.47743771	5.80431298	16.60362698
H	7.45971229	3.36608702	2.77487698
H	7.45971229	1.21911298	16.60362698
H	7.47743771	7.95128702	2.77487698
H	2.48066229	3.36608702	11.05387302
H	2.49838771	5.80431298	24.88262303
H	4.57017041	8.83311269	10.43849365
H	0.40887959	0.33728731	24.26724365
H	9.54922041	4.92248731	17.21900635
H	5.38792959	4.24791269	3.39025635
H	5.38792959	0.33728731	17.21900635
H	9.54922041	8.83311269	3.39025635
H	0.40887959	4.24791269	10.43849365
H	4.57017041	4.92248731	24.26724365
H	4.72720965	1.17931344	8.68473158

H	0.25184035	7.99108656	22.51348158
H	9.70625965	3.40588656	18.97276843
H	5.23089035	5.76451344	5.14401842
H	5.23089035	7.99108656	18.97276843
H	9.70625965	1.17931344	5.14401842
H	0.25184035	5.76451344	8.68473158
H	4.72720965	3.40588656	22.51348158
VEC1	9.95810000	0.00000000	0.00000000
VEC2	0.00000000	9.17040000	0.00000000
VEC3	0.00000000	0.00000000	27.65750000

PhASCBz (experimental)

O	7.28916183	13.37852596	5.26001395
O	0.11026698	27.15037596	10.28958287
O	0.89822404	14.16517404	5.10638393
O	8.07711889	0.39332404	0.07681501
O	6.85028313	15.72635095	1.95841989
O	2.12505980	1.95450095	3.22477905
O	1.33710274	11.81734905	8.40797799
O	6.06232607	25.58919905	7.14161882
O	7.96617630	18.15019655	4.17060919
O	1.00916664	4.37834655	1.01258974
O	0.22120957	9.39350345	6.19578868
O	7.17821923	23.16535345	9.35380813
N	6.14238179	14.16985647	3.46165124
N	2.83296114	0.39800646	1.72154770
N	2.04500408	13.37384354	6.90474663
N	5.35442473	27.14569353	8.64485018
N	8.06109394	15.44099822	3.84551896
N	0.91424899	1.66914822	1.33767998
N	0.12629193	12.10270178	6.52087892
N	7.27313688	25.87455178	9.02871789
N	9.03905304	16.31743875	3.39872721
N	-0.06371010	2.54558875	1.78447173
N	-0.85166717	11.22626125	6.96767067
N	8.25109597	24.99811125	8.58192614
C	5.22164883	12.31313565	4.78243400
C	3.75369410	26.08498565	0.40076494
C	2.96573704	15.23056435	5.58396388
C	4.43369177	1.45871435	9.96563293
O	1.84970510	17.05230467	9.00570449
O	5.54972370	3.28045467	6.54389232
O	6.33768077	10.49139533	1.36069339
O	2.63766217	24.26324533	3.82250555
C	4.13952430	12.10435440	3.94213378
C	4.83581864	25.87620440	1.24106515
C	4.04786157	15.43934560	6.42426409
C	3.35156723	1.66749560	9.12533272
O	4.10661775	14.09383585	1.39635379
O	4.86872518	0.32198585	3.78684514
O	4.08076812	13.44986415	8.97004408
O	3.31866069	27.22171415	6.57955273
C	3.19182154	11.13812141	4.25540633
C	5.78352139	24.90997141	0.92779261
C	4.99556433	16.40557859	6.11099155
C	2.40386448	2.63372859	9.43860527

O	0.94347082	14.67610967	1.79411248
O	8.03187211	0.90425967	3.38908646
O	7.24391505	12.86759033	8.57228539
O	0.15551376	26.63944033	6.97731142
C	3.31689469	10.37295742	5.39083789
C	4.08253412	24.14480742	10.15875893
C	4.87049118	17.17074258	4.97555999
C	4.10485175	3.39889258	0.20763895
C	4.37507193	10.59771401	6.24865731
C	3.02435687	24.36956401	9.30093950
C	3.81231394	16.94598599	4.11774056
C	5.16302900	3.17413599	1.06545837
C	5.31804226	11.56890487	5.95238566
C	2.08138654	25.34075487	9.59721115
C	2.86934361	15.97479513	4.41401222
C	6.10599933	2.20294513	0.76918672
C	6.30091509	13.31958245	4.53882365
C	2.67442785	27.09143245	0.64437529
C	1.88647078	14.22411755	5.82757423
C	5.51295802	0.45226755	9.72202258
C	7.03091879	15.15537005	3.03984251
C	1.94442414	1.38352005	2.14335642
C	1.15646708	12.38832995	7.32655536
C	6.24296173	26.16017995	8.22304145
C	8.88779568	17.65633801	3.55173524
C	0.08754726	3.88448801	1.63146370
C	-0.70040981	9.88736199	6.81466264
C	8.09983862	23.65921199	8.73493418
C	0.20464446	18.48237357	2.91762268
C	8.77069848	4.71052357	2.26557626
C	7.98274142	9.06132643	7.44877519
C	-0.58331261	22.83317643	8.10082162
C	0.86588816	18.09345653	1.75855574
C	8.10945478	4.32160653	3.42464320
C	7.32149771	9.45024347	8.60784214
C	0.07793109	23.22209347	6.94175467
C	1.81580290	18.92775520	1.18861118
C	7.15954003	5.15590520	3.99458776
C	6.37158297	8.61594480	9.17778669
C	1.02784584	22.38779480	6.37181012
C	2.13092867	20.13747451	1.78353875
C	6.84441426	6.36562451	3.39966018
C	6.05645720	7.40622549	8.58285912
C	1.34297161	21.17807549	6.96673769
C	1.48113339	20.52666699	2.94115441
C	7.49420954	6.75481699	2.24204453
C	6.70625248	7.01703301	7.42524347
C	0.69317633	20.78888301	8.12435334
C	0.50834827	19.71192434	3.50290951
C	8.46699467	5.94007434	1.68028943
C	7.67903760	7.83177566	6.86348837
C	-0.27960880	21.60362566	8.68610844
N	4.53068004	16.06816827	0.36914743
N	4.44466290	2.29631827	4.81405151
N	3.65670583	11.47553173	9.99725045
N	3.74272297	25.24738173	5.55234637

N	1.11156254	14.75874077	10.12600111
N	6.28786627	0.98689077	5.42359570
N	7.07582334	12.78495923	0.24039677
N	1.89951960	26.55680923	4.94280217
N	1.87568913	13.66250151	0.01243968
N	7.09965381	27.43435151	5.17075926
N	6.31169674	13.88119849	10.35395820
N	1.08773206	0.10934849	5.19563862
C	3.72300735	18.21409794	9.89379380
C	3.67642146	4.44224794	5.65580302
C	4.46437852	9.32960206	0.47260408
C	4.51096441	23.10145206	4.71059486
C	6.06005244	18.50909096	0.65526001
C	2.91529050	4.73724096	4.52793893
C	2.12733343	9.03460904	9.71113787
C	5.27209537	22.80645904	5.83845895
C	6.91760112	19.61221615	0.65308307
C	2.05774182	5.84036615	4.53011587
C	1.26978475	7.93148385	9.71331481
C	6.12964405	21.70333385	5.83628200
C	5.41604778	20.41759394	9.90094661
C	1.98338102	6.64574394	5.64865020
C	2.77133809	7.12610606	0.46545126
C	6.20400485	20.89795606	4.71774767
C	4.66106242	20.13582188	8.79174204
C	2.73836639	6.36397188	6.75785477
C	3.52632345	7.40787811	1.57465584
C	5.44901948	21.17972811	3.60854310
C	3.81570813	19.02939146	8.76893596
C	3.58372068	5.25754146	6.78066085
C	4.37167774	8.51430854	1.59746191
C	4.60366519	22.28615854	3.58573702
C	2.76066963	17.07130982	9.81780810
C	4.63875918	3.29945982	5.73178871
C	5.42671625	10.47239018	0.54858978
C	3.54862669	24.24424018	4.63460916
C	3.77318147	14.91353637	0.55066306
C	5.20216146	1.14168636	4.63253588
C	4.41420440	12.63016364	9.81573482
C	2.98522441	26.40201363	5.73386199
C	1.14883986	13.64542442	1.16570144
C	7.82650307	27.41727442	4.01749750
C	7.03854601	13.89827558	9.20069643
C	0.36088280	0.12642558	6.34890038
C	0.61737027	12.31616546	1.60212679
C	8.35797267	26.08801546	3.58107215
C	7.57001561	15.22753454	8.76427108
C	-0.17058680	1.45568454	6.78532573
C	-0.26065098	12.30487254	2.68562270
C	9.23599391	26.07672254	2.49757624
C	8.44803685	15.23882746	7.68077518
C	-1.04860804	1.46697746	7.86882164
C	9.03292463	11.10975139	3.20269862
C	-0.05758169	24.88160140	1.98050031
C	-0.84553876	16.43394861	7.16369925
C	8.24496756	2.66209861	8.38589756

C	-0.31904956	9.90857064	2.64332779
C	9.29439250	23.68042064	2.53987114
C	8.50643543	17.63512936	7.72307008
C	-1.10700662	3.86327936	7.82652673
C	0.52990586	9.90691802	1.55578899
C	8.44543708	23.67876802	3.62740994
C	7.65748001	17.63678198	8.81060888
C	-0.25805121	3.86493198	6.73898793
C	1.00077107	11.10479353	1.03249323
C	7.97457187	24.87664353	4.15070571
C	7.18661480	16.43890647	9.33390465
C	0.21281400	2.66705647	6.21569217
H	5.45470857	14.08860255	2.88393189
H	3.52063437	0.31675255	2.29926705
H	2.73267730	13.45509745	7.48246599
H	4.66675150	27.22694745	8.06713083
H	4.04573925	12.62245140	3.15128129
H	4.92960369	26.39430140	2.03191765
H	4.14164662	14.92124860	7.21511659
H	3.25778218	1.14939860	8.33448023
H	8.20433507	14.97550969	4.55188531
H	0.77100787	1.20365969	0.63131363
H	-0.01694920	12.56819031	5.81451257
H	7.41637800	26.34004031	9.73508424
H	2.44885960	11.00453446	3.67851629
H	6.52648333	24.77638446	1.50468265
H	5.73852627	16.53916554	6.68788159
H	1.66090254	2.76731554	8.86171522
H	-0.08055188	15.94504793	2.92539748
H	9.05589481	2.17319793	2.25780146
H	8.26793775	11.59865207	7.44100039
H	-0.86850894	25.37050207	8.10859642
H	2.68011016	9.69483153	5.58365289
H	4.71931865	23.46668153	9.96594393
H	5.50727571	17.84886847	4.78274499
H	3.46806722	4.07701847	0.40045395
H	4.45690427	10.08485032	7.04427835
H	2.94252454	23.85670032	8.50531846
H	3.73048160	17.45884968	3.32211953
H	5.24486133	3.68699968	1.86107941
H	6.03606717	11.72755659	6.55394773
H	1.36336164	25.49940659	8.99564908
H	2.15131870	15.81614341	3.81245015
H	6.82402423	2.04429341	1.37074879
H	0.66689204	17.25612805	1.35665049
H	8.30845090	3.48427805	3.82654845
H	7.52049383	10.28757195	9.00974739
H	-0.12106503	24.05942195	6.53984943
H	2.25249709	18.66774267	0.38594099
H	6.72284584	4.89589267	4.79725794
H	5.93488878	8.87595732	9.98045688
H	1.46454003	22.64780732	5.56913993
H	2.79259712	20.69936599	1.39749410
H	6.18274581	6.92751599	3.78570484
H	5.39478875	6.84433401	8.96890378
H	2.00464006	20.61618401	6.58069304

H	1.70144392	21.35435517	3.35249307
H	7.27389901	7.58250517	1.83070586
H	6.48594195	6.18934483	7.01390480
H	0.91348686	19.96119483	8.53569201
H	0.04911883	19.99149290	4.28619453
H	8.92622411	6.21964290	0.89700441
H	8.13826704	7.55220710	6.08020335
H	-0.73883824	21.32405710	9.46939347
H	5.26590569	16.08001206	0.90187662
H	3.70943724	2.30816206	4.28132232
H	2.92148018	11.46368794	9.46452126
H	4.47794863	25.23553794	6.08507555
H	5.99624735	17.95959415	1.42755665
H	2.97909558	4.18774415	3.75564229
H	2.19113852	9.58410585	8.93884122
H	5.20829029	23.35595585	6.61075559
H	0.83751182	15.38040208	9.53190285
H	6.56191699	1.60855208	6.01769397
H	7.34987405	12.16329792	0.83449503
H	1.62546888	25.93514792	4.34870391
H	7.44682922	19.80667467	1.41760491
H	1.52851372	6.03482467	3.76559403
H	0.74055665	7.73702533	8.94879297
H	6.65887215	21.50887533	6.60080385
H	0.53864539	12.91524093	9.93722900
H	6.86078342	26.68709093	5.61236781
H	7.64874049	14.62845907	0.42916887
H	1.32660245	0.85660907	4.75403007
H	5.99425885	21.17174044	9.90011730
H	1.40516995	7.39989044	5.64947951
H	2.19312702	6.37195956	0.46628058
H	6.78221592	20.14380956	4.71691836
H	4.71476600	20.70156948	8.03001912
H	2.68466281	6.92971948	7.51957769
H	3.47261987	6.84213052	2.33637875
H	5.50272306	20.61398052	2.84682018
H	3.30576864	18.83217856	7.99249276
H	4.09366017	5.06032856	7.55710405
H	4.88161723	8.71152144	2.37390511
H	4.09372570	22.48337144	2.80929382
H	9.22387184	13.12622567	3.07311865
H	-0.24852890	26.89807567	2.11008029
H	-1.03648597	14.41747433	7.29327923
H	8.43591477	0.64562433	8.25631759
H	8.43125416	11.11195489	3.93777990
H	0.54408877	24.88380489	1.24541904
H	-0.24386829	16.43174511	6.42861798
H	7.64329710	2.65989511	9.12097883
H	9.14096035	9.08611576	3.00967630
H	-0.16561741	22.85796576	2.17352264
H	-0.95357448	18.45758424	7.35672158
H	8.35300328	4.68573424	8.19287523
H	0.79368597	9.08308595	1.16290251
H	8.18165696	22.85493595	4.02029642
H	7.39369990	18.46061405	9.20349536
H	0.00572891	4.68876405	6.34610145

H	1.58572892	11.09735673	0.28403930
H	7.38961401	24.86920673	4.89915964
H	6.60165695	16.44634327	10.08235857
H	0.79777186	2.67449327	5.46723824
VEC1	9.76330000	0.00000000	0.00000000
VEC2	0.00000000	27.54370000	0.00000000
VEC3	-1.57591413	0.00000000	10.36639788

Table S12. Cartesian coordinates (in Å) and bonding energies (in kcal mol^{-1}) for the stationary points of the optimized (crystal) structures PhASCPh and PhASCBz, computed with periodic DFT (BAND engine) at ZORA-BLYP-D3(BJ)/TZP.

PhASCPh (monomer)
E = –4683.5 kcal mol^{-1}
H = –4519.8 kcal mol^{-1}
G = –4559.8 kcal mol^{-1}
N_{imag} = 0

H	3.44702710	2.99021236	-2.81536452
H	6.10563695	-0.55718412	-5.06616312
H	6.43605614	1.82616897	-5.70339811
H	5.11040777	3.60695102	-4.57515158
C	2.79787934	0.58319942	-1.93044576
O	2.37975527	1.41945994	-1.11452004
N	2.34750499	-0.72121930	-1.88412751
H	2.25866920	-1.29587531	-2.72284236
N	1.29454750	-0.97752397	-0.97728880
H	1.07482496	-0.09280461	-0.50432809
C	0.24908430	-1.74685723	-1.52627361
O	0.36858931	-2.31734553	-2.61240528
N	-0.83818759	-1.82781024	-0.67873765
H	-0.73292778	-1.37953051	0.22558850
H	-1.64927419	-3.28564793	-2.83966803
C	4.02862780	2.22717357	-3.32453592
H	4.46628014	-1.16077552	-3.31809245
C	4.96169808	2.56372133	-4.30578692
C	3.82385518	0.88179743	-2.97484127
C	4.58131213	-0.11958422	-3.60829961
C	5.51728663	0.22190626	-4.58701235
C	5.70626450	1.56264577	-4.94120179
C	-2.06039271	-2.51429579	-0.86812858
C	-2.99805486	-2.45220487	0.17993646
C	-4.22761286	-3.09952670	0.06587922
C	-4.54338795	-3.81497156	-1.09489238
C	-3.60994064	-3.87328130	-2.13428593
C	-2.37098873	-3.23353925	-2.03525891
H	-2.75916786	-1.89448585	1.08487739
H	-4.93970555	-3.04161841	0.88584299
H	-5.50237073	-4.31861196	-1.18591204
H	-3.84206018	-4.42691591	-3.04145985

PhASCPh (theoretical)
E = –37752.1 kcal mol^{-1}
N_{imag} = 0

O	2.23606797	1.39612460	4.09516042
O	2.67675998	7.59764894	17.59077418
O	7.14267809	3.07605901	22.89989893
O	7.63125451	5.89871259	9.39939602
O	7.60462339	7.58745007	22.89319180
O	7.16473315	1.38784289	9.39928092
O	2.69979349	5.90722535	4.08918741
O	2.20931608	3.08627908	17.58904595
O	3.99943346	2.38139082	6.39265735
O	0.91159915	6.61038058	19.88902306
O	8.90307761	2.09001824	20.59517792
O	5.86927930	6.88574152	7.09399015
O	5.84138636	6.61069721	20.59680536
O	8.93014837	2.36785203	7.10109854
O	0.93903394	6.90040133	6.39423815
O	3.97196275	2.09158136	19.89476096
N	2.59066110	3.39947793	2.98952398
N	2.31957504	5.59452132	16.48616425
N	7.50128465	1.07230239	24.00320647
N	7.26737899	7.90229053	10.50104569
N	7.25086187	5.58433654	23.99870047
N	7.52166522	3.39090054	10.50399833
N	2.34131565	7.91120397	2.98569609
N	2.57400076	1.08246038	16.48755181
N	1.81908738	3.39097338	5.17907989
N	3.09217448	5.60254922	18.67522478
N	6.72642279	1.08144977	21.81472655
N	8.04610385	7.89347703	8.31389135
N	8.01991144	5.59323840	21.80789199
N	6.75172762	3.38287522	8.31360020
N	3.11784531	7.90208161	5.17329102
N	1.79325833	1.09107466	18.67358202
N	1.75390536	2.71227680	6.39792922
N	3.15728126	6.28058684	19.89443889
N	6.65706687	1.76233583	20.59721390
N	8.11519659	7.21322015	7.09597086
N	8.08615368	6.27329466	20.58972639
N	6.68511409	2.70351343	7.09506582
N	3.18564122	7.22249396	6.39149614
N	1.72539414	1.77030052	19.89198756
C	3.29961214	2.92554347	1.85174682
C	1.61314018	6.07054424	15.34759487
C	8.21508463	1.54456309	25.13855836
C	6.55508761	7.42715792	11.63629614
C	6.54283842	6.05938524	25.13658975
C	8.22880736	2.91439655	11.64191794
C	1.62788035	7.43946616	1.84990261
C	3.28686102	1.55650108	15.35218179
C	3.13707631	3.60601143	0.63601620
C	1.77784362	5.39225491	14.13104587
C	8.06141057	0.85860556	26.35235750
C	6.71106295	8.10829127	12.85236973
C	6.70818901	5.38218465	26.35369092
C	8.06291215	3.59010516	12.85976098
C	1.78100705	8.12700169	0.63692271
C	3.13373285	0.87198952	14.13754483

C	3.86331229	3.19034968	26.50830547
C	1.05060797	5.79215360	13.00709458
C	8.80052793	1.27125006	0.47764698
C	5.97687089	7.71021686	13.97251734
C	5.98263028	5.79899435	0.48154299
C	8.79118806	3.18993139	13.98296620
C	1.04260415	7.71448232	26.51119821
C	3.86793216	1.26952441	13.01732428
C	4.77036688	2.12941037	26.58837186
C	0.14510128	6.85448592	13.08670656
C	9.70411512	2.33488331	0.39714310
C	5.07234508	6.64748258	13.88905992
C	5.07379608	6.85816611	0.40033318
C	9.69883333	2.12975110	13.90149430
C	0.14003274	6.64975023	26.59061943
C	4.76991158	2.33466753	13.09923169
C	4.95508205	1.49078091	0.81640461
C	-0.03792570	7.50963187	14.31086233
C	9.87262339	2.97919568	26.17075873
C	4.89763895	5.98957552	12.66498666
C	4.88615351	7.49368579	26.17094146
C	9.88286112	1.47678747	12.67619688
C	-0.02805674	6.00421841	0.81626425
C	4.94168297	2.99574403	14.32185602
C	4.22175839	1.86868758	1.94085256
C	0.69162535	7.12798794	15.43659559
C	9.13386227	2.60442426	25.04862680
C	5.63496381	6.36870433	11.54345368
C	5.61836450	7.11432782	25.04619036
C	9.15220762	1.85856559	11.55111785
C	0.71011341	6.37880706	1.93872306
C	4.20404242	2.61742381	15.44340311
C	2.25094019	2.64436178	4.07881465
C	2.66011153	6.34939947	17.57529295
C	7.15893143	1.82784588	22.91517272
C	7.61188980	7.14696728	9.41350305
C	7.58869967	6.33927125	22.90877026
C	7.18138320	2.63606613	9.41462799
C	2.68383948	7.15550241	4.07358779
C	2.22708635	1.83798846	17.57414067
C	2.88583274	2.12794650	6.90108688
C	2.02501348	6.86431785	20.39769066
C	7.78812655	2.34650353	20.09147938
C	6.98409646	6.63015177	6.58938679
C	6.95527143	6.86080800	20.08750933
C	7.81622225	2.11672301	6.59231131
C	2.05358488	6.64078792	6.89738226
C	2.85758832	2.35079834	20.39865384
C	2.72347197	1.16520667	8.03508731
C	2.18687507	7.82768730	21.53118168
C	7.62433585	3.30942639	18.95798415
C	7.14824518	5.66763213	5.45558048
C	7.11853594	7.82201197	18.95226454
C	7.65325216	1.15480274	5.45765898
C	2.21631238	5.67762966	8.03072946
C	2.69475051	3.31489087	21.53122533

C	1.47587714	0.66468537	8.45430561
C	3.43419812	8.32964928	21.94966899
C	6.37635027	3.81340989	18.54405371
C	8.39621948	5.16259863	5.04296241
C	8.36713073	8.31754349	18.53004173
C	6.40490189	0.65779481	5.03632710
C	3.46338637	5.16951016	8.44225271
C	1.44782643	3.82393723	21.94207100
C	1.39347393	8.75444541	9.48936313
C	3.51619505	0.23975287	22.99721995
C	6.30689976	4.74362336	17.50336912
C	8.46601062	4.23239168	4.00217836
C	8.45093850	0.22626997	17.49359366
C	6.32141018	8.74853974	3.98807001
C	3.53159076	4.23803105	9.48182179
C	1.37977284	4.75512914	22.98202972
C	2.55884746	8.31174514	10.12233199
C	2.35065044	0.68176309	23.63030890
C	7.47085145	5.18410636	16.86664977
C	7.30243708	3.79390588	3.36326175
C	7.28600154	0.67261701	16.86274760
C	7.48637365	8.30349029	3.35640433
C	2.36725376	3.80045782	10.12015576
C	2.54411569	5.19068538	23.62200195
C	3.80085131	8.79939837	9.69993271
C	1.10898933	0.19277693	23.20856570
C	8.71312681	4.69246000	17.28338830
C	6.06016173	4.28670470	3.77871814
C	6.04322482	0.18933726	17.28755418
C	8.72890927	8.78788382	3.78059509
C	1.12575590	4.29605941	9.70561163
C	3.78550475	4.69434670	23.20778200
C	3.89168327	0.70499015	8.66760706
C	1.01848407	8.28706284	22.16392696
C	8.79134919	3.76610212	18.32068033
C	5.98159381	5.21220187	4.81673015
C	5.95062067	8.28515548	18.32105228
C	8.82125760	0.69237309	4.82620112
C	1.04905677	5.22375962	8.66940271
C	3.86195419	3.76789155	22.17052278
H	2.55005610	4.42063107	3.11299840
H	2.35942173	4.57325560	16.60956424
H	7.46300891	0.05117593	23.87833014
H	7.30446383	8.92345191	10.37637180
H	7.29149280	4.56305907	23.87620319
H	7.48207801	4.41217360	10.38116026
H	2.37956089	8.93226803	3.11137601
H	2.53701784	0.06140124	16.61314276
H	2.44866151	4.44522819	0.58069531
H	2.46566896	4.55252885	14.07573331
H	7.37569951	0.01725248	26.40825010
H	7.39760590	8.94883352	12.91047647
H	7.39800085	4.54417862	26.41017649
H	7.37362483	4.42848032	12.91681553
H	2.46605051	8.96899066	0.58218059
H	2.44914826	0.02977215	14.08072016

H	2.16390831	4.35467649	5.22673502
H	2.74734505	4.63878519	18.72256555
H	7.07549201	0.11936852	21.76418615
H	7.69792146	8.85595299	8.26352211
H	7.67433024	4.62985546	21.75891478
H	7.09864419	4.34586653	8.26519900
H	2.77044157	8.86480004	5.22272810
H	2.14142838	0.12854795	18.72278918
H	3.72887311	3.71917240	25.57131170
H	1.18598878	5.26455455	12.06958041
H	8.67221061	0.73835298	1.41330927
H	6.10698134	8.23933093	14.91014173
H	6.12000136	5.27284108	1.41978535
H	8.65423030	3.71552581	14.92148623
H	1.16957696	8.24879866	25.57633170
H	3.74064632	0.73780932	12.08100157
H	0.79874048	2.50865730	6.72149382
H	4.11236991	6.48537689	20.21753071
H	5.70081836	1.96638945	20.27678517
H	9.07137112	7.00937264	6.77536143
H	9.04199311	6.47526559	20.26688385
H	5.72930972	2.50101109	6.77236028
H	4.14120546	7.01642649	6.71242479
H	0.76991508	1.97594193	20.21327652
H	5.34735686	1.83445844	25.71672203
H	9.43123050	7.13522476	12.21286184
H	0.42456638	2.64416518	1.26810827
H	4.49210738	6.35192905	14.75834413
H	4.49766096	7.15447266	1.27211266
H	0.41345937	1.84860605	14.77470518
H	9.41997424	6.34096720	25.71923267
H	5.35037309	2.62933912	12.22980962
H	5.67880236	0.68818185	0.90725673
H	9.10023901	8.29683663	14.39990470
H	0.73339392	3.80039059	26.08044263
H	4.17522867	5.18598283	12.57104016
H	4.16100409	8.29495524	26.07936922
H	0.74640642	0.69120152	12.58582596
H	9.11213788	5.18213912	0.90581747
H	5.66197477	3.80130191	14.41480462
H	4.39130343	1.37854124	2.89064378
H	0.52032507	7.61634795	16.38699688
H	9.29702816	3.09910068	24.09984602
H	5.47016677	5.87815377	10.59285824
H	5.44644189	7.60210952	24.09532911
H	9.32430642	1.37170763	10.59983598
H	0.54748300	5.88319994	2.88687424
H	4.36655016	3.11036244	16.39291919
H	0.55399252	0.97550480	7.97406968
H	4.35624233	8.01951195	21.46934055
H	5.45544735	3.50388120	19.02700911
H	9.31663490	5.47031969	5.52797388
H	9.28883887	8.00395685	19.00885377
H	5.48309889	0.97083807	5.51525031
H	4.38434299	5.47588619	7.95743833
H	0.52694234	3.51809163	21.45676551

H	0.42790900	8.35255260	9.77933835
H	4.48150221	0.64227901	23.28709753
H	5.34114349	5.14769514	17.21702912
H	9.43168141	3.82699178	3.71726709
H	9.41729804	0.62438043	17.20088723
H	5.35525797	8.34983932	3.69566386
H	4.49654925	3.83017298	9.76536746
H	0.41485126	5.16332299	23.26558733
H	2.50346224	7.57702262	10.92227748
H	2.40567762	1.41631327	24.43041532
H	7.41426293	5.91858970	16.06659532
H	7.35921908	3.05991172	2.56276562
H	7.34235156	1.40570669	16.06140413
H	7.43034748	7.56995577	2.55545211
H	2.42300215	3.06473594	10.91915957
H	2.48856603	5.92574341	24.42160566
H	4.71080213	8.44899781	10.17035830
H	0.19903118	0.54205099	23.67974821
H	9.62168664	5.04051443	16.80827052
H	5.15193039	3.94002924	3.30216081
H	5.13409606	0.54225197	16.81717442
H	9.63816736	8.43532106	3.31015104
H	0.21659571	3.95049920	10.18109834
H	4.69470516	5.03866947	23.68392422
H	4.86031274	1.06512022	8.34413473
H	0.05005002	7.92588634	21.84095536
H	9.76022796	3.40222892	18.63953842
H	5.01270935	5.57665000	5.13484509
H	4.98127724	7.92862479	18.64663570
H	9.79039675	1.05008393	5.15104973
H	0.08075537	5.59039901	8.35209448
H	4.83003138	3.40038357	21.85372927
VEC1	9.86069685	-0.01654658	-0.00135035
VEC2	-0.01489352	9.01956031	-0.00618761
VEC3	-0.00375840	-0.01846718	26.99537083

PhASCBz (monomer)
E = –5039.5 kcal mol^{-1}
H = –4868.8 kcal mol^{-1}
G = –4910.4 kcal mol^{-1}
N_{imag} = 0

C	3.08754903	-5.45302315	-2.60913728
C	2.14121240	-3.21108024	-1.20948112
N	0.31427045	-0.08289369	-0.37611821
H	3.33574826	-6.36057712	-0.66420159
H	-2.70077235	4.38448886	4.71491798
H	-3.62003350	5.88807316	0.78215168
H	-2.33949365	4.04867180	-0.23210402
H	1.94593946	-2.29735340	-3.16978012
C	2.68974909	-4.30768059	-3.30786897
C	3.02188353	-5.47415801	-1.21081994
O	-0.17168878	1.38644026	1.80992160
O	1.89641982	-1.89603630	0.80289897
C	-1.01302879	1.98103069	1.12917136

N	0.88530450	-1.13388355	-1.08740358
H	0.40348723	-1.31897927	-1.96374427
C	-3.25308353	5.24970373	2.81356799
C	-1.90244189	3.25489277	3.06530027
H	0.56551665	0.02305473	0.61249278
H	-3.81371844	6.06936510	3.25696792
O	-1.12538275	0.34954762	-2.10291534
C	-2.62633471	4.30306718	3.63304331
H	-1.40093650	2.51765239	3.68529412
H	2.50720074	-4.35182000	0.57127160
N	-1.29215266	1.61759210	-0.18366423
H	2.75507273	-4.27993229	-4.39310709
C	2.55676397	-4.35842857	-0.51377017
C	-0.71003012	0.58393008	-0.96257252
C	2.21899760	-3.19080174	-2.61332684
C	-3.15018735	5.14528576	1.42229880
C	-2.43396997	4.09103955	0.85064704
H	-2.06130642	2.06556461	-0.67031133
C	-1.80931747	3.13259760	1.66825017
C	1.64475708	-2.05385417	-0.39607707
H	3.45400644	-6.32149582	-3.15179207

PhASCBz (theoretical)
E = –40579.0 kcal mol^{-1}
$\boldsymbol{N_{imag}}$ = 0

O	7.34187725	13.31860083	5.23926969
O	0.39909537	27.07602448	9.74507470
O	1.11734829	14.01560384	4.76442294
O	8.07213154	0.27853728	0.27804922
O	6.87314034	15.69274622	1.92558196
O	2.31521721	2.02192451	3.10521113
O	1.58427769	11.64985374	8.08181393
O	6.16698431	25.34366736	6.90865136
O	8.09917243	18.11477301	4.11658263
O	1.09324493	4.43483201	0.93089975
O	0.35232653	9.22199917	5.89143782
O	7.37351884	22.92226039	9.07170260
N	6.15790173	14.10911946	3.43507449
N	3.03352441	0.43461804	1.60092924
N	2.29930037	13.23320623	6.57291312
N	5.44170762	26.92369889	8.41783217
N	8.10304095	15.37083387	3.82653461
N	1.08636468	1.69254448	1.20416703
N	0.35672045	11.96626256	6.17876726
N	7.38741752	25.66349579	8.81610042
N	9.12704611	16.19808328	3.38518064
N	0.05975595	2.51711363	1.64494349
N	-0.66687518	11.14159789	6.62752078
N	8.41549241	24.84120718	8.37400303
C	5.30629379	12.18225498	4.74555896
C	3.90895180	25.90650818	0.39839963
C	3.15008715	15.15716162	5.25697697
C	4.56370548	1.44967766	9.62130793

O	1.98375080	16.84246714	8.41523097
O	5.72996993	3.13119105	6.47646882
O	6.47779154	10.51020181	1.59978195
O	2.74078823	24.22403016	3.54779852
C	4.21585121	11.92549324	3.89093462
C	4.99477613	25.64741413	1.25810306
C	4.23707589	15.42068724	6.11382373
C	3.47465334	1.70388996	8.76424342
O	4.13411282	13.94760187	1.47577714
O	5.05283215	0.28930206	3.55803027
O	4.32294670	13.39430963	8.53295779
O	3.42130009	27.07599905	6.45593097
C	3.31181265	10.90731218	4.20013809
C	5.90059884	24.63012234	0.95063188
C	5.14037512	16.43865198	5.80167993
C	2.56848811	2.72108154	9.07069920
O	0.89216057	14.60210256	1.70841048
O	8.31172410	0.93327658	3.33461680
O	7.56232492	12.74202645	8.29702530
O	0.16809631	26.42228372	6.67942977
C	3.48572012	10.12764104	5.34984469
C	4.25965040	23.89059902	9.64294861
C	4.96889537	17.21164948	4.64698313
C	4.21282547	3.46609022	0.37411230
C	4.56863916	10.37706048	6.20247651
C	3.18106106	24.14242913	8.78534103
C	3.88907315	16.95547282	3.79231644
C	5.29502503	3.21981292	1.22875292
C	5.46756692	11.40227909	5.90928071
C	2.28020681	25.16638109	9.07704472
C	2.99116458	15.93018726	4.08833151
C	6.19574393	2.19520403	0.93854130
C	6.33776368	13.23421719	4.50792298
C	2.87517853	26.95713438	0.63383189
C	2.12013082	14.10426654	5.49687134
C	5.59782428	0.39902691	9.38725225
C	7.04993173	15.09997933	3.01829045
C	2.13890369	1.42471421	2.01444080
C	1.40752626	12.24222076	6.98894079
C	6.33741714	25.93511797	8.00347354
C	9.02090569	17.56326628	3.49716481
C	0.17122434	3.88272475	1.54842246
C	-0.56502629	9.77655789	6.51485214
C	8.30177065	23.47530040	8.46453777
C	0.21210024	18.33744188	2.73772067
C	8.98991891	4.66872939	2.32647823
C	8.24382836	9.00399734	7.27642420
C	-0.51255259	22.68980213	7.69364219
C	0.87487182	17.89606926	1.57970418
C	8.32775227	4.21371556	3.47970041
C	7.57659566	9.45139439	8.42980918
C	0.15454350	23.14397175	6.54288051
C	1.86056869	18.69323585	0.99015419
C	7.35271198	5.01029530	4.08812203
C	6.58885655	8.65698832	9.01946463
C	1.13098557	22.34609942	5.93839370

C	2.21616842	19.91719306	1.56656289
C	7.00700886	6.24766983	3.53496364
C	6.23628111	7.42979687	8.44826770
C	1.47361883	21.10877394	6.49352253
C	1.56587542	20.35745146	2.72762675
C	7.65618107	6.70166971	2.37855770
C	6.89038798	6.98414140	7.29161867
C	0.81967274	20.65571678	7.64763599
C	0.55571758	19.58119694	3.29941257
C	8.65575031	5.92554736	1.78818154
C	7.90199673	7.75787793	6.71920134
C	-0.18171350	21.43280911	8.23378355
N	4.57975718	15.89861213	0.36381630
N	4.60411391	2.23648536	4.67926707
N	3.87959386	11.44429988	9.64818638
N	3.86753545	25.12572636	5.34068664
N	1.28188700	14.57356356	9.59077053
N	6.43502821	0.87672561	5.28405745
N	7.17978001	12.76883232	0.41410540
N	2.04119576	26.48833799	4.72762501
N	1.91262793	13.47056894	0.02429677
N	7.28883022	27.20388314	5.11337238
N	6.54216645	13.87618553	9.97833431
N	1.18468976	0.15882737	4.90128408
C	3.87783788	18.04377765	9.23197705
C	3.83004578	4.33614416	5.68509830
C	4.58345385	9.30366602	0.79247278
C	4.63709832	23.01803760	4.35087931
C	6.17847330	18.34411434	0.47650401
C	2.98570174	4.68189114	4.61146522
C	2.28305550	8.99461119	9.55048160
C	5.47556959	22.67853868	5.43110404
C	7.04735295	19.43402198	0.38041389
C	2.12407759	5.77624796	4.72790918
C	1.41865679	7.90154468	9.65313950
C	6.34204899	21.58721663	5.32420929
C	5.61509143	20.24491318	9.05881830
C	2.10448980	6.54404736	5.90004691
C	2.85409583	7.09804020	0.97963720
C	6.37087424	20.81459248	4.15570615
C	4.78195136	19.91798896	7.98046412
C	2.95102973	6.20482881	6.96382782
C	3.68598268	7.43493677	2.05591912
C	5.52675071	21.14437707	3.08657706
C	3.92481587	18.82357276	8.06212096
C	3.80281378	5.10806670	6.86107253
C	4.53971485	8.53116885	1.96712558
C	4.67105832	22.23925238	3.17938058
C	2.91569412	16.90462086	9.23890631
C	4.79348133	3.19786201	5.65821528
C	5.54466732	10.44337008	0.77790598
C	3.67557037	24.15840975	4.36768726
C	3.82010148	14.74303238	0.57353010
C	5.36689841	1.08292682	4.46173543
C	4.63867821	12.59912579	9.43498123
C	3.10717170	26.28125160	5.55340498

C	1.12442784	13.51565425	1.15115043
C	8.08591287	27.24550425	3.99332895
C	7.33000802	13.82992133	8.85162059
C	0.38793271	0.11185887	6.02176150
C	0.57495667	12.21316146	1.63469240
C	8.63215756	25.94071791	3.51297174
C	7.87873536	15.13163245	8.36571170
C	-0.16703400	1.41289965	6.50212556
C	-0.39174009	12.25348200	2.65680991
C	9.60362594	25.97515025	2.49508167
C	8.84669915	15.09116538	7.34482728
C	-1.14078782	1.37215946	7.51750085
C	9.01983837	11.08503014	3.31879021
C	0.19061286	24.79083454	1.83829142
C	-0.56307879	16.25962686	6.68458242
C	8.26376654	2.55314771	8.17340342
C	-0.43514206	9.83865348	2.75079185
C	9.63920055	23.55981123	2.40720539
C	8.89225645	17.50603151	7.25301671
C	-1.19121387	3.78724256	7.60633140
C	0.51290603	9.78471476	1.72667065
C	8.68598148	23.51228148	3.42668526
C	7.94218076	17.56005707	8.27525246
C	-0.23620169	3.84106701	6.58891152
C	1.01869632	10.96257173	1.16684462
C	8.18217301	24.69312564	3.98168723
C	7.43508180	16.38208228	8.83369325
C	0.27620291	2.66350195	6.03485742
H	5.35735998	14.01258463	2.78658289
H	3.83358796	0.34347710	2.25073343
H	3.09767894	13.33092420	7.22392318
H	4.64175060	27.01613442	7.76856203
H	4.05134299	12.50510162	2.99102108
H	5.15412798	26.22495453	2.16038933
H	4.39949179	14.84593990	7.01729556
H	3.31276869	1.12241118	7.86491092
H	8.21622719	14.80102744	4.67349567
H	0.97350227	1.12094506	0.35853041
H	0.24063418	12.53456470	5.33154765
H	7.49796798	26.23088278	9.66465791
H	2.46585331	10.72175157	3.54565281
H	6.74288437	24.44274144	1.60925916
H	5.98399296	16.62933785	6.45768948
H	1.72350706	2.90446990	8.41437090
H	-0.07253422	15.71153299	2.71518668
H	9.26264564	2.03925362	2.31521079
H	8.53603693	11.63542563	7.29540447
H	-0.78796484	25.31897154	7.70260034
H	2.75925001	9.35637817	5.58366348
H	4.98813185	23.12062761	9.41052151
H	5.69512697	17.98266321	4.41134231
H	3.48469161	4.23662326	0.60560459
H	4.71251915	9.77979011	7.09948251
H	3.04197013	23.54791911	7.88552344
H	3.74678155	17.54744661	2.89145295
H	5.43690320	3.81884264	2.12516228

H	6.28649463	11.63282624	6.58065744
H	1.46471040	25.39849647	8.40207377
H	2.17501754	15.69407651	3.41545000
H	7.01398169	1.96698788	1.61144982
H	0.62230552	16.94577488	1.12165321
H	8.57227938	3.25304557	3.91998251
H	7.82666757	10.40440159	8.88376270
H	-0.08800875	24.10446734	6.10103062
H	2.33465670	18.35446558	0.07500645
H	6.87991670	4.66052306	5.00001630
H	6.11085856	8.99988615	9.93093539
H	1.60708722	22.69455483	5.02777150
H	2.98855683	20.52908775	1.10733503
H	6.24333143	6.85962810	4.00828382
H	5.46318594	6.81964252	8.90828697
H	2.23875988	20.49609824	6.02337164
H	1.84284881	21.30730290	3.17610746
H	7.38670044	7.66239474	1.94916565
H	6.61514079	6.03203969	6.84700615
H	1.08687469	19.69504736	8.07859095
H	0.03075207	19.92150494	4.18729293
H	9.18024345	6.27602202	0.90404929
H	8.42959441	7.41408166	5.83439766
H	-0.71007458	21.08293492	9.11593111
H	5.41835168	15.91279362	0.96837450
H	3.76599450	2.25179661	4.07452701
H	3.03947598	11.42929035	9.04655051
H	4.70570384	25.11036181	5.94482057
H	6.15976290	17.77212012	1.39738197
H	2.98738220	4.11494278	3.68685625
H	2.29979611	9.56167561	8.62635849
H	5.46726723	23.24877079	6.35347365
H	1.02303718	15.29945069	8.91420298
H	6.69203560	1.59738899	5.96697416
H	7.44015959	12.04684688	1.09400955
H	1.78209601	25.76482854	4.04856157
H	7.69370289	19.67785737	1.22021318
H	1.46705288	6.02958069	3.89924051
H	0.77329297	7.64952127	8.81491204
H	6.99620362	21.34128149	6.15721399
H	0.71889860	12.63064277	9.42281011
H	7.00651370	26.33047527	5.56500308
H	7.73437315	14.71416929	0.58232767
H	1.46494704	1.03487267	4.45327593
H	6.29777283	21.08938380	8.99411645
H	1.43236080	7.39628381	5.98061467
H	2.17601056	6.25044947	1.05167425
H	7.05070774	19.96808299	4.08023868
H	4.81052952	20.50914411	7.07109971
H	2.93885324	6.79043904	7.87721246
H	3.65935551	6.84926436	2.96891958
H	5.54523619	20.55433701	2.17605310
H	3.29167338	18.54295656	7.22653176
H	4.44888224	4.82028142	7.68404355
H	5.17284348	8.81880227	2.80014451
H	4.02882660	22.52134299	2.35126630

```
H        9.19944111      13.22396854       3.13385140
H        0.01735363      26.93080245       2.01727080
H       -0.74443792      14.12071058       6.86787014
H        8.45029165       0.41449573       7.99431641
H        8.27368331      11.13637968       4.10484506
H        0.94005795      24.83746815       1.05516593
H        0.18388823      16.20845936       5.89921072
H        7.51276063       2.50185416       8.95459116
H        9.10738993       8.92770841       3.30524452
H        0.09574766      22.63325533       1.85752242
H       -0.64843869      18.41706129       6.70028322
H        8.34627261       4.71128059       8.15621466
H        0.87334102       8.82781461       1.36524865
H        8.32088491      22.55780808       3.78906653
H        7.58152354      18.51693373       8.63668365
H        0.12408267       4.79788720       6.22795478
H        1.76569413      10.87888529       0.38381693
H        7.43271412      24.61442141       4.76279751
H        6.68717639      16.46546413       9.61592646
H        1.02732886       2.74735653       5.25594987
VEC1       9.91725475       0.00636021       0.11198182
VEC2       0.01700942      27.39854418       0.10552317
VEC3      -1.47387232       0.03675855       9.84538224
```

8. References

1 A. M. M. Schreurs, X. Xian, L. M. J. Kroon-Batenburg. "*EVAL15*: a diffraction data integration method based on *ab initio* predicted profiles". *J. Appl. Cryst.,* **2010**, 43, 70-82.

2 L. Krause, R. Herbst-Irmer, G.M. Sheldrick, D. Stalke. "Comparison of silver and molybdenum microfocus X-ray sources for single-crystal structure determination". *J. Appl. Cryst.*, **2015**, 48, 3-10.

3 G. M. Sheldrick. "*SHELXT* - Integrated space-group and crystal-structure determination". *Acta Cryst.*, **2015**, A71, 3-8.

4 G. M. Sheldrick. "Crystal structure refinement with *SHELXL*". *Acta Cryst.*, **2015**, C71, 3-8.

5 A. L. Spek. "Structure validation in chemical crystallography". *Acta Cryst.*, **2009**, D65, 148-155.

6 V. A. Blatov, A. P. Shevchenko, D. M. Proserpio. "Applied Topological Analysis of Crystal Structures with the Program Package ToposPro". *Cryst. Growth Des.*, **2014**, 14, 3576-3586.

7 Spackman, P. R., Turner, M. J., McKinnon, J. J., Wolff, S. K., Grimwood, D. J., Jayatilaka, D. & Spackman, M. A. *J. Appl. Cryst.*, **2021**, 54, **3**, 1006–1011.

8 C. Nieuwland, S. Lekanne Deprez, C. de Vries, C. Fonseca Guerra, Chalcogen Atom Size Dictates Stability of Benzene-1,3,5-triamide Polymers: Overlooked Role of Geometrical Fit for Enhanced Hydrogen Bonding. *Chem. Eur. J.*, **2023**, 29 (34).

9 S. C. C. Van Der Lubbe, C. Fonseca Guerra, The Nature of Hydrogen Bonds: A Delineation of the Role of Different Energy Components on Hydrogen Bond Strengths and Lengths. *Chem. Asian J.*, **2019**, 14 (16), 2760-2769.

10 C. Nieuwland, C. Fonseca Guerra, Chalcogen Atom Size: A Key Parameter in Modulating Carbonyl Compound Properties. *Chem. Eur. J.*, **2024**, 30 (24).

11 L. De Azevedo Santos, D. Cesario, P. Vermeeren, S. C. C. Van Der Lubbe, F. Nunzi, C. Fonseca Guerra, σ-Electrons Responsible for Cooperativity and Ring Equalization in Hydrogen-Bonded Supramolecular Polymers. *ChemPlusChem*, **2022**, 87 (2).

12 C. Fonseca Guerra, H. Zijlstra, G. Paragi, F. M. Bickelhaupt, Telomere Structure and Stability: Covalency in Hydrogen Bonds, Not Resonance Assistance, Causes Cooperativity in Guanine Quartets. *Chem. Eur. J.*, **2011**, 17 (45), 12612-12622.

13 BAND 2023.1; SCM Theoretical Chemistry, Vrije Universiteit: Amsterdam, the Netherlands, **2023**. http://www.scm.com (accessed January 11, 2024).

14 G. Te Velde, E. J. Baerends, Precise density-functional method for periodic structures. *Phys. Rev. B*, **1991**, 44 (15), 7888-7903.

15 C. Fonseca Guerra, J. G. Snijders, G. te Velde, E. J. Baerends, Towards an order-N DFT method. *Theor. Chem. Acc.*, **1998**, 99 (6), 391-403.
16 G. te Velde, F. M. Bickelhaupt, E.J. Baerends, C. Fonseca Guerra, S. J. A. van Gisbergen, J. G. Snijders, T. Ziegler, Chemistry with ADF. *J. Comput. Chem.*, **2001**, 22 (9), 931-967.
17 ADF2023.104; SCM Theoretical Chemistry, Vrije Universiteit: Amsterdam, the Netherlands, **2023**. http://www.scm.com (accessed January 11, 2024).
18 A. D. Becke, Density-functional exchange-energy approximation with correct asymptotic behavior. *Phys. Rev. A*, **1988**, 38 (6), 3098-3100.
19 C. Lee, W. Yang, R. G. Parr, Development of the Colle-Salvetti correlation-energy formula into a functional of the electron density. *Phys. Rev. B*, **1988**, 37 (2), 785-789.
20 S. Grimme, J. Antony, S. Ehrlich, H. Krieg, A consistent and accurate ab initio parametrization of density functional dispersion correction (DFT-D) for the 94 elements H-Pu. *J. Chem. Phys.*, **2010**, 132 (15).
21 S. Grimme, S. Ehrlich, L. Goerigk, Effect of the damping function in dispersion corrected density functional theory. *J. Comput. Chem.*, **2011**, 32 (7), 1456-1465.
22 C. Nieuwland, F. Zaccaria, C. Fonseca Guerra, Understanding alkali metal cation affinities of multi-layer guanine quadruplex DNA. *Phys. Chem. Chem. Phys*., **2020**, 22 (37), 21108-21118.
23 C. Fonseca Guerra, F. M. Bickelhaupt, J. G. Snijders, E. J. Baerends, Hydrogen Bonding in DNA Base Pairs: Reconciliation of Theory and Experiment. *J. Am. Chem. Soc.*, **2000**, 122 (17), 4117-4128.
24 P. Vermeeren, L. P. Wolters, G. Paragi, C. Fonseca Guerra, Cooperative Self-Assembly in Linear Chains Based on Halogen Bonds. *ChemPlusChem*, **2021**, 86 (6), 812-819.
25 E. van Lenthe, E. J. Baerends, J. G. Snijders, Relativistic total energy using regular approximations. *J. Chem. Phys.*, **1994**, 101 (11), 9783-9792.
26 M. Franchini, P. H. T. Philipsen, E. van Lenthe, L. Visscher, Accurate Coulomb Potentials for Periodic and Molecular Systems through Density Fitting. *J. Chem. Theory Comput.*, **2014**, 10 (5), 1994-2004.
27 A. Bérces, R. M. Dickson, L. Fan, H. Jacobsen, D. Swerhone, T. Ziegler, An implementation of the coupled perturbed Kohn-Sham equations: perturbation due to nuclear displacements. *Comput. Phys. Commun.*, **1997**, 100, 247-262.
28 H. Jacobsen, A. Bérces, D. P. Swerhone, T. Ziegler, Analytic second derivatives of molecular energies: a density functional implementation. *Comput. Phys. Commun.*, **1997**, 100 (3), 263-276.
29 CYLview2.0; Université de Sherbrooke, 2020. http://www.cylview.org (accessed July 11, 2024).
30 PLAMS; SCM, Theoretical Chemistry, Vrije Universiteit: Amsterdam, the Netherlands, 2023. https://www.scm.com https://github.com/SCM-NV/PLAMS (accessed July 11, 2024).
31 W. -J. Van Zeist, F. M. Bickelhaupt, The activation strain model of chemical reactivity. *Org. Biomol. Chem.*, **2010**, 8 (14), 3118.
32 P. Vermeeren, P.; S. C. C. Van Der Lubbe, C. Fonseca Guerra, F. M. Bickelhaupt, T. A. Hamlin, Understanding chemical reactivity using the activation strain model. *Nat. Protoc.*, **2020**, 15 (2), 649-667.
33 P. Vermeeren, P.; T. A. Hamlin, F. M. Bickelhaupt, Chemical reactivity from an activation strain perspective. *Chem. Commun.*, **2021**, 57 (48), 5880-5896.
34 F. M. Bickelhaupt, Understanding reactivity with Kohn–Sham molecular orbital theory: E2–SN2 mechanistic spectrum and other concepts. *J. Comput. Chem.*, **1999**, 20 (1), 114-128.
35 F. M. Bickelhaupt, E. J. Baerends, Kohn-Sham Density Functional Theory: Predicting and Understanding Chemistry. In Reviews in Computational Chemistry, John Wiley & Sons, Inc., **2007**; pp 1-86.
36 T. A. Hamlin, P. Vermeeren, C. Fonseca Guerra, F. M. Bickelhaupt, 8 Energy decomposition analysis in the context of quantitative molecular orbital theory. In Complementary Bonding Analysis, G. Simon, Ed.; De Gruyter, **2021**; pp 199-212.
37 C. Fonseca Guerra, J. W. Handgraaf, E. J. Baerends, F. M. Bickelhaupt, Voronoi deformation density (VDD) charges: Assessment of the Mulliken, Bader, Hirshfeld, Weinhold, and VDD methods for charge analysis. *J. Comput. Chem.*, **2004**, 25 (2), 189-210.